DELIRA: A 1D 3T hydrodynamic code for simulating targets driven by laser and fast-ion beams; version 2019-11.

M.M. Basko
Keldysh Institute of Applied Mathematics, Moscow[*]
(Dated: February 7, 2020)

Contents

[*]Electronic address: mmbasko@kiam.ru

1. INTRODUCTION

The DELIRA code is a 2019 upgrade of the DEIRA-4 code (version 4.2 dated 2006-11-24) to the full fortran-90 version. It is practically fully based on the physical and mathematical model of DEIRA-4, described below. New extensions include (i) an expanded interface for inclusion of a broad selection of the equation-of-state (EOS) models (with such new additions as the generalized van-der-Waals EOS and the "phase-flip" EOS model), and (ii) a wave-optics model for the laser energy deposition.

The original DEIRA physical and mathematical model was formulated with the aim to develop a one-dimensional (1D) single-fluid numerical code for simulating inertial confinement fusion (ICF) targets driven by the beams of fast ions. The target geometry may be of one of the following three types: plane-parallel, cylindrical, and spherical. It is assumed that such a target can be irradiated by ion (or laser) beams only strictly symmetrically within the prescribed geometry, and that the ions (laser rays) propagate along the target radii. An arbitrary mixture of the deuterium, tritium, helium-3, hydrogen, and boron-11 isotopes can be used as a thermonuclear fuel. In particular, our model includes

1. the equations of 1D single-fluid three-temperature (3T) dissipative magnetohydrodynamics (MHD) with the electron and ion heat conduction and the ion physical viscosity;

2. the diffusion equation for the axial component of the magnetic field; the MHD option is restricted to the plane-parallel and cylindrical geometries only, and only the magnetic field component perpendicular to the radial direction (i.e. along the cylinder axis in the cylindrical case) is treated;

3. the diffusion equation for the energy density of radiation in the approximation of one frequency group (the approximation of a separate radiation temperature);

4. three diffusion equations for the energy densities of the three species of fast charged fusion products, namely, the 3.5-MeV alpha particles, the 3-MeV protons, and the 14.7-MeV protons;

5. four nuclear burn equations for the relative abundances of the deuterium, tritium, ^{3}He, and ^{11}B isotopes;

6. a stopping equation for propagation of fast ions in the approximation of straight-line trajectories.

The energy deposition by slow charged fusion products with short ranges, for which no diffusion equations are solved, is included as a local heat source. For the non-local heating by any of the two sorts of fast neutrons two options are provided: the approximation of first scattering and the approximation of uniform heating; note that in the present model the heating by thermonuclear neutrons is evaluated for the central fuel sphere only.

The equation of state is supposed to be given in the form of functions $P_e(V, T_e)$, $P_i(V, T_i)$, $\epsilon_e(V, T_e)$, and $\epsilon_i(V, T_i)$, where P_e, P_i and ϵ_e, ϵ_i are, respectively, the electron and the ion components of the pressure and the internal energy (per unit mass), $V \equiv 1/\rho$ is the specific volume. As a universal basic option, inherited from the DEIRA code, the EOS from Ref. [1] is used in a tabular form (EOS model #3 named "DEITA3"); it approximates realistic properties of materials in the region of strong coupling, treats properly multiple ionization of

atoms (both the pressure and the thermal ionization), and accounts for the Fermi degeneracy of the electron gas at high densities. The numerical version of the EOS #3 exists only for materials, consisting of a single chemical element.

To solve the hydrodynamic equations numerically, an explicit finite-difference scheme with artificial viscosity is used on a Lagrangian mesh. For all the diffusion equations and the heat conduction terms in the hydrodynamic energy equations, a linearized implicit scheme is used, in which the values of heat capacities and all the transport coefficients are taken from the previous time step.

2. NOTATION AND UNITS

The target to be simulated is assumed to consist of $N_z = \texttt{nz}$ different planar, cylindrical, or spherical shells (layers, or zones). Its geometry is specified by the value of parameter $s = \texttt{igeo}$: $s = 0$ for a planar target, $s = 1$ for a cylindrical target, and $s = 2$ for a spherical target. Every target layer is supposed to consist of a single material, distinguished by the index $i_{mat} = \texttt{imat} = 1, 2, \ldots, \texttt{nnmatrls}$, i.e. allowing up to `nnmatrls` different materials in any single job; `nnmatrls` is a user-defined parameter with the default value of 30. No mixing between different materials is possible.

Everywhere below we assume that all the physical variables should have a subscript corresponding to the shell number, which is omitted for brevity. Except for shells containing thermonuclear fuel, matter in each target shell is assumed to consist of atoms of a single element with an atomic number Z and an atomic mass A (different shells may have different A and Z). The mean degree of ionization (the mean number of free electrons per atom) is denoted as y, and is assumed to be a known function of the density $\rho \equiv 1/V$ and the electron temperature T_e.

In target shells containing thermonuclear fuel, the following fusion nuclear reactions are accounted for:

$$\mathrm{D} + \mathrm{T} \rightarrow {}^4\mathrm{He}\ (3.52\ \mathrm{MeV}) + \mathrm{n}\ (14.07\ \mathrm{MeV}), \tag{2.1}$$

$$\mathrm{D} + \mathrm{D} \rightarrow {}^3\mathrm{He}\ (0.82\ \mathrm{MeV}) + \mathrm{n}\ (2.45\ \mathrm{MeV}), \tag{2.2}$$

$$\mathrm{D} + \mathrm{D} \rightarrow \mathrm{T}\ (1.01\ \mathrm{MeV}) + \mathrm{p}\ (3.02\ \mathrm{MeV}), \tag{2.3}$$

$$\mathrm{D} + {}^3\mathrm{He} \rightarrow {}^4\mathrm{He}\ (3.67\ \mathrm{MeV}) + \mathrm{p}\ (14.68\ \mathrm{MeV}), \tag{2.4}$$

$$\mathrm{H} + {}^{11}\mathrm{B} \rightarrow 3{}^4\mathrm{He}\ (8.682\ \mathrm{MeV}). \tag{2.5}$$

The H+^{11}B reaction is treated in a simplified manner by assuming that all its energy (8.682 MeV) is released in the form of 3.5-MeV alpha particles.

When describing matter which undergoes nuclear transformations, it is convenient to imagine that it consists of identical "molecules", with each "molecule" containing X_k atoms (nuclei) of species k. The total number of such imaginary "molecules" in each target shell is arbitrary: it is defined by the initial normalization of concentrations X_k. Later on, in the course of nuclear transformations of one species into another, the number of "molecules" in each Lagrangian mass interval remains constant, and only concentrations X_k change. It is convenient to introduce a "molecular" mass A_{mol} defined as

$$A_{mol} = \sum_k X_k A_k. \tag{2.6}$$

This quantity changes only little in the course of nuclear transformations (2.1)–(2.4), and we assume that

$$A_{mol} = \sum_k X_{k0} A_k = \text{constant}, \tag{2.7}$$

where X_{k0} are the initial values of the element concentrations. In addition to A_{mol}, we will need the quantities

$$X_{mol} = \sum_k X_{k0}, \quad Z_{mol} = \sum_k X_{k0} Z_k, \quad \bar{A} = \frac{A_{mol}}{X_{mol}}, \quad \bar{Z} = \frac{Z_{mol}}{X_{mol}}, \tag{2.8}$$

$$\left(Z^2\right)_{mol} = \sum_k X_{k0} Z_k^2, \quad S_{mol} = \sum_k X_{k0} A_k^{-1/2} Z_k^{-2}, \quad \overline{Z^2} = \frac{\left(Z^2\right)_{mol}}{X_{mol}}, \tag{2.9}$$

which allow adequate evaluation of the transport and relaxation coefficients of a fully ionized plasma in the fuel layers, where matter can be a mixture of different elements. However, since we assume X_{mol}, A_{mol}, Z_{mol}, ... to be constant, we neglect the effect of the change in the nuclear composition due to nuclear reactions on the values of the transport and relaxation coefficients.

It should be noted here that the present model does not provide for the EOS and the rigorous treatment of the transport and relaxation phenomena in mixtures of different elements, i.e. the EOS in each target layer is always calculated for a single element with certain mean values of A and Z. Hence, a special attention should be paid to a judicial choice of the mean A and Z values for a given fuel mixture. For example, if an equimolar mixture of H and ^{11}B is considered, one can choose $Z = 5$ and $A = 9$ — so that a correct value of the total plasma pressure $P_e + P_i$ is recovered for given ρ and $T_e = T_i$ in the fully ionized state. If, on the other hand, a $(\mathrm{H})_1\,(^{11}\mathrm{B})_{11}$ mixture is considered, a more adequate choice would be $Z = 1$, $A = 11/7$, where again the value of A is chosen such as to obtain a correct value of the total plasma pressure $P_e + P_i$ in the fully ionized state. Note that the EOS always provides a single value of the ionization degree $y = y(\rho, T_e)$ with $0 < y \leq Z$.

In the shells which contain no fuel [for which `IFMFU∅(I)=∅`], we assume $X_{mol} = 1$, $A_{mol} = \bar{A} = A$, $Z_{mol} = \bar{Z} = Z$, $\left(Z^2\right)_{mol} = \overline{Z^2} = Z^2$, $S_{mol} = A^{-1/2} Z^{-2}$. Then, the general expressions for the number of nuclei n_k of species k, the number of free electrons n_e, and the total number of nuclei n_n per unit volume become

$$n_k = \frac{\rho X_k}{m_u A_{mol}}, \quad n_e = \frac{\rho \bar{Z}}{m_u \bar{A}} \left(\frac{\bar{y}}{\bar{Z}}\right), \quad n_n = \frac{\rho}{m_u \bar{A}}, \tag{2.10}$$

where m_u is the atomic mass unit, and $\bar{y}$ is the mean ionization degree.

In all the equations below, if not stated to the contrary, the following units are used (the DEIRA units):

t	(time)	10^{-8} s = 10 ns
r	(length)	10^{-1} cm = 1 mm
u	(velocity)	10^{7} cm s^{-1} = 100 km s^{-1}
$\rho = V^{-1}$	(density)	1 g cm^{-3} = 1 mg mm^{-3}
B	(magnetic field strength)	10^{7} Gauss
M, m	(mass)	10^{-3} g mm^{s-2} = 1 mg mm^{s-2}
E	(energy)	10^{11} ergs mm^{s-2} = 10 kJ mm^{s-2}
P_e, P_i	(pressure)	10^{14} ergs cm^{-3} = 100 Mbar

ϵ_e, ϵ_i	(mass-specific internal energy)	10^{14} ergs g^{-1} = 10 MJ g^{-1}
T_e, T_i, T_r	(temperature)	1 keV = 1.1604×10^7 K
q_{ik}	(nuclear reaction rate)	10^8 cm^3 g^{-1} s^{-1}
$Q_e, Q_i, \ldots$	(mass-specific heating rate)	10^{22} ergs g^{-1} s^{-1} = 1 TW mg^{-1}
$\mathcal{E}_r, \mathcal{E}_\alpha, \ldots$	(energy density)	10^{14} ergs cm^{-3}
ν_{ee}, ν_{ei}	(collision frequency)	10^8 s^{-1}
$\kappa_e, \kappa_i, \kappa_r$	(heat conduction coefficients)	10^{20} ergs cm^{-1} s^{-1} keV^{-1}
χ_{ei}, χ_{er}	(temperature relaxation coeff-s)	10^{22} ergs g^{-1} s^{-1} keV^{-1}
$\eta_\perp$	(specific resistivity)	10^{-8} s
$\eta_{i,sc}$, $\eta_{i,tn}$	(ion viscosity coeff-s)	10^6 g cm^{-1} s^{-1}
$\chi_\alpha, \chi_{p3}, \chi_{p14}$	(fusion energy relaxation coeff-s)	10^8 cm^3 g^{-1} s^{-1}
$d_\alpha, d_{p3}, d_{p14}$	(fusion energy diffusion coeff-s)	10^6 cm^2 s^{-1}
W_b	(beam power)	10^{19} ergs s^{-1} mm^{s-2} = 1 TW mm^{s-2}
E_b	(fast ion energy)	1 GeV per nucleus
S_b	(stopping power)	1 GeV mm^2 mg^{-1}

This system of units is self-consistent in the sense that all the equations below, where the values of dimensional physical constants are not specified as decimal numbers, are valid in any other self-consistent (like CGS) system of units.

3. DIFFERENTIAL EQUATIONS

1. Equations in the Eulerian form

We solve the following system of single-fluid dissipative three-temperature (3T) MHD equations:

$$\frac{\partial \rho}{\partial t} + \frac{1}{r^s}\frac{\partial}{\partial r}\left(\rho u r^s\right) = 0, \tag{3.1}$$

$$\rho\frac{\partial u}{\partial t} + \rho u\frac{\partial u}{\partial r} + \frac{\partial}{\partial r}\left[P_e + P_i - \eta_{i,sc}\frac{1}{r^s}\frac{\partial}{\partial r}\left(u r^s\right) + \frac{B^2}{8\pi} + \frac{\mathcal{E}_r}{3} + \frac{2}{3}\left(\mathcal{E}_\alpha + \mathcal{E}_{p3} + \mathcal{E}_{p14}\right)\right] = \\ = \frac{1}{r^{s+1}}\frac{\partial}{\partial r}\left[r^{s+2}\eta_{i,tn}\frac{\partial}{\partial r}\left(\frac{u}{r}\right)\right], \tag{3.2}$$

$$\frac{\partial \epsilon_e}{\partial t} + u\frac{\partial \epsilon_e}{\partial r} + \frac{P_e}{\rho}\frac{1}{r^s}\frac{\partial}{\partial r}\left(u r^s\right) = \frac{1}{\rho r^s}\frac{\partial}{\partial r}\left(r^s\hat{\kappa}_e\frac{\partial T_e}{\partial r}\right) + \frac{\eta_\perp}{\rho}\left(\frac{c}{4\pi}\frac{\partial B}{\partial r}\right)^2 - \chi_{ei}(T_e - T_i) - \\ -\chi_{er}(T_e - T_r) + \chi_{e\alpha}\mathcal{E}_\alpha + \chi_{ep3}\mathcal{E}_{p3} + \chi_{ep14}\mathcal{E}_{p14} + Q_{ecl} + Q_{en} + Q_{dr}, \tag{3.3}$$

$$\frac{\partial \epsilon_i}{\partial t} + u\frac{\partial \epsilon_i}{\partial r} + \left[P_i - \eta_{i,sc}\frac{1}{r^s}\frac{\partial}{\partial r}(u r^s)\right]\frac{1}{\rho r^s}\frac{\partial}{\partial r}\left(u r^s\right) = \frac{1}{\rho r^s}\frac{\partial}{\partial r}\left(r^s\hat{\kappa}_i\frac{\partial T_i}{\partial r}\right) + \frac{\eta_{i,tn}}{\rho}\left[r\frac{\partial}{\partial r}\left(\frac{u}{r}\right)\right]^2 + \\ +\chi_{ei}(T_e - T_i) + \chi_{i\alpha}\mathcal{E}_\alpha + \chi_{ip3}\mathcal{E}_{p3} + \chi_{ip14}\mathcal{E}_{p14} + Q_{icl} + Q_{in}, \tag{3.4}$$

$$\frac{\partial \mathcal{E}_r}{\partial t} + u\frac{\partial \mathcal{E}_r}{\partial r} + \frac{4}{3}\mathcal{E}_r\frac{1}{r^s}\frac{\partial}{\partial r}\left(u r^s\right) = \frac{1}{r^s}\frac{\partial}{\partial r}\left(r^s\hat{\kappa}_r\frac{\partial T_r}{\partial r}\right) + \rho\chi_{er}(T_e - T_r), \tag{3.5}$$

$$\frac{\partial B}{\partial t} + \frac{1}{r^s}\frac{\partial}{\partial r}\left(B u r^s\right) = \frac{c^2}{4\pi}\frac{1}{r^s}\frac{\partial}{\partial r}\left(r^s\eta_\perp\frac{\partial B}{\partial r}\right). \tag{3.6}$$

Here $\eta_{i,sc}$ and $\eta_{i,tn}$ are the coefficients of the ion (physical) viscosity, defined as

$$\eta_{i,sc} = \begin{cases} \frac{1}{3}\eta_0^i + \eta_1^i, & s = 0, \\ \frac{1}{3}\eta_0^i, & s = 1, \\ 0, & s = 2, \end{cases} \qquad \eta_{i,tn} = \begin{cases} 0, & s = 0, \\ \eta_1^i, & s = 1, \\ \frac{4}{3}\eta_0^i, & s = 2, \end{cases} \tag{3.7}$$

where η_0^i and η_1^i are the coefficients of the ion viscosity of the magnetized plasmas as defined by Braginskii [2]; without magnetic field $\eta_0^i = \eta_1^i$. Then, $\hat{\kappa}_e$, $\hat{\kappa}_i$, and $\hat{\kappa}_r$ are, respectively, the electron, the ion, (both transverse with respect to the magnetic field), and the radiative, heat conduction coefficients corrected for the corresponding flux limits (see §§ 6.1 and 6.2); $\eta_\perp$ is the transverse electrical resistivity; Q_{ecl} and Q_{icl} are the mass-specific heating rates for plasma electrons and ions by slow charged fusion products which deposit their energy locally, Q_{en} and Q_{in} are the corresponding heating rates by thermonuclear neutrons; Q_{dr} is the mass-specific energy deposition by an external power source (the driver) like a beam of fast ions or a laser beam. The energy density of radiation is given by

$$\mathcal{E}_r = a_{SB} T_r^4, \tag{3.8}$$

where $a_{SB} = 4\sigma_{SB}/c \stackrel{\text{D}}{=} 1.372$ is the radiation density constant related to the Stefan-Boltzmann constant σ_{SB}. Here and everywhere below the DEIRA units are used after the symbol $\stackrel{\text{D}}{=}$. Equation (3.6) for the axial magnetic field B has a physical meaning only in the cases of $s = 0$ and $s = 1$. It is derived from the system of two-fluid 2-T Braginskii equations [2], where the Nernst effect has been neglected.

The diffusion equations for the volumetric energy densities of the three species of fast charged fusion products are

$$\frac{\partial \mathcal{E}_\alpha}{\partial t} + u\frac{\partial \mathcal{E}_\alpha}{\partial r} + \frac{5}{3}\mathcal{E}_\alpha \frac{1}{r^s}\frac{\partial}{\partial r}\left(u r^s\right) + \rho\chi_\alpha \mathcal{E}_\alpha = \frac{1}{r^s}\frac{\partial}{\partial r}\left(r^s d_\alpha \frac{\partial \mathcal{E}_\alpha}{\partial r}\right) + \rho Q_\alpha, \tag{3.9}$$

$$\frac{\partial \mathcal{E}_{p3}}{\partial t} + u\frac{\partial \mathcal{E}_{p3}}{\partial r} + \frac{5}{3}\mathcal{E}_{p3} \frac{1}{r^s}\frac{\partial}{\partial r}\left(u r^s\right) + \rho\chi_{p3} \mathcal{E}_{p3} = \frac{1}{r^s}\frac{\partial}{\partial r}\left(r^s d_{p3} \frac{\partial \mathcal{E}_{p3}}{\partial r}\right) + \rho Q_{p3}, \tag{3.10}$$

$$\frac{\partial \mathcal{E}_{p14}}{\partial t} + u\frac{\partial \mathcal{E}_{p14}}{\partial r} + \frac{5}{3}\mathcal{E}_{p14} \frac{1}{r^s}\frac{\partial}{\partial r}\left(u r^s\right) + \rho\chi_{p14} \mathcal{E}_{p14} = \frac{1}{r^s}\frac{\partial}{\partial r}\left(r^s d_{p14} \frac{\partial \mathcal{E}_{p14}}{\partial r}\right) + \rho Q_{p14}. \tag{3.11}$$

When calculating the diffusion coefficients d_α, d_{p3}, and d_{p14}, no flux limits are imposed.

The depletion of the thermonuclear fuel is described by the equations

$$\frac{\partial X_D}{\partial t} + u\frac{\partial X_D}{\partial r} = \frac{\rho}{A_{mol}}\left(-X_D X_T\, q_{DT} - 2X_D^2\, q_{DD} - X_D X_{He}\, q_{DHe}\right), \tag{3.12}$$

$$\frac{\partial X_T}{\partial t} + u\frac{\partial X_T}{\partial r} = \frac{\rho}{A_{mol}}\left(-X_D X_T\, q_{DT} + \frac{1}{2}X_D^2\, q_{DD}\right), \tag{3.13}$$

$$\frac{\partial X_{He}}{\partial t} + u\frac{\partial X_{He}}{\partial r} = \frac{\rho}{A_{mol}}\left(-X_D X_{He}\, q_{DHe} + \frac{1}{2}X_D^2\, q_{DD}\right), \tag{3.14}$$

$$\frac{\partial X_B}{\partial t} + u\frac{\partial X_B}{\partial r} = -\frac{\rho}{A_{mol}}\, X_B X_H\, q_{BH} = \frac{\partial X_H}{\partial t} + u\frac{\partial X_H}{\partial r}. \tag{3.15}$$

Here

$$q_{ik} = \frac{\langle \sigma v \rangle_{ik}}{m_u} \tag{3.16}$$

is the rate of an $i+k$ nuclear reaction. The two reactions (2.2) and (2.3) are assumed to have the same rate q_{DD}. The total mass of a fuel component k is given by

$$M_k(t) = K(s)\frac{A_k}{A_{mol}}\int\limits_0^R \rho(t,r)X_k(t,r)\,r^s\,dr, \tag{3.17}$$

where

$$K(0)=1, \quad K(1)=2\pi, \quad K(2)=4\pi. \tag{3.18}$$

2. Equations in the Lagrangian form with artificial viscosity

Here we write down the basic differential equations in the form that will be used for constructing the finite difference scheme. At this stage, we introduce the terms with artificial viscosity. As independent Lagrangian variables, we use the time t and the quantity

$$m = \int\limits_0^r \rho r^s\,dr. \tag{3.19}$$

The coordinate m differs from the true mass coordinate by the factor $K(s)$ given in Eq. (3.18). The principal dependent variables are

$$r, \quad u, \quad T_e, \quad T_i, \quad T_r, \quad B, \quad \mathcal{E}_\alpha, \quad \mathcal{E}_{p3}, \quad \mathcal{E}_{p14}, \quad X_D, \quad X_T, \quad X_{He}, \quad X_B. \tag{3.20}$$

Transformation of differential operators from the Eulerian to the Lagrangian form is accomplished as

$$\frac{\partial}{\partial t}+u\frac{\partial}{\partial r}\to\frac{\partial}{\partial t}, \qquad \frac{\partial}{\partial r}\to\rho\,r^s\frac{\partial}{\partial m}. \tag{3.21}$$

The equations of magnetohydrodynamics become:

$$\frac{\partial r}{\partial t}=u, \tag{3.22}$$

$$\frac{\partial u}{\partial t}+r^s\frac{\partial}{\partial m}\left[P_{av}+P_e+P_i-\eta_{i,sc}\rho\frac{\partial}{\partial m}(ur^s)+\frac{B^2}{8\pi}+\frac{a_{SB}T_r^4}{3}+\frac{2}{3}\left(\mathcal{E}_\alpha+\mathcal{E}_{p3}+\mathcal{E}_{p14}\right)\right]= \\ =\frac{1}{r}\frac{\partial}{\partial m}\left[\left(\eta_{av,tn}+\eta_{i,tn}\rho r^{2s+2}\right)\frac{\partial}{\partial m}\left(\frac{u}{r}\right)\right], \tag{3.23}$$

$$\left(\frac{\partial\epsilon_e}{\partial T_e}\right)_V\frac{\partial T_e}{\partial t}+\left[P_e+\left(\frac{\partial\epsilon_e}{\partial V}\right)_{T_e}\right]\frac{\partial\left(ur^s\right)}{\partial m}=\frac{\partial}{\partial m}\left(r^s\hat{\kappa}_e\frac{\partial T_e}{\partial r}\right)+\left(\frac{c}{4\pi}\right)^2\eta_\perp V\left(\frac{\partial B}{\partial r}\right)^2- \\ -\chi_{ei}(T_e-T_i)-\chi_{er}(T_e-T_r)+\chi_{e\alpha}\mathcal{E}_\alpha+\chi_{ep3}\mathcal{E}_{p3}+\chi_{ep14}\mathcal{E}_{p14}+Q_{ecl}+Q_{en}+Q_{dr}, \tag{3.24}$$

$$\left(\frac{\partial\epsilon_i}{\partial T_i}\right)_V\frac{\partial T_i}{\partial t}+\left[P_{av}+P_i+\left(\frac{\partial\epsilon_i}{\partial V}\right)_{T_i}-\eta_{i,sc}\rho\frac{\partial\left(ur^s\right)}{\partial m}\right]\frac{\partial\left(ur^s\right)}{\partial m}=\frac{\partial}{\partial m}\left(r^s\hat{\kappa}_i\frac{\partial T_i}{\partial r}\right)+\chi_{ei}(T_e-T_i)+ \\ +\left(\eta_{av,tn}+\eta_{i,tn}\rho r^{2s+2}\right)\left[\frac{\partial}{\partial m}\left(\frac{u}{r}\right)\right]^2+\chi_{i\alpha}\mathcal{E}_\alpha+\chi_{ip3}\mathcal{E}_{p3}+\chi_{ip14}\mathcal{E}_{p14}+Q_{icl}+Q_{in}, \tag{3.25}$$

$$4a_{SB}T_r^3V\frac{\partial T_r}{\partial t}+\frac{4}{3}a_{SB}T_r^4\frac{\partial\left(ur^s\right)}{\partial m}=\frac{\partial}{\partial m}\left(r^s\hat{\kappa}_r\frac{\partial T_r}{\partial r}\right)+\chi_{er}(T_e-T_r), \tag{3.26}$$

$$\frac{\partial(BV)}{\partial t}=\frac{c^2}{4\pi}\frac{\partial}{\partial m}\left(r^s\eta_\perp\frac{\partial B}{\partial r}\right). \tag{3.27}$$

Diffusion of the energy density of fast fusion products:

$$V\frac{\partial \mathcal{E}_\alpha}{\partial t} + \frac{5}{3}\mathcal{E}_\alpha \frac{\partial\,(ur^s)}{\partial m} + \chi_\alpha \mathcal{E}_\alpha = \frac{\partial}{\partial m}\left(r^s d_\alpha \frac{\partial \mathcal{E}_\alpha}{\partial r}\right) + Q_\alpha, \tag{3.28}$$

$$V\frac{\partial \mathcal{E}_{p3}}{\partial t} + \frac{5}{3}\mathcal{E}_{p3} \frac{\partial\,(ur^s)}{\partial m} + \chi_{p3} \mathcal{E}_{p3} = \frac{\partial}{\partial m}\left(r^s d_{p3} \frac{\partial \mathcal{E}_{p3}}{\partial r}\right) + Q_{p3}, \tag{3.29}$$

$$V\frac{\partial \mathcal{E}_{p14}}{\partial t} + \frac{5}{3}\mathcal{E}_{p14} \frac{\partial\,(ur^s)}{\partial m} + \chi_{p14} \mathcal{E}_{p14} = \frac{\partial}{\partial m}\left(r^s d_{p14} \frac{\partial \mathcal{E}_{p14}}{\partial r}\right) + Q_{p14}. \tag{3.30}$$

Fuel depletion:

$$\frac{\partial X_D}{\partial t} = \frac{1}{VA_{mol}}\left(-X_D X_T\, q_{DT} - 2X_D^2\, q_{DD} - X_D X_{He}\, q_{DHe}\right), \tag{3.31}$$

$$\frac{\partial X_T}{\partial t} = \frac{1}{VA_{mol}}\left(-X_D X_T\, q_{DT} + \frac{1}{2}X_D^2\, q_{DD}\right), \tag{3.32}$$

$$\frac{\partial X_{He}}{\partial t} = \frac{1}{VA_{mol}}\left(-X_D X_{He}\, q_{DHe} + \frac{1}{2}X_D^2\, q_{DD}\right), \tag{3.33}$$

$$\frac{\partial X_B}{\partial t} = \frac{\partial X_H}{\partial t} = -\frac{1}{VA_{mol}} X_B X_H\, q_{BH}. \tag{3.34}$$

The specific volume $V \equiv 1/\rho$ (not among the principal dependent variables) is given by

$$V = \frac{1}{s+1}\frac{\partial r^{s+1}}{\partial m}. \tag{3.35}$$

In particular, from Eqs. (3.22) and (3.35) we have

$$\frac{\partial V}{\partial t} = \frac{\partial\,(ur^s)}{\partial m} \equiv \dot{V}. \tag{3.36}$$

The additive pressure component due to the scalar artificial viscosity is given by

$$P_{av} = -\eta_{av,sc}\frac{\partial\,(ur^s)}{\partial m} \equiv -\eta_{av,sc}\dot{V}. \tag{3.37}$$

Here $\eta_{av,sc} \geq 0$ and $\eta_{av,tn} \geq 0$ are, respectively, the coefficients of scalar and tensor components of the artificial viscosity [3]. In equations (3.24)–(3.30), the derivative $\dfrac{\partial}{\partial r}$ should be understood as the operator $\rho r^s \dfrac{\partial}{\partial m}$.

4. BOUNDARY CONDITIONS

At the inner (left) boundary $r = R_l$ three different types of boundary conditions are envisaged.

1. A fixed center of symmetry at $R_l = u_l = 0$, all the diffusion fluxes are zero:

$$u(t,0) = 0, \tag{4.1}$$

$$\frac{\partial T_e}{\partial r} = \frac{\partial T_i}{\partial r} = \frac{\partial T_r}{\partial r} = \frac{\partial B}{\partial r} = 0, \tag{4.2}$$

$$\frac{\partial \mathcal{E}_\alpha}{\partial r} = \frac{\partial \mathcal{E}_{p3}}{\partial r} = \frac{\partial \mathcal{E}_{p14}}{\partial r} = 0. \tag{4.3}$$

2. A closed void cavity at $0 < r < R_l$ with a prescribed boundary pressure $P_{bl}(t)$; all the diffusion fluxes are zero:

$$\frac{\partial T_e}{\partial r} = \frac{\partial T_i}{\partial r} = \frac{\partial T_r}{\partial r} = \frac{\partial B}{\partial r} = 0, \tag{4.4}$$

$$P(t, R_l) = P_{bl}(t) + \frac{1}{3} a_{SB} T_{r,l}^4 + \frac{B_l^2}{8\pi} + \frac{2}{3}(\mathcal{E}_{\alpha,l} + \mathcal{E}_{p3,l} + \mathcal{E}_{p14,l}), \tag{4.5}$$

$$\frac{\partial \mathcal{E}_\alpha}{\partial r} = \frac{\partial \mathcal{E}_{p3}}{\partial r} = \frac{\partial \mathcal{E}_{p14}}{\partial r} = 0. \tag{4.6}$$

   Here $T_{r,l}$, B_l, $\mathcal{E}_{\alpha,l}$, ..., are the values of the corresponding physical quantities calculated at $r = R_l + 0$. The condition for the magnetic field B in this case may appear as questionable, but no other physically more adequate condition can be suggested immediately.

3. An open halfspace at $-\infty < r < R_l$ with a prescribed boundary pressure $P_{bl}(t)$, an external radiation temperature $T_{rlex}(t)$, and a boundary magnetic field $B_{bl}(t)$:

$$\frac{\partial T_e}{\partial r} = \frac{\partial T_i}{\partial r} = 0, \tag{4.7}$$

$$\kappa_r \frac{\partial T_r}{\partial r} = \frac{1}{4} c\, a_{SB} \left(T_r^4 - T_{rlex}^4 \right), \tag{4.8}$$

$$P(t, R) = P_{bl}(t) + \frac{1}{3} a_{SB} T_{rlex}^4 + \frac{B_{bl}^2}{8\pi}, \tag{4.9}$$

$$B(t, R) = B_{bl}(t), \tag{4.10}$$

$$\mathcal{E}_\alpha(t, R_l - 0) = \mathcal{E}_{p3}(t, R_l - 0) = \mathcal{E}_{p14}(t, R_l - 0) = 0. \tag{4.11}$$

   This latter type of the left boundary condition is possible for plane-parallel targets only.

The conditions at the outer (right) boundary $r = R$ are:

$$\frac{\partial T_e}{\partial r} = 0, \quad \kappa_r \frac{\partial T_r}{\partial r} = \frac{1}{4} c\, a_{SB} \left(T_{rex}^4 - T_r^4 \right), \tag{4.12}$$

$$P(t, R) = P_{br}(t) + \frac{1}{3} a_{SB} T_{rex}^4 + \frac{B_{br}^2}{8\pi}, \tag{4.13}$$

$$B(t, R) = B_{br}(t), \tag{4.14}$$

$$\mathcal{E}_\alpha(t, R + 0) = \mathcal{E}_{p3}(t, R + 0) = \mathcal{E}_{p14}(t, R + 0) = 0. \tag{4.15}$$

Here, the right boundary pressure $P_{br}(t)$, the right boundary magnetic field $B_{br}(t)$, and the right boundary radiation temperature $T_{rex}(t)$ are assumed to be given functions of their arguments. Default values are $P_{bl} = P_{br} = 0$, $T_{rlex} = T_{rex} = 0$, $B_{bl} = B_{br} = B_0 \equiv B(0, r)$.

5. EQUATION OF STATE

Under the equation of state we understand the algorithm for calculating the thermodynamic functions

$$y = y(V, T_e), \tag{5.1}$$
$$P_e = P_e(V, T_e), \tag{5.2}$$
$$P_i = P_i(V, T_i), \tag{5.3}$$
$$\epsilon_e = \epsilon_e(V, T_e), \tag{5.4}$$
$$\epsilon_i = \epsilon_i(V, T_i), \tag{5.5}$$

and their first derivatives. Functions (5.2)–(5.5) must satisfy the following thermodynamic identities and inequalities:

$$\frac{\partial \epsilon_e}{\partial V} = T_e \frac{\partial P_e}{\partial T_e} - P_e, \tag{5.6}$$
$$\frac{\partial \epsilon_i}{\partial V} = T_i \frac{\partial P_i}{\partial T_i} - P_i, \tag{5.7}$$
$$\frac{\partial P_e}{\partial V} + \frac{\partial P_i}{\partial V} < 0, \tag{5.8}$$
$$\frac{\partial \epsilon_e}{\partial T_e} > 0, \quad \frac{\partial \epsilon_i}{\partial T_i} > 0. \tag{5.9}$$

The adiabatic sound velocity u_s is given by the formula

$$u_s^2 = V\frac{B^2}{4\pi} + \frac{4}{9} V a_{SB} T_r^4 + V^2 \left[-\frac{\partial P_e}{\partial V} - \frac{\partial P_i}{\partial V} + T_e \frac{(\partial P_e/\partial T_e)^2}{\partial \epsilon_e/\partial T_e} + T_i \frac{(\partial P_i/\partial T_i)^2}{\partial \epsilon_i/\partial T_i} \right]. \tag{5.10}$$

Initially, each target layer $\texttt{I} = 1, 2, \ldots, \texttt{nz}$ is supposed to be composed of a single material, identified by index $i_{mat} = \texttt{imat} = \texttt{imatz0(I)}$, where `imatz0(1:nz)` is a user-defined array. Different layers may have either different or the same values of $1 \le i_{mat} \le \texttt{nnmatrls}$. Later on, in the course of simulation, the material index i_{mat} is set individually for every mesh cell $\texttt{j} = 1, 2, \ldots, \texttt{nn}$ as the value `matnum(j)` of the integer array `matnum(1:nn)`. The EOS of materials with different values of $i_{mat} = \texttt{imat}$ can (but not must) be calculated from different *EOS models*. The switchyard between different EOS models is programmed in the `subroutine EOSDRV`.

The values of all user-defined parameters, governing the EOS for each material `imat`, must be specified within the subset `propmat(1:29,imat)` of the user-defined array `propmat(1:100,1:nnmatrls)` via the `namelist/input/` in the input file `"input/deinput.ii"`. The type of EOS, chosen for a given material $i_{mat} = \texttt{imat}$, is defined by the value of $\texttt{propmat(1,imat)} = 1, 2, 3, \ldots = EOS\#$, serving as the sequential number of the EOS model from the predefined list of all available models. The total number of available EOS models is, in principle, unlimited: it is determined by the number of programmed cases in the latest version of the `subroutine EOSDRV`. The meaning of different elements $\texttt{i} = 2, 3, \ldots, 29$ of the array `propmat(i,imat)`, depending on the value of $\texttt{propmat(1,imat)} = EOS\#$, is explained in Table B.1. For more information on how to set the values of the array `propmat(i,imat)` see Appendix B.

Generally, we distinguish between two types of EOS models: the analytic (i.e. calculated in-line from analytic formulae) and the tabular EOS models. Several implemented analytic models are described in the subsections below. In a tabular EOS, functions (5.1)–(5.5) are supposed to be calculated by interpolation between grid nodes of a separately generated table. In this case the interpolation algorithm is assumed to maintain the continuity of functions (5.1)–(5.5) between the grid cells of the (V, T_e, T_i) parameter space, while their first derivatives may generally have jumps. In the (V, T_e, T_i) parameter space, there may exist certain restricted domains, where the inequality (5.8) is violated (domains of thermodynamic instability). In contrast, the inequalities (5.9) must be fulfilled for all $V > 0$, $T_e > 0$, $T_i > 0$. The tabular EOS #3, named "DEITA3", has been inherited from the DEIRA code: it uses the tables generated by a separate code package TABIN3.

1. EOS #1: polytropic ideal gas (analytic)

The two-temperature polytropic EOS #1 is defined as

$$P_e = K_e \frac{T_e}{V}, \qquad P_i = K_i \frac{T_i}{V}, \tag{5.11}$$

$$\epsilon_e = \frac{K_e}{\gamma_e - 1} T_e, \qquad \epsilon_i = \frac{K_i}{\gamma_i - 1} T_i, \tag{5.12}$$

$$u_s^2 = V\left(\gamma_e P_e + \gamma_i P_i\right). \tag{5.13}$$

The polytropic EOS has no direct relation to matter ionization. However, it can be applied to describe a plasma with a constant degree of ionization. In such a case, a reasonable definition of the ionization degree would be

$$y = \frac{P_e}{P_i} = \frac{K_e}{K_i}. \tag{5.14}$$

This EOS model has 4 free (user-defined) parameters:

$$\begin{aligned} &K_e = \texttt{propmat(2,imat)},\ K_i = \texttt{propmat(3,imat)}, \\ &\gamma_e = \texttt{propmat(4,imat)},\ \ \gamma_i = \texttt{propmat(5,imat)}. \end{aligned} \tag{5.15}$$

This EOS model is selected by setting $\texttt{propmat(1,imat)} = 1$.

In the simplest case of the Boltzmann gas of free electrons and a mixture of different ion species k with ionization degrees y_k we have

$$P_e = \frac{\rho T_e}{m_u} \frac{\sum\limits_k X_k y_k}{\sum\limits_k X_k A_k} \overset{\text{D}}{=} 9.65 \frac{\sum\limits_k X_k y_k}{\sum\limits_k X_k A_k} \frac{T_e}{V} \overset{\text{D, fi}}{=} 9.65\ \frac{\bar{Z}}{\bar{A}} \frac{T_e}{V}, \quad K_e = 9.65 \frac{\bar{Z}}{\bar{A}}, \tag{5.16}$$

$$P_i = \frac{\rho T_i}{m_u} \frac{\sum\limits_k X_k}{\sum\limits_k X_k A_k} \overset{\text{D}}{=} 9.65 \frac{\sum\limits_k X_k}{\sum\limits_k X_k A_k} \frac{T_i}{V} \overset{\text{D, fi}}{=} 9.65 \frac{T_i}{\bar{A} V}, \quad K_i = \frac{9.65}{\bar{A}}, \tag{5.17}$$

$$\epsilon_e = \frac{3}{2} P_e V, \quad \epsilon_i = \frac{3}{2} P_i V, \quad \gamma_e = \gamma_i = \frac{5}{3}, \tag{5.18}$$

where the equality sign $\overset{\text{D, fi}}{=}$ indicates a particular case of the DEIRA units and full plasma ionization.

2. EOS #2: ideal Fermi-Boltzmann gas (analytic)

Here, for the EOS #2, we assume that matter is an electrically neutral mixture of the ideal non-relativistic Fermi-gas of free electrons at temperature T_e with the ideal Boltzmann gas of ions at temperature T_i. This EOS has two free dimensionless parameters, namely, the mean atomic mass $\bar{A}$ and the mean ionization degree $\bar{y}$:

$$\bar{A} = \frac{\sum_k A_k X_k}{\sum_k X_k} \equiv \frac{A_{mol}}{X_{mol}}, \qquad \bar{y} = \frac{\sum_k y_k X_k}{\sum_k X_k} \equiv \frac{y_{mol}}{X_{mol}}. \tag{5.19}$$

Note that the mean ionization degree $\bar{y}$ is assumed to be independent of temperature and density. The values of $\bar{A}$ and $\bar{y}$ are set by the user by assigning

$$\texttt{propmat(25,imat)} = \bar{A}, \qquad \texttt{propmat(2,imat)} = \bar{y} \tag{5.20}$$

in the `namelist/input/` in the input file `"input/deinput.ii"`. If positive values have not been assigned to either `propmat(2,imat)` or `propmat(25,imat)`, the code stops.

The present EOS is most conveniently represented when using the atomic units for the volume V per ion, the temperatures, T_e, T_i, the pressures P_e, P_i, the internal energies E_e, E_i per ion

$$\begin{aligned} &[V] = a_0^3 = 1.4818 \times 10^{-25}\ \text{cm}^3/\text{ion}, && [T_e] = [T_i] = e^2/a_0 = 27.21\ \text{eV}, \\ &[P_e] = [P_i] = e^2/a_0^4 = 2.942 \times 10^{14}\ \text{ergs/cm}^3, && [E_e] = [E_i] = e^2/a_0 = 27.21\ \text{eV/ion}, \end{aligned} \tag{5.21}$$

where $a_0 = \hbar^2/(m_e e^2)$ is the Bohr radius. Transformation between the DEIRA and the atomic units is given by

$$\begin{aligned} &V_{\text{au}} = \frac{11.206\bar{A}}{\rho_{\text{D}}}, && T_{e(i),\,\text{au}} = \frac{T_{e(i),\,\text{D}}}{0.02721}, \\ &P_{e(i),\,\text{D}} = 2.942\, P_{e(i),\,\text{au}}, && \epsilon_{e(i),\,\text{D}} = 0.2625 \frac{E_{e(i),\,\text{au}}}{\bar{A}}. \end{aligned} \tag{5.22}$$

In the atomic units, the equation of state of the considered Fermi-Boltzmann mixture can be sufficiently accurately approximated by simple formulae

$$\theta_e = \frac{T_e}{E_F}, \qquad E_F = \frac{1}{2}(3\pi^2)^{2/3} n_e^{2/3}, \qquad n_e = \frac{\bar{y}}{V}, \tag{5.23}$$

$$P_e = n_e \left(\frac{2}{5} E_F + T_e \frac{\theta_e}{a_F + \theta_e} \right), \qquad P_i = \frac{T_i}{V}, \tag{5.24}$$

$$E_e = \frac{3}{2} V P_e, \qquad E_i = \frac{3}{2} V P_i, \tag{5.25}$$

where a_F is a dimensionless fit parameter. The electron components of the Helmholtz free energy F_e, the specific entropy S_e, and the chemical potential μ_e are given by

$$F_e = \frac{3}{5}\bar{y} E_F - \frac{3}{2}\bar{y} T_e \ln\left(1 + a_F^{-1}\theta_e\right), \tag{5.26}$$

$$S_e = \frac{3}{2}\bar{y}\left[\ln\left(1 + a_F^{-1}\theta_e\right) + \frac{\theta_e}{a_F + \theta_e} \right], \tag{5.27}$$

$$\mu_e = E_F + T_e \left[\frac{\theta_e}{a_F + \theta_e} - \frac{3}{2} \ln\left(1 + a_F^{-1}\theta_e\right) \right]. \tag{5.28}$$

The corresponding ion components are given by

$$F_i \;=\; -T_i\left(\ln V + \frac{3}{2}\ln T_i\right), \tag{5.29}$$

$$S_i \;=\; \ln V + \frac{3}{2}\ln T_i + \frac{3}{2}, \tag{5.30}$$

$$\mu_i \;=\; F_i + P_i V = T_i\left(1 - \ln V - \frac{3}{2}\ln T_i\right). \tag{5.31}$$

The non-trivial derivatives of the electron pressure are calculated as

$$V\frac{\partial P_e}{\partial V} \;=\; -n_e\left[\frac{2}{3}E_F + T_e\,\frac{\theta_e(\theta_e + a_F/3)}{(\theta_e + a_F)^2}\right], \tag{5.32}$$

$$T_e\frac{\partial P_e}{\partial T_e} \;=\; n_e T_e\,\frac{\theta_e(\theta_e + 2a_F)}{(\theta_e + a_F)^2}. \tag{5.33}$$

The dimensionless entropy parameter α, defined as the ratio of the total pressure $P_e(V,T_e) + P_i(V,T_i)$ to the degenerate pressure $P_e(V,0)$ for the same specific volume V, is given by

$$\alpha = 1 + \frac{5}{2}\left(\frac{T_i}{\bar{y}E_F} + \frac{\theta_e^2}{a_F + \theta_e}\right). \tag{5.34}$$

On possible values of the fit parameter a_F: for $a_F = 0.4$, the error in approximating the exact Fermi integrals for P_e never exceeds 1.5%; $a_F = 6/\pi^2 = 0.6079$ corresponds to the exact limit of the electron heat capacity at $T_e \to 0$; $a_F = \frac{2}{3}[6/\exp(2)]^{1/3} = 0.424665$ corresponds to the exact limit of the chemical potential for $\theta_e \to \infty$.

If the electron pressure P_e and the specific volume V are known (in atomic units), then the electron temperature T_e is calculated as

$$T_e = \tau_e + \sqrt{\tau_e^2 + 2a_F E_F \tau_e}, \quad \tau_e = \frac{P_e}{2n_e} - \frac{E_F}{5}. \tag{5.35}$$

In the single-temperature case $T_e = T_i = T$, the temperature T can be calculated as a function of V and $P = P_e + P_i$ as

$$\begin{aligned} T \;&=\; \frac{1}{2(\bar{y}+1)}\left[\tau - a_F E_F + \sqrt{(\tau + a_F E_F)^2 + 4\bar{y}\tau a_F E_F}\right] = \\ &= \frac{2\tau a_F E_F}{\sqrt{(\tau + a_F E_F)^2 + 4\bar{y}\tau a_F E_F} - (\tau - a_F E_F)}, \end{aligned} \tag{5.36}$$

where

$$\tau = P_{th}V \equiv (P_e + P_i)\,V - \frac{2}{5}\bar{y}E_F. \tag{5.37}$$

3. EOS #3: tabular EOS model "DEITA3"

For material `imat`, this EOS model is selected by assigning `propmat(1,imat)` = 3; the value of `propmat(2,imat)` = m is the sequential number m of material `imat` in the "DEITA3" table. The input folder `"input/"` must contain the file `"eosta3.ii"` with the "DEITA3" EOS table, generated by running the code package `TABIN3`. The values of variables `propmat(27,imat)` and `propmat(28,imat)` are either forced to be equal to $\bar{A}$ and $\bar{Z}$ from the "DEITA3" EOS table (non-fuel layers) or calculated from the initial composition in the fuel-layers.

4. EOS #4: quasi-linear Mie-Grüneisen EOS (analytic)

This is a particular case of the Mie-Grüneisen EOS written in the form

$$P_e = P_c(V) + \Gamma_e\, c_{Ve} \frac{T_e}{V}, \quad P_i = \Gamma_i\, c_{Vi} \frac{T_i}{V}, \tag{5.38}$$

$$\epsilon_e = \epsilon_c(V) + c_{Ve} T_e, \quad \epsilon_i = c_{Vi} T_i, \tag{5.39}$$

where the cold components are given by

$$P_c(V) = \frac{\rho_0 c_0^2}{\nu + 1} \left[(\rho_0 V)^{-\nu-1} - 1 \right], \tag{5.40}$$

$$\epsilon_c(V) = \frac{c_0^2}{\nu + 1} \left[\nu^{-1} (\rho_0 V)^{-\nu} + \rho_0 V \right] - \frac{c_0^2}{\nu}, \tag{5.41}$$

and the square of the sound velocity is calculated as

$$u_s^2 = c_0^2 (\rho_0 V)^{-\nu} + \Gamma_e(\Gamma_e + 1) c_{Ve} T_e + \Gamma_i(\Gamma_i + 1) c_{Vi} T_i. \tag{5.42}$$

In the above equations, Γ_e, Γ_i, c_{Ve}, c_{Vi}, ν, ρ_0, and c_0 are user-defined constants. For $\Gamma_e = \Gamma_i = \nu = \Gamma$, the pressure as a function of energy takes the form $P = a + b\epsilon$, where a and b are linear functions of density $\rho = V^{-1}$, and Γ is the usual Grüneisen parameter. This EOS has no van-der-Waals loops and no phase transitions.

The present EOS model has 7 user-defined free parameters

$$\begin{aligned} &\rho_0 = \texttt{propmat(2,imat)}, \quad c_0^2 = \texttt{propmat(3,imat)}, \quad \nu = \texttt{propmat(4,imat)}, \\ &\Gamma_e = \texttt{propmat(5,imat)}, \quad \Gamma_i = \texttt{propmat(6,imat)}, \\ &c_{Ve} = \texttt{propmat(7,imat)}, \; c_{Vi} = \texttt{propmat(8,imat)}. \end{aligned} \tag{5.43}$$

For material $i_{mat} = \texttt{imat}$ this model is selected by assigning $\texttt{propmat(1,imat)} = 4$.

5. EOS #5: generalized van der Waals EOS (analytic)

The one-temperature version of the generalized van der Waals EOS (GWEOS), considered here, has 5 user-defined free parameters

$$\rho_{cr}, \quad T_{cr}, \quad P_{cr}, \quad n, \quad c_V, \tag{5.44}$$

of which the first three (the parameters of the liquid-gas critical point) are dimensional, and the last two — dimensionless; n is the exponent in the attraction term, c_V is the heat capacity per one atom (molecule) at constant volume. The values of these parameters for each individual material $i_{mat} = \texttt{imat}$ can be assigned via `namelist/input/` in file `"input/deinput.ii"` (in the DEIRA units) as

$$\begin{aligned} &n = \texttt{propmat(2,imat)}, \quad c_V = \texttt{propmat(3,imat)}, \quad \rho_{cr} = \texttt{propmat(4,imat)}, \\ &T_{cr} = \texttt{propmat(5,imat)}, \; P_{cr} = \texttt{propmat(6,imat)}. \end{aligned} \tag{5.45}$$

For material `imat` this model is selected by assigning `propmat(1,imat)` = 5. If none of the three variables `propmat(4,imat)`, `propmat(5,imat)`, `propmat(6,imat)` has been assigned a positive value by the user, all three are automatically set equal to 1. If only one or two out of the three these variables have been assigned positive values, the code stops.

The analytical GWEOS has two different options (branches) in the liquid-gas phase coexistence region (below the binodal curve), namely, the metastable (MS) and the fully equilibrium (EQ) branches. The EQ-GWEOS is calculated by applying the Maxwell rule. The user can select which branch to use by setting the value of the *pf-Maxwell flag*

$$\texttt{propmat(10,imat)} = \begin{cases} 0.0, \text{ MS branch, no Maxwell construction,} \\ 1.0, \text{ EQ branch with Maxwell construction,} \\ 2.0, \text{ the "phase-flip" kinetics,} \end{cases} \tag{5.46}$$

equal to 0 or 1. The value `propmat(10,imat)` = 2.0 turns on the mode of "phase-flip" (PF) kinetics for material `imat`, in which the MS-GWEOS is applied in any given mesh cell all the way down to the spinodal, where an irreversable transition to the EQ-GWEOS is made. The complete set of analytical formulae for calculating both branches of GWEOS in-line is presented in Ref. [28].

In addition to the above mentioned parameters, one might also have to assign the value of

$$z_{ion} = \texttt{propmat(7,imat)} = \text{mean ionization degree}, \tag{5.47}$$

which might be needed when calculating various transport and relaxation coefficients. If no value has been explicitly assigned to `propmat(27,imat)` in the `namelist/input/`, it is automatically set equal to

$$\bar{A} = \frac{n^2-1}{4n}\,\frac{\rho_{cr}T_{cr}}{m_u P_{cr}}, \tag{5.48}$$

where m_u is the atomic mass unit; see Ref. [28].

6. SOURCES

Under the term *sources* we understand non-diffusion and non-relaxation terms on the right-hand sides of Eqs. (3.3), (3.4), (3.9)–(3.15), (3.24), (3.25), (3.28)–(3.34).

1. Ion driver: energy deposition by a beam of fast ions

The driver is defined as an external source of energy. In our case, this is a beam of fast ions propagating normally with respect to spherical ($s = 2$), cylindrical ($s = 1$), or planar ($s = 0$) surfaces in the corresponding geometry. In Eulerian coordinates, the energy of individual ions $E_b(t, r)$ is determined by solving the equation of beam propagation

$$\frac{\partial E_b}{\partial r} = \rho S_b(E_b, \rho, T_e, T_i) \tag{6.1}$$

with the boundary condition $E_b(t, R) = E_{b0}$; here $R = R(t)$ is the outer target radius, $S_b = S_b(E_b, \rho, T_e, T_i)$ is the stopping power of matter (a known function of its arguments

[4]). Integration of Eq. (6.1) is conducted from outside ($r = R$) inwards (towards $r = 0$) and can be terminated at a point $r = r_1$ defined by

$$E_b(t, r_1)\ [\text{GeV}]\ \leq 10^{-5} A_b, \tag{6.2}$$

where A_b is the atomic mass of the beam ions.

In the present model, we assume for simplicity that the driver energy is transferred exclusively to the electron component of the plasma. The specific heating rate is given by

$$Q_{dr}(t, r) = \frac{W_b(t)}{K(s) r^s} \frac{S_b(E_b, \rho, T_e, T_i)}{E_{b0}}, \tag{6.3}$$

where $W_b(t)$ [TW mm^{s-2}] is the total beam power. As a finite-difference approximation to the heating rate in the j-th mesh interval, we use the following energy conserving expression

$$Q_{dr,j} = \frac{W_b(t)}{K(s)} \frac{E_b(t, r_{j+1}) - E_b(t, r_j)}{E_{b0}\, \Delta m_j}. \tag{6.4}$$

There is no need to solve Eq. (6.1) at each time step: it should be integrated only after changes in temperatures and density of the irradiated region accumulate to a noticeable level.

2. Thermonuclear burn rates

All the formulae given below in this section for the thermonuclear reaction rates q and the energy deposition rates Q are in the DEIRA units. The $\langle \sigma v \rangle$ value for each fusion reaction is related to the corresponding q value as

$$\langle \sigma v \rangle_{ik}\ [\text{cm}^3\ \text{s}^{-1}]\ = 1.66 \times 10^{-16}\, q_{ik}, \tag{6.5}$$

where q_{ik} is in the DEIRA units.

For the thermonuclear burn rates, the following approximate formulae [6] are used

$$q_{DT} \overset{\text{D}}{=} 1.58 \times 10^4\, T_i^{-2/3} \left\{ (1 + 0.16\, T_i)\ \exp\left[-\frac{19.98}{T_i^{1/3}} - \left(\frac{T_i}{10.34} \right)^2 \right] + \right.$$
$$\left. +0.0108\ \exp\left(-\frac{45.07}{T_i} \right) \right\}, \tag{6.6}$$

$$q_{DD} \overset{\text{D}}{=} 81.4\, T_i^{-2/3} (1 + 0.01\, T_i) \exp\left(-\frac{18.81}{T_i^{1/3}} \right), \tag{6.7}$$

$$q_{DHe} \overset{\text{D}}{=} 1.3 \times 10^4\, T_i^{-2/3} (1 + 5 \times 10^{-4}\, T_i^2)\ \exp\left[-\frac{31.72}{T_i^{1/3}} - \left(\frac{T_i}{27.14} \right)^2 \right] +$$
$$+40.5\, T_i^{-1/2} \exp\left(-\frac{148.2}{T_i} \right), \tag{6.8}$$

$$q_{BH} \stackrel{\text{D}}{=} 5.05 \times 10^4\, T_i^{-2/3} \Big(1 + 0.008\, T_i^{1/3} + 0.063\, T_i^{2/3} + 0.0034\, T_i + 0.0056\, T_i^{4/3} + \\ + 7.9 \times 10^{-4}\, T_i^{5/3}\Big) \exp\left[-\frac{53.423}{T_i^{1/3}} - \left(\frac{T_i}{174.06}\right)^2\right] + \\ + 59.2\, T_i^{-3/2} \exp\left[-\frac{149.33}{T_i}\right] + 6.51 \times 10^4\, T_i^{-3/2} \exp\left[-\frac{618.45}{T_i}\right] + \\ + 333.6\, T_i^{-2/3} \exp\left[-\frac{1094}{T_i}\right]. \tag{6.9}$$

Formulae (6.6)-(6.8) approximate more lengthy expressions [like Eq. (6.9)] from Ref. [6] to an accuracy of about 10%, which is the accuracy of the original formulae in Ref. [6]. It is assumed that each of the two reactions (2.2) and (2.3) occurs with the same rate (6.7).

Recently [27] a new (more accurate?) approximation for the H+B reaction was proposed,

$$\langle \sigma v \rangle_{BH} = \langle \sigma v \rangle_{BH,nr} + 5.41 \times 10^{-15} T_i^{-3/2} \exp\left(-\frac{148.0}{T_i}\right), \tag{6.10}$$

where for $T_i < 70$ keV

$$\langle \sigma v \rangle_{BH,nr} = 4.455 \times 10^{-16}\, S\, T_i^{-2/3} \exp\left(-\frac{53.42365}{T_i^{1/3}}\right), \tag{6.11}$$

$$S = 1.97 \times 10^5 \left(1 + \frac{5T_i}{36E_0}\right) + 240 \left(E_0 + \frac{35}{36} T_i\right) + 0.231 \left(E_0^2 + \frac{89}{36} E_0 T_i\right), \tag{6.12}$$

$$E_0 = 17.8079\, T_i^{2/3}, \tag{6.13}$$

and for 50 keV $< T_i <$ 500 keV

$$\langle \sigma v \rangle_{BH,nr} = 6.3825 \times 10^{-13}\, \zeta^{-5/6} \tau^2\, \exp\left(-3\zeta^{1/3}\tau\right), \tag{6.14}$$

$$\tau = \frac{17.8079}{T_i^{1/3}}, \tag{6.15}$$

$$\zeta = 1 - T_i \frac{-5.9357 \times 10^{-2} + T_i(1.0404 \times 10^{-3} - 9.1653 \times 10^{-6} T_i)}{1 + T_i\,[0.20165 + T_i(2.7621 \times 10^{-3} + 9.8305 \times 10^{-7} T_i)]}. \tag{6.16}$$

The specific rate of local heating by slow charged products (helium-3 and tritium) of thermonuclear reactions is

$$Q_{ecl} \stackrel{\text{D}}{=} \frac{\rho}{A_{mol}^2} \frac{1}{2} X_D^2\, q_{DD} (0.97 \times 10^4\, f_{eHe} + 0.79 \times 10^4\, f_{eT}), \tag{6.17}$$

$$Q_{icl} \stackrel{\text{D}}{=} \frac{\rho}{A_{mol}^2} \frac{1}{2} X_D^2\, q_{DD} \left[0.97 \times 10^4\, (1 - f_{eHe}) + 0.79 \times 10^4\, (1 - f_{eT})\right], \tag{6.18}$$

$$f_{eHe} \stackrel{\text{D}}{=} \frac{5.6}{5.6 + T_e}, \quad f_{eT} \stackrel{\text{D}}{=} \frac{7.0}{7.0 + T_e}. \tag{6.19}$$

The total specific power of the local energy deposition by slow charged fusion products is

$$Q_{cl} = Q_{ecl} + Q_{icl} \stackrel{\text{D}}{=} 1.76 \times 10^4 \frac{\rho}{A_{mol}^2} \frac{1}{2} X_D^2\, q_{DD}. \tag{6.20}$$

The specific powers of non-local energy sources of charged fusion products (source terms in the corresponding diffusion equations for the energy densities of these products) are

$$Q_\alpha \stackrel{\text{D}}{=} \frac{\rho}{A_{mol}^2}\left(3.40\times10^4\, X_D\, X_T\, q_{DT} + 3.54\times10^4\, X_D\, X_{He}\, q_{DHe} + \right.$$
$$\left. + 8.38\times10^4\, X_B X_H\, q_{BH}\right), \tag{6.21}$$

$$Q_{p3} \stackrel{\text{D}}{=} \frac{\rho}{A_{mol}^2}\, 2.91\times10^4\, \frac{1}{2}\, X_D^2\, q_{DD}, \tag{6.22}$$

$$Q_{p14} \stackrel{\text{D}}{=} \frac{\rho}{A_{mol}^2}\, 14.16\times10^4\, X_D\, X_{He}\, q_{DHe}. \tag{6.23}$$

The total specific power of thermonuclear energy sources (including the energy of neutrons) is given by

$$Q_{fus} \stackrel{\text{D}}{=} \frac{\rho}{A_{mol}^2}\left(1.70\times10^5\, X_D\, X_T\, q_{DT} + 7.04\times10^4\, \frac{1}{2}\, X_D^2\, q_{DD} + \right.$$
$$\left. + 1.77\times10^5\, X_D\, X_{He}\, q_{DHe} + 8.38\times10^4\, X_B X_H\, q_{BH}\right). \tag{6.24}$$

3. Heating by neutrons

Heating by thermonuclear neutrons is only evaluated for the target shells which contain thermonuclear fuel. Temporal retardation of the neutron flux is neglected. The specific neutron energy deposition rates are written as

$$Q_{en} = Q_{n14} f_{en14} + Q_{n2} f_{en2}, \tag{6.25}$$

$$Q_{in} = Q_{n14}(1 - f_{en14}) + Q_{n2}(1 - f_{en2}). \tag{6.26}$$

Here Q_{n14} and Q_{n2} are the total specific deposition powers by 14-MeV [reaction (2.1)] and 2.5-MeV [reaction (2.2)] neutrons. Coefficients $0 < f_{en14} < 1$ and $0 < f_{en2} < 1$ represent the energy fractions left by the recoil nuclei in the plasma electrons. Similar to Eq. (6.19), we approximate them as

$$f_{en14} \stackrel{\text{D}}{=} \left[1 + (1+\bar{A})^2 T_e/750\right]^{-1}, \tag{6.27}$$

$$f_{en2} \stackrel{\text{D}}{=} \left[1 + (1+\bar{A})^2 T_e/130\right]^{-1}. \tag{6.28}$$

When fuel is present in the central region $0 < r < R_{fu}$ only (which may consist of more than one shell), each of the quantities Q_{n14} and Q_{n2} can be evaluated according to one of the following three options.

I. Approximation of the first scattering. This approximation can be self-consistently implemented only in the cylindrical and spherical geometries:

$$Q_{n14}(r) \stackrel{\text{D}}{=} \frac{1100}{\bar{A}} \int_0^{R_{fu}} q_{DT}(r')\, X_D(r')\, X_T(r') \left[\frac{\rho(r')}{A_{mol}}\right]^2 \mathcal{G}(r,r')\, dr', \tag{6.29}$$

$$Q_{n2}(r) \stackrel{\text{D}}{=} \frac{650}{\bar{A}} \int_0^{R_{fu}} \frac{1}{2} q_{DD}(r') \left[\frac{X_D(r')\,\rho(r')}{A_{mol}}\right]^2 \mathcal{G}(r,r')\, dr', \tag{6.30}$$

where

$$\mathcal{G}(r,r') = \begin{cases} \dfrac{2r'}{r+r'}\,\mathcal{K}\left(\dfrac{2\sqrt{rr'}}{r+r'}\right), & s=1, \\ \dfrac{r'}{r}\,\ln\left|\dfrac{r+r'}{r-r'}\right|, & s=2, \end{cases} \tag{6.31}$$

$\mathcal{K}(x)$ is the full elliptic integral of the first kind. Constants 1100 and 650 in front of the integrals in Eqs. (6.29) and (6.30) are the numerical values of the quantity

$$\frac{1}{2}\frac{A_D}{\langle\rho l\rangle_D}\left\langle\frac{\Delta E_n}{m_u}\right\rangle_D,$$

where $\left\langle\frac{\Delta E_n}{m_u}\right\rangle_D$ is the mean energy loss (in units 10^{14} ergs/g) by neutrons after the first scattering off a deuterium nucleus, $\langle\rho l\rangle_D$ is the mean range of neutrons (in units mg/mm^2) in pure deuterium (admixture of tritium has no practical effect on the value of this constant). Strictly speaking, Eqs. (6.29) and (6.30) are valid in the limits $\tau_{n14} \ll 1$, $\tau_{n2} \ll 1$ only [definitions of τ_{n14} and τ_{n2} are given below in Eq. (6.36)], and it should be remembered that for $\tau_{n14} > 1$ ($\tau_{n2} > 1$) the neutron heating calculated from Eq. (6.29) [(6.30)] can exceed even the total thermonuclear energy liberation (6.24).

II. Local deposition. When the optical thickness of the fuel with respect to the neutron scattering is large, $\tau_{n14} \gg 1$, $\tau_{n2} \gg 1$, the neutron heating can be evaluated in the local approximation

$$Q_{n14} \stackrel{\text{D}}{=} 13.6\times10^4\, q_{DT}\, X_D X_T \frac{\rho}{A_{mol}^2}, \tag{6.32}$$

$$Q_{n2} \stackrel{\text{D}}{=} 2.37\times10^4\,\frac{1}{2}\, q_{DD}\, X_D^2 \frac{\rho}{A_{mol}^2}. \tag{6.33}$$

III. Approximation of a uniform spread. In this approximation we assume that the total fraction of the neutron energy left inside the fuel region $0 < r < R_{fu}$ is spread uniformly over the fuel mass in this region; we evaluate this fraction as $(1+\tau_0/\tau_n)^{-1}$, where τ_0 is a constant, and τ_n is the optical thickness of the fuel region $0 < r < R_{fu}$ with respect to the scattering of the corresponding neutron species. The value of τ_0 can be calculated in the limit of $\tau_n \to 0$, when Eqs. (6.29) and (6.30) become valid. As a result, we obtain $\tau_0 = 3.0$ for a neutron source in the center of a fuel sphere, $\tau_0 = 4.0$ for a neutron source spread uniformly over a fuel sphere, and $\tau_0 = 6.0$ for a neutron source along the outer rim of a fuel sphere. Assuming $\tau_0 = 4.0$ as a reasonable compromise, we obtain

$$Q_{n14} \stackrel{\text{D}}{=} 13.6\times10^4\,\frac{\tau_{n14}}{\tau_{n14}+4.0}\,\frac{\int\limits_0^{R_{fu}} q_{DT}\, X_D X_T\,(\rho/A_{mol})^2\, r^s\, dr}{\int\limits_0^{R_{fu}} \rho r^s\, dr}, \tag{6.34}$$

$$Q_{n2} \stackrel{\text{D}}{=} 2.37\times10^4\,\frac{\tau_{n2}}{\tau_{n2}+4.0}\,\frac{\frac{1}{2}\int\limits_0^{R_{fu}} q_{DD}\,(\rho X_D/A_{mol})^2\, r^s\, dr}{\int\limits_0^{R_{fu}} \rho r^s\, dr}, \tag{6.35}$$

where

$$\tau_{n14} \stackrel{\text{D}}{=} \frac{1}{20} \int\limits_0^{R_{fu}} \frac{\rho}{\bar{A}}\, dr, \qquad \tau_{n2} \stackrel{\text{D}}{=} \frac{1}{6.5} \int\limits_0^{R_{fu}} \frac{\rho}{\bar{A}}\, dr. \tag{6.36}$$

IV. Approximation of a diffusion-profile spread (version 4.2 of 2006-11-24). This approximation has been implemented for 14-MeV neutrons only, and for the spherical ($s = 2$) geometry only. In this approximation we assume that all the energy of 14-MeV neutrons, generated in the fuel sphere $0 < r < R_{fu}$, is spread over the fuel mass according to the diffusion profile $\phi(\tau)$, namely,

$$Q_{n14}(r) \stackrel{\text{D}}{=} \frac{13.6 \times 10^4}{20\bar{A}} \left[\int\limits_0^{R_{fu}} q_{DT} X_D X_T \left(\frac{\rho}{A_{mol}} \right)^2 r^2\, dr \right] \frac{\tau^2}{r^2}\, \phi(\tau), \tag{6.37}$$

where

$$\tau(r) \stackrel{\text{D}}{=} \frac{1}{20} \int\limits_0^{r} \frac{\rho}{\bar{A}}\, dr, \tag{6.38}$$

and

$$\phi(\tau) = \frac{3}{\tau_0^3} \begin{cases} 1 - \dfrac{1+\tau_0}{2\tau} \left(e^{\tau-\tau_0} - e^{-\tau-\tau_0} \right), & 0 < \tau < \tau_0, \\ \dfrac{\tau_0 - 1 + (\tau_0+1)e^{-2\tau_0}}{2\tau} e^{\tau_0-\tau}, & \tau > \tau_0. \end{cases} \tag{6.39}$$

The profile $\phi(\tau)$ has one free parameter τ_0. For any $\tau_0 > 0$ it is normalized by the condition

$$\int\limits_0^{\infty} \phi(\tau)\, \tau^2\, d\tau = 1. \tag{6.40}$$

By its meaning from the derivation of the diffusion profile, τ_0 is the "optical" radius of the 14-MeV generating fuel core. In the DEIRA code the value of τ_0 is determined as the position (along the τ coordinate) where the function

$$q_{DT} X_D X_T \left(\frac{\rho}{A_{mol}} \right)^2 r^2 \tag{6.41}$$

drops by a factor 2 from its maximum value; if the function (6.41) is uniform to within a factor 2, then $\tau_0 = \tau_{n14}$ is the optical thickness for 14-MeV neutrons of the entire fuel sphere $0 < r < R_{fu}$.

In the framework of the present model, the neutron heating of non-central fuel shells can only be evaluated in the local approximation (6.32), (6.33) (or neglected altogether).

7. KINETIC COEFFICIENTS

The above equations of magnetohydrodynamics, and of the radiation and fast-product energy diffusion contain the following kinetic coefficients: κ_e, κ_i, κ_r, χ_{ei}, χ_{er} are the coefficients of transverse (with respect to the magnetic field) heat conduction (radiation diffusion)

and temperature relaxation; η_0^i and η_1^i are the physical ion-viscosity coefficients; $\eta_\perp$ is the transverse electrical conductivity coefficient; d_α, d_{p3}, d_{p14}, $\chi_\alpha = \chi_{e\alpha} + \chi_{i\alpha}$, $\chi_{p3} = \chi_{ep3} + \chi_{ip3}$, $\chi_{p14} = \chi_{ep14} + \chi_{ip14}$ are the coefficients of diffusion and relaxation of the energy of fast fusion products. The formulae for these coefficients given below are based on the expressions published earlier in Refs. [2, 5, 7–10].

1. Electron heat conduction, electrical resistivity, and relaxation between the electron and ion temperatures

Following Ref. [11], we adopt the following expression for the limiting heat flux due to the electron heat conduction

$$F_{em} = f_{\kappa e} n_e \left(\frac{T_e}{m_e}\right)^{1/2} T_e = 1.28 \times 10^3 \, f_{\kappa e} \left(\frac{\rho y Z_{mol}}{Z A_{mol}}\right) T_e^{3/2}, \tag{7.1}$$

where $f_{\kappa e}$ is the flux limiting factor; regularly, $f_{\kappa e} = 0.5$ is assumed. Accordingly, the coefficient of the electron heat conduction corrected for the flux limit is defined as

$$\hat{\kappa}_e = \min\left\{\kappa_e;\ \frac{F_{em}}{|\nabla T_e|}\right\}. \tag{7.2}$$

Here we only need the transverse (with respect to the magnetic field) conduction coefficient κ_e. Following Ref. [10], we write it in the form

$$\kappa_e = \frac{n_e T_e}{m_e \nu_{\kappa en}} \, \Gamma_1(x_{\kappa ei}, w_{\kappa e}) \stackrel{\text{D}}{=} 1.697 \times 10^5 \left(\frac{\rho y Z_{mol}}{Z A_{mol}}\right) \frac{T_e}{\nu_{\kappa en}} \, \Gamma_1(x_{\kappa ei}, w_{\kappa e}), \tag{7.3}$$

where

$$\Gamma_1(x, w) = \frac{x^2 \Gamma_{1,1}(w) + \Gamma_{1,2}(w)}{x^4 + x^2 \Gamma_{7,1}(w) + [\Gamma_{7,2}(w)]^2}, \tag{7.4}$$

$$\Gamma_{1,1}(w) = \Gamma_{1,10} + \Gamma_{1,11} w, \tag{7.5}$$

$$\Gamma_{1,2}(w) = \Gamma_{1,20} + \Gamma_{1,21} w + \Gamma_{1,22} w^2 + \Gamma_{1,23} w^3, \tag{7.6}$$

$$\Gamma_{7,1}(w) = \Gamma_{7,10} + \Gamma_{7,11} w + \Gamma_{7,12} w^2, \tag{7.7}$$

$$\Gamma_{7,2}(w) = \Gamma_{7,20} + \Gamma_{7,21} w + \Gamma_{7,22} w^2, \tag{7.8}$$

$$x_{\kappa ei} = \frac{eB}{m_e c \nu_{\kappa en}} \stackrel{\text{D}}{=} 1.759 \times 10^6 \frac{B}{\nu_{\kappa en}}. \tag{7.9}$$

Here

$$w_{\kappa e} = \frac{\nu_{\kappa ee}}{\nu_{\kappa en}} \tag{7.10}$$

is the ratio between the frequencies of the electron-electron and electron-ion collisions. We

include the effects of the electron degeneracy and of the electron-atom scattering by writing

$$\nu_{\kappa ee} = \frac{4\sqrt{\pi}}{3} \frac{e^4 n_e L_{ee}}{m_e^{1/2} T_e \left[T_e^2 + (\beta_{\kappa ee} E_F)^2\right]^{1/4}} \stackrel{\text{D}}{=}$$

$$\stackrel{\text{D}}{=} 3.914 \times 10^5 \left(\frac{\rho y Z_{mol}}{Z A_{mol}}\right) \frac{L_{ee}}{T_e \left[T_e^2 + (\beta_{\kappa ee} E_F)^2\right]^{1/4}}, \tag{7.11}$$

$$\nu_{\kappa en} = \nu_{ei}(\beta_{\kappa ei}) + \nu_{ea}, \tag{7.12}$$

$$\nu_{ei}(\beta) = \frac{4\sqrt{2\pi}}{3} \frac{e^4 n_i y^2 L_{ei}}{m_e^{1/2} \left[T_e^2 + (\beta E_F)^2\right]^{3/4}} \stackrel{\text{D}}{=}$$

$$\stackrel{\text{D}}{=} 5.536 \times 10^5 \left(\frac{\rho \left(Z^2\right)_{mol}}{Z^2 A_{mol}}\right) \frac{L_{ei}}{\left[T_e^2 + (\beta E_F)^2\right]^{3/4}} \times \begin{cases} y, & y < 1, \\ y^2, & y \geq 1, \end{cases} \tag{7.13}$$

$$\nu_{ea} = \sigma_{ea} n_a \left(\frac{T_F}{m_e}\right)^{1/2} \exp\left[-(E_F/13 \text{ eV})^2\right] \stackrel{\text{D}}{=}$$

$$\stackrel{\text{D}}{=} 7.987 \times 10^9 \sqrt{T_F} \frac{\rho}{\bar{A}} \exp\left[-(E_F/0.013)^2\right] \times \begin{cases} (1-y), & y < 1, \\ 0, & y \geq 1. \end{cases} \tag{7.14}$$

For the electron-atom collisions we simply assume a fixed cross-section of $\sigma_{ea} = 10^{-15}$ cm^2.

In the non-degenerate limit $E_F = 0$, the formulae (7.11) and (7.13) for the electron-electron and electron-ion collision frequencies coincide with those in Refs. [2] and [10]. We calculate the values of the interpolation coefficients

$$\beta_{\kappa ee} = \left[\frac{20\pi^3\sqrt{2\pi}}{216} \frac{(\Gamma_{7,22})^2}{\Gamma_{1,23}}\right]^2 = 3.394, \tag{7.15}$$

$$\beta_{\kappa ei} = \pi \left[\frac{4}{9} \frac{(\Gamma_{7,20})^2}{\Gamma_{1,20}}\right]^{2/3} = 0.3402, \tag{7.16}$$

from the condition that in the limit of strong degeneracy, $E_F \gg T_e$, the above formulae yield the expressions for κ_{ei} (in the limit of $w \to 0$) and κ_{ee} (in the limit of $w \to \infty$) calculated by Lee [12] and Lampe [13].

The transverse electrical resistivity is given by [10]

$$\eta_\perp = \frac{m_e \nu_{\eta en}}{e^2 n_e} \left[1 - \Gamma_5(x_{\eta ei}, w_\eta)\right] \stackrel{\text{D}}{=} 6.556 \times 10^{-17} \left(\frac{Z A_{mol}}{\rho y Z_{mol}}\right) \nu_{\eta en} \left[1 - \Gamma_5(x_{\eta ei}, w_\eta)\right], \tag{7.17}$$

where

$$\Gamma_5(x, w) = \frac{x^2 \Gamma_{5,1}(w) + \Gamma_{5,2}(w)}{x^4 + x^2 \Gamma_{7,1}(w) + \left[\Gamma_{7,2}(w)\right]^2}, \tag{7.18}$$

$$\Gamma_{5,1}(w) = \Gamma_{5,10} + \Gamma_{5,11} w, \tag{7.19}$$

$$\Gamma_{5,2}(w) = \Gamma_{5,20} + \Gamma_{5,21} w + \Gamma_{5,22} w^2 + \Gamma_{5,23} w^3, \tag{7.20}$$

$$x_{\eta ei} = \frac{eB}{m_e c \nu_{\eta en}} \stackrel{\text{D}}{=} 1.759 \times 10^6 \frac{B}{\nu_{\eta en}}, \tag{7.21}$$

$$w_\eta = \frac{\nu_{\eta ee}}{\nu_{\eta en}} = \frac{\nu_{\kappa ee}}{\nu_{\eta en}}, \tag{7.22}$$

$$\nu_{\eta en} = \nu_{ei}(\beta_{\eta ei}) + \nu_{ea}. \tag{7.23}$$

The interpolation coefficient

$$\beta_{\eta ei} = \left[\frac{4}{3\sqrt{\pi}}\left(1 - \frac{\Gamma_{5,20}}{(\Gamma_{7,20})^2}\right)\right]^{2/3} = 0.3665 \tag{7.24}$$

is chosen such as to give the correct degenerate limit calculated by Lampe [14] for $\nu_{\eta ee} = 0$. We assume for simplicity $\nu_{\eta ee} = \nu_{\kappa ee}$ because the contribution of the electron-electron collisions to resistivity can be neglected in the degenerate limit [14].

The coefficient χ_{ei} of the electron-ion temperature relaxation, defined such that $\rho\chi_{ei}(T_e - T_i)$ [ergs cm^{-3} s^{-1}] is the rate of the energy transfer from the electrons to the ions per unit plasma volume, is given by [2]

$$\chi_{ei} = \frac{1}{\rho}\,\frac{3m_e}{m_i}\,n_e\nu_{\chi en} \stackrel{\text{D}}{=} 1.588\times 10^{-2}\,\left(\frac{Z_{mol}y}{\bar{A}A_{mol}Z}\right)\,\nu_{\chi en}. \tag{7.25}$$

Here, similar to Eqs. (7.12) and (7.23), the collision frequency is defined as

$$\nu_{\chi en} = \nu_{ei}(\beta_{\chi ei}) + \nu_{ea}, \tag{7.26}$$

where the interpolation coefficient

$$\beta_{\chi ei} = \left(\frac{4}{3\sqrt{\pi}}\right)^{2/3} = 0.8271 \tag{7.27}$$

is chosen such as to yield the correct degenerate limit calculated in Refs. [15, 16]. Table 7.1 lists the values of coefficients $\Gamma_{i,jk}$ — which are all rational fractions — as calculated in Ref. [10].

The Coulomb logarithms are approximated as

$$L_{ei} \;=\; \ln\left[1 + \frac{g_{fit,\kappa}\Lambda_{ei}}{1 + (6.5 g_{fit,\kappa}\Lambda_{ei})^{-1}}\right], \tag{7.28}$$

$$L_{ee} \;=\; \frac{2}{3}\ln\left[1 + \frac{\Lambda_{ee}^{3/2}}{1 + (8.5\Lambda_{ee}^{3/2})^{-1}}\right], \tag{7.29}$$

where

$$\Lambda_{ei} = \frac{3\,T_F\,D_{ei}}{e^2\left[y^2 + \frac{3}{4}\,(T_F\,\hbar^2/m_e\,e^4)\right]^{1/2}} \stackrel{\text{D}}{=} 631\,T_F\left[D_{ei}^{-2}(y^2 + 27.56T_F)\right]^{-1/2}, \tag{7.30}$$

$$\Lambda_{ee} = \frac{\frac{3}{2}\,T_e\,D_{ee}}{e^2\left[1 + \frac{3}{4}\,(T_F\,\hbar^2/m_e\,e^4)\right]^{1/2}} \stackrel{\text{D}}{=} 315.5\,T_e\left[D_{ee}^{-2}(1 + 27.56T_F)\right]^{-1/2}, \tag{7.31}$$

$$D_{ei}^{-2} = D_{ee}^{-2} + \frac{4\pi\,e^2\,n_i\,y^2}{T_i} \stackrel{\text{D}}{=} D_{ee}^{-2} + \frac{\rho\,(Z^2)_{mol}}{A_{mol}}\left(\frac{y}{Z}\right)^2\frac{1}{T_i}, \tag{7.32}$$

$$D_{ee}^{-2} = \frac{4\pi\,e^2\,n_e}{T_F} \stackrel{\text{D}}{=} \frac{\rho y Z_{mol}}{Z A_{mol}\,T_F}, \qquad T_F = \left[T_e^2 + \left(\frac{2}{3}E_F\right)^2\right]^{1/2}, \tag{7.33}$$

$$E_F = \frac{\hbar^2}{2\,m_e}\,\left(3\pi^2\,n_e\right)^{2/3} \stackrel{\text{D}}{=} 0.026\,\left(\frac{\rho y Z_{mol}}{Z A_{mol}}\right)^{2/3}, \qquad \theta_e = \frac{T_e}{E_F}. \tag{7.34}$$

TABLE 7.1: The values of $\Gamma_{i,jk}$ as calculated in Ref. [10]

	$j=1$			$j=2$			
	$k=0$	$k=1$	$k=2$	$k=0$	$k=1$	$k=2$	$k=3$
$i=1$	$\frac{13}{4}$	2	0	$\frac{93961}{4900\cdot16}$	$\frac{37574}{4900}$	$\frac{42768}{4900}$	$\frac{1296}{490}$
2	$\frac{5}{2}$	0	0	$\frac{320797}{490\cdot64}$	$\frac{632025}{49000}$	$\frac{2277}{490}$	0
3	$\frac{2127}{560}$	$\frac{1032}{560}$	0	$\frac{7161}{49000}$	$\frac{59394}{49000}$	$\frac{127728}{49000}$	$\frac{5184}{4900}$
4	$\frac{3}{2}$	0	0	$\frac{429675}{490000}$	$\frac{100665}{49000}$	$\frac{7092}{4900}$	0
5	$\frac{363033}{4900\cdot16}$	$\frac{123705}{49000}$	0	$\frac{33201}{490000}$	$\frac{341064}{490000}$	$\frac{957888}{490000}$	$\frac{41472}{49000}$
6	$\frac{477}{280}$	0	0	$\frac{4608}{49000}$	$\frac{21744}{49000}$	$\frac{36432}{49000}$	0
7	$\frac{586601}{4900\cdot16}$	$\frac{41269}{4900}$	$\frac{13252}{4900}$	$\frac{31}{100}$	$\frac{1208}{700}$	$\frac{576}{700}$	0
8	$\frac{6}{5}$	$\frac{6}{5}$	0	$\frac{58752}{49000}$	$\frac{243252}{49000}$	$\frac{294051}{49000}$	$\frac{10947}{4900}$
9	1	0	0	$\frac{1494}{490}$	$\frac{25446}{4900}$	$\frac{46561}{4900\cdot4}$	0
10	$\frac{26532}{4900}$	$\frac{44094}{4900}$	$\frac{79321}{4900\cdot4}$	$\frac{576}{700}$	$\frac{1806}{700}$	$\frac{1068}{700}$	0

TABLE 7.2: The values of the fit parameter $g_{fit,\kappa}$

Element	Z	$g_{fit,\kappa}$
Cu	29	3.0
W	74	10.0
Au	79	6.0

Eqs. (7.28) and (7.29) are written such as to approach $\ln\Lambda_{ei}$ ($\ln\Lambda_{ee}$) in the limit of $\Lambda_{ei}\gg 1$ ($\Lambda_{ee}\gg 1$), and to reproduce (for $g_{fit,\kappa}=1$) correct asymptotic behaviors in the limits of $\Lambda_{ei}\ll 1$ and $\Lambda_{ee}\ll 1$ as calculated in Refs. [17] and [14]. The parameter $g_{fit,\kappa}$ (see Table 7.2) is introduced in order to fit the experimental values of κ_e and $\eta_\perp$ in metals at room temperatures; its default value is $g_{fit,\kappa}=1$. Expressions (7.30) and (7.31) are taken from Ref. [18]; Eq. (7.31) agrees well in all limiting cases with the formulae used in Ref. [19]. Note that, when written in the DEIRA units, the quantities D_{ei} and D_{ee} in Eqs. (7.30)–(7.33) are redefined such as to contain no numerical factors.

2. Radiation diffusion and relaxation between the electron and radiation temperatures

The coefficient of radiative heat conduction $\hat{\kappa}_r$, corrected for the flux limit, is defined as

$$\hat{\kappa}_r=\min\left\{\kappa_r;\ \frac{F_{rm}}{|\nabla T_r|}\right\}, \tag{7.35}$$

where

$$F_{rm} = f_{\kappa r}\, a_{SB}\, c\, T_r^4 \tag{7.36}$$

is the limiting flux for the radiation energy, and $0 < f_{\kappa r} < 1$ is the flux limiting factor; regularly, the value $f_{\kappa r} = 0.5$ is assumed, which would be adequate for the propagation of a steep plane-parallel radiation front.

The uncorrected coefficient of radiative heat conduction κ_r is expressed in terms of the Rosseland mean free path l_R,

$$\kappa_r = \frac{4}{3}\, c\, a_{SB}\, l_R\, T_r^3 = l_R\, \frac{4\pi^2}{45\hbar^3 c^2}\, T_r^3 \stackrel{\text{D}}{=} 5484.0\, l_R\, T_r^3, \tag{7.37}$$

where

$$l_R = l_R(\rho, T_e, T_r) = \frac{15}{4\pi^4} \int\limits_0^\infty \frac{1}{\sigma_T n_e + \tilde{k}_a(\nu, \rho, T_e)}\, \frac{x^4 e^{-x}}{(1-e^{-x})^2}\, dx, \qquad x \equiv \frac{h\nu}{T_r}, \tag{7.38}$$

σ_T is the Thomson scattering cross-section, $\tilde{k}_a(\nu, \rho, T_e)$ [cm^{-1}] is the absorption coefficient of a photon $h\nu$ corrected for stimulated emission. If the values of l_R are provided from elsewhere as a function of one temperature only, $l_R = l_R(\rho, T)$, it is recommended to assign $l_R(\rho, T_e, T_r) = l_R(\rho, T_r)$. Analogously, the relaxation coefficient χ_{er} is defined as

$$\chi_{er}(\rho, T_e, T_r) = \frac{4\sigma_T}{m_e c}\, \frac{n_e}{\rho}\, a_{SB}\, T_r^4 + \frac{c a_{SB} T_e^4}{\rho(T_e - T_r)} \left[\frac{1}{l_P(\rho, T_e)} - \frac{15\, h^4}{\pi^4 T_e^4} \int\limits_0^\infty \tilde{k}_a(\nu, \rho, T_e)\, \frac{\nu^3\, d\nu}{\exp(h\nu/T_r) - 1} \right], \tag{7.39}$$

where the Planckian mean free path $l_P(\rho, T_e)$ is given by

$$\frac{1}{l_P(\rho, T_e)} = \frac{15\, h^4}{\pi^4\, T_e^4} \int\limits_0^\infty \tilde{k}_a(\nu, \rho, T_e)\, \frac{\nu^3\, d\nu}{\exp(h\nu/T_e) - 1}. \tag{7.40}$$

Equations (7.39) and (7.40) imply that

$$\chi_{er}(\rho, T_e, 0) = \frac{\pi^2}{15\hbar^3 c^2}\, \frac{T_e^3}{\rho\, l_P(\rho, T_e)} \stackrel{\text{D}}{=} 4113.0\, \frac{T_e^3}{\rho\, l_P}. \tag{7.41}$$

If one wants to express $\chi_{er}(\rho, T_e, T_r)$ in terms of externally provided values of $l_P(\rho, T_e)$, one can, to a first approximation, assume $\chi_{er}(\rho, T_e, T_r) = \chi_{er}(\rho, T_e, 0)$.

Below we present simple analytical formulae for approximate evaluation of l_R and χ_{er} that have been adopted in the opacity model DEIRA-2. The more involved opacity model DEIRA-3 is described in the Appendix A. The DEIRA-3 formulae describe the same physical processes but employ straightforward frequency integration instead of analytical approximations.

The present model describes radiation-matter interaction by taking into account the processes of Compton scattering, free-free absorption, and free-bound + bound-bound absorption. The free-free absorption (inverse bremsstrahlung) coefficient is calculated for a partially degenerate Fermi gas of free electrons. The contribution of the bound-bound and

bound-free transitions is evaluated on the basis of the model proposed in Ref. [9]. In the DEIRA-2 version of the model the following approximate formulae are used:

$$l_R = \frac{1}{k_{cs} + k_{ff} + k_{ph}}, \tag{7.42}$$

$$\chi_{er} = \chi_{cs} + \chi_{ff} + \chi_{ph}. \tag{7.43}$$

Compton scattering:

$$k_{cs} \stackrel{\text{D}}{=} 0.04\,\frac{\rho\, y Z_{mol}}{Z A_{mol}}, \qquad \chi_{cs} \stackrel{\text{D}}{=} 0.94\,\frac{y Z_{mol}}{Z A_{mol}}\,\mathcal{E}_r \stackrel{\text{D}}{=} 1.290\,\frac{y Z_{mol}}{Z A_{mol}}\,T_r^4. \tag{7.44}$$

Inverse bremsstrahlung:

$$k_{ff} \stackrel{\text{D}}{=} \left(\frac{y}{Z}\right)^2 \frac{\rho\,(Z^2)_{mol}}{A_{mol}}\,\frac{1}{T_r^2\left[1 + 9.3\,\theta_e^{3/2}(T_r/T_e)\right]}, \tag{7.45}$$

$$\chi_{ff} \stackrel{\text{D}}{=} 1.12 \times 10^5\,\left(\frac{y}{Z}\right)^2 \frac{(Z^2)_{mol}}{A_{mol}}\,\frac{T_e + T_r}{1 + 2.19\,\theta_e^{3/2}}. \tag{7.46}$$

The quantity θ_e is defined in Eq. (7.34).
Photoelectric absorption by hydrogen-like ions, $0 < Z - y \leq 1$:

$$k_{ph} \stackrel{\text{D}}{=} 1.2\,(Z-y)_H\,\frac{\rho\, Z^4}{\bar{A} T_r^3}\,\Phi_1(\omega_{r1}, -1.397), \tag{7.47}$$

$$\chi_{ph} \stackrel{\text{D}}{=} 759\,\frac{Z^4}{\bar{A}}\,(Z-y)_H\,\frac{T_e\Phi_2(\omega_{e1}, -1.397) - T_r\Phi_2(\omega_{r1}, -1.397)}{T_e - T_r}, \tag{7.48}$$

where

$$\omega_{e1} \stackrel{\text{D}}{=} \left(\frac{T_e}{0.0136\,Z^2}\right)^2, \qquad \omega_{r1} \stackrel{\text{D}}{=} \left(\frac{T_r}{0.0136\,Z^2}\right)^2. \tag{7.49}$$

When y is close to Z, the equation-of-state data may lead to a large error in the small quantity $(Z-y)_H$. Hence, we use the following approximation in Eqs. (7.47) and (7.48)

$$(Z-y)_H \stackrel{\text{D}}{=} \left[1 + 0.665\,\theta_e^{3/2}\,\exp\left(\frac{1}{\theta_e} - \frac{0.0136\,Z^2}{T_e}\right)\right]^{-1}. \tag{7.50}$$

Photoelectric absorption by helium-like ions, $1 < Z - y \leq 2$:

$$k_{ph} \stackrel{\text{D}}{=} 1.2\,\frac{\rho Z^4}{\bar{A} T_r^3}\,\left[(2 + y - Z)\Phi_1(\omega_{r1}, -1.397) + 2(Z - y - 1)\Phi_1(\omega_{r2}, b_2)\right], \tag{7.51}$$

$$\chi_{ph} \stackrel{\text{D}}{=} 759\,\frac{Z^4}{\bar{A}}\,\left[(2 + y - Z)\,\frac{T_e\Phi_2(\omega_{e1}, -1.397) - T_r\Phi_2(\omega_{r1}, -1.397)}{T_e - T_r} + \right.$$
$$\left. + 2(Z - y - 1)\,\frac{T_e\Phi_2(\omega_{e2}, b_2) - T_r\Phi_2(\omega_{r2}, b_2)}{T_e - T_r}\right], \tag{7.52}$$

where

$$\omega_{e2} \stackrel{\text{D}}{=} \left[\frac{T_e}{0.0136\,(Z - 0.65)^2}\right]^2, \qquad \omega_{r2} \stackrel{\text{D}}{=} \left[\frac{T_r}{0.0136\,(Z - 0.65)^2}\right]^2, \tag{7.53}$$

$$b_2 \stackrel{\text{D}}{=} -1.397 + \frac{13.25}{(Z - 0.4)^2}. \tag{7.54}$$

Photoelectric absorption by lithium-like ions, $2 < Z - y \le 3$:

$$k_{ph} \stackrel{\text{D}}{=} 2.4\,\frac{\rho Z^4}{\bar{A}T_r^3}\,\left[(3+y-Z)\Phi_1(\omega_{r2},b_2)+(Z-y-2)\Phi_1(\omega_{r3},b_3)\right], \tag{7.55}$$

$$\chi_{ph} \stackrel{\text{D}}{=} 1518.0\,\frac{Z^4}{\bar{A}}\left[(3+y-Z)\,\frac{T_e\Phi_2(\omega_{e2},b_2)-T_r\Phi_2(\omega_{r2},b_2)}{T_e-T_r}+\right.$$
$$\left.+(Z-y-2)\,\frac{T_e\Phi_2(\omega_{e3},b_3)-T_r\Phi_2(\omega_{r3},b_3)}{T_e-T_r}\right], \tag{7.56}$$

where

$$\omega_{e3} \stackrel{\text{D}}{=} \left[\frac{T_e}{0.0036\,(Z-1.77)^2}\right]^2, \qquad \omega_{r3} \stackrel{\text{D}}{=} \left[\frac{T_r}{0.0036\,(Z-1.77)^2}\right]^2, \tag{7.57}$$

$$b_3 \stackrel{\text{D}}{=} \frac{5.53}{(1-1.77/Z)^4}\,\ln\frac{11}{(1-1.77/Z)^4}. \tag{7.58}$$

Photoelectric absorption by higher ions, $3 < Z - y \le Z$:

$$k_{ph} \stackrel{\text{D}}{=} 2.4\,\frac{\rho\,Z^4}{\bar{A}T_r^3}\,\Phi_1(\omega_{ry},b_y), \tag{7.59}$$

$$\chi_{ph} \stackrel{\text{D}}{=} 1518.0\,\frac{Z^4}{\bar{A}}\,\frac{T_e\Phi_2(\omega_{ey},b_y)-T_r\Phi_2(\omega_{ry},b_y)}{T_e-T_r}, \tag{7.60}$$

where

$$\omega_{ey} = \left(\frac{T_e}{I_y}\right)^2, \qquad \omega_{ry} = \left(\frac{T_r}{I_y}\right)^2, \tag{7.61}$$

$$b_y \stackrel{\text{D}}{=} \frac{0.245}{Z-y}\left(\frac{0.0272\,Z^2}{I_y}\right)^2\,\ln\left[\frac{1}{Z-y}\left(\frac{0.0272\,Z^2}{I_y}\right)^2\right]. \tag{7.62}$$

In the above formulae we used the functions

$$\Phi_1(\omega,b) = \frac{\omega}{210\omega+5b+\frac{1}{4}(b+3)/\omega}, \tag{7.63}$$

$$\Phi_2(\omega,b) = \frac{\omega}{\omega+\frac{1}{2}(b+2.5)[1+1/(12\omega)]}. \tag{7.64}$$

The ionization potential of higher ions can be evaluated as

$$I_y \stackrel{\text{D}}{=} \begin{cases} 0.0063\,(1+y)^{3/2}+1.5\times10^{-7}\,(1+y)^4, & 10 < Z-y \le Z,\\ 0.0036\,(y+1.3)^2, & 2 < Z-y \le 10,\\ 0.0136\,(y+1.3)^2, & 0 < Z-y \le 2. \end{cases} \tag{7.65}$$

3. Ion heat conduction and viscosity

The limiting heat flux due to the ion heat conduction is taken to be equal to

$$F_{im} = f_{\kappa i} n_i \left(\frac{T_i}{m_i}\right)^{1/2} T_i \stackrel{\text{D}}{=} 29.97\,f_{\kappa i}\,\rho\left(\frac{T_i}{\bar{A}}\right)^{3/2}, \tag{7.66}$$

where $f_{\kappa i}$ is the flux limiting factor; regularly, $f_{\kappa i} = 0.5$ is assumed. Accordingly, the coefficient of the ion heat conduction corrected for the flux limit is given by

$$\hat{\kappa}_i = \min\left\{\kappa_i;\ \frac{F_{im}}{|\nabla T_i|}\right\}. \tag{7.67}$$

The transverse (with respect to the magnetic field) ion heat conduction coefficient is taken from Ref. [2]:

$$\kappa_i = \frac{n_i T_i}{m_i(\nu_{ii}+\nu_{ia})}\ \frac{2x_{ii}^2+2.645}{x_{ii}^4+2.70x_{ii}^2+0.677} \stackrel{\text{D}}{=} 93.89\left(\frac{S_{mol}Z^2}{A_{mol}\sqrt{\bar{A}}}\right)\frac{\rho T_i}{\nu_{ii}+\nu_{ia}}\ \frac{2x_{ii}^2+2.645}{x_{ii}^4+2.70x_{ii}^2+0.677}, \tag{7.68}$$

where

$$x_{ii} = \frac{eBy_*}{m_i c(\nu_{ii}+\nu_{ia})} \stackrel{\text{D}}{=} 964.9\ \frac{By_*}{\bar{A}(\nu_{ii}+\nu_{ia})}. \tag{7.69}$$

To the ion-ion collision frequency

$$\nu_{ii} = \frac{4\sqrt{\pi}}{3}\ \frac{e^4 n_i L_{ii}}{m_i^{1/2}T_i^{3/2}} \times \begin{cases} y, & y<1, \\ y^4, & y\geq 1, \end{cases} \stackrel{\text{D}}{=} 9166.0\ \frac{\rho\,(Z^2)_{mol}\,L_{ii}}{Z^2 A_{mol}\sqrt{\bar{A}}T_i^{3/2}} \times \begin{cases} y, & y<1, \\ y^4, & y\geq 1, \end{cases} \tag{7.70}$$

we add the ion-atom collision frequency

$$\begin{aligned}\nu_{ia} = \sigma_{ia} n_a \left(\frac{T_i}{m_i}\right)^{1/2} = \sigma_{ia}\frac{\rho}{m_i}\left(\frac{T_i}{m_i}\right)^{1/2} \times \begin{cases} (1-y), & y<1, \\ 0, & y\geq 1, \end{cases} \stackrel{\text{D}}{=} \\ \stackrel{\text{D}}{=} 1.871\times 10^7\ \frac{\rho T_i^{1/2}}{\bar{A}^{3/2}} \times \begin{cases} (1-y), & y<1, \\ 0, & y\geq 1, \end{cases}\end{aligned} \tag{7.71}$$

evaluated for the ion-atom scattering cross-section $\sigma_{ia} = 10^{-16}$ cm^2.

The two ion viscosity coefficients, η_0^i and η_1^i, that we need in our case are taken from Ref. [2]:

$$\eta_0^i = \frac{0.96 n_i T_i}{\nu_{ii}+\nu_{ia}} \stackrel{\text{D}}{=} 9.263\frac{\rho T_i}{\bar{A}(\nu_{ii}+\nu_{ia})}, \tag{7.72}$$

$$\begin{aligned}\eta_1^i = \frac{n_i T_i}{\nu_{ii}+\nu ia}\ \frac{1.2(2x_{ii})^2+2.23}{(2x_{ii})^4+4.03(2x_{ii})^2+2.33} \stackrel{\text{D}}{=} \\ \stackrel{\text{D}}{=} 9.649\ \frac{\rho T_i}{\bar{A}(\nu_{ii}+\nu_{ia})}\ \frac{1.2(2x_{ii})^2+2.23}{(2x_{ii})^4+4.03(2x_{ii})^2+2.33}.\end{aligned} \tag{7.73}$$

The ion-ion Coulomb logarithm L_{ii} is calculated as

$$L_{ii} = \frac{1}{2}\ln\left(1+\Lambda_{ii}^2\right), \tag{7.74}$$

where

$$\Lambda_{ii} = \frac{\frac{3}{2}T_i D_{ei}}{e^2\left[y_*^4 + \frac{3}{4}\frac{m_e}{m_i}\left(\frac{\hbar^2 T_i}{m_e e^4}\right)\right]^{1/2}} \stackrel{\text{D}}{=} \frac{315.5 T_i}{\left[D_{ei}^{-2}(y_*^4+1.512\times 10^{-2}T_i/\bar{A})\right]^{1/2}}, \tag{7.75}$$

$$D_{ei}^{-2} \stackrel{\text{D}}{=} \frac{\rho y Z_{mol}}{Z A_{mol}\,T_F} + \left(\frac{y_*}{Z}\right)^2 \frac{\rho\,(Z^2)_{mol}}{A_{mol}\,T_i} \times \begin{cases} y, & y<1, \\ 1, & y\geq 1, \end{cases} \qquad y_* = \begin{cases} 1, & y<1, \\ y, & y\geq 1. \end{cases} \tag{7.76}$$

The functional form (7.75) has been chosen in agreement with the classical Coulomb scattering in the limit of $\Lambda_{ii} \ll 1$; the classical and quantum asymptotic formulae are matched in Eq. (7.75) by analogy with the electron-electron and electron-ion scattering [18].

4. Diffusion and relaxation of the energy of fast fusion products

In this subsection we assume that index (α) takes one of the three possible values, namely, α, $p3$, or $p14$. Each of the three sorts of fast charged fusion products is characterized by the set of constants listed in Table 7.3. Here, the principal quantity is the energy relaxation coefficient $\chi_{(\alpha)}$, defined such that $(\rho\chi_{(\alpha)})^{-1}$ is the decay time of the energy density $\mathcal{E}_{(\alpha)}$ [see Eqs. (3.9)-(3.11)]. Its value does not depend on the presence of the magnetic field and can be split into two components,

$$\chi_{(\alpha)} = \chi_{(\alpha),n} + \chi_{(\alpha),c}, \tag{7.77}$$

representing, respectively, the loss of energy by nuclear scattering and by the Coulomb stopping. The contribution of nuclear scattering is important for the 14-MeV protons only, so that $\chi_{\alpha,n} = \chi_{p3,n} = 0$ in this DEIRA version.

TABLE 7.3: Constants for fast charged fusion products (in the DEIRA units).

(α)	α	$p3$	$p14$
$Z_{(\alpha)}$	2	1	1
$A_{(\alpha)}$	4	1	1
$v_{0(\alpha)}$	130.3	240.5	530.2
$c_{(\alpha)}$	0.077	0.12	0.13
$T_{(\alpha)}$	20	60	300

The energy relaxation coefficient of the 14-MeV protons due to the nuclear scattering is given by [5]

$$\rho\chi_{p14,n} = v_{0p14} \sum_k \left\langle \frac{\Delta E}{E} \right\rangle_k \sigma_{nk}\, n_k, \tag{7.78}$$

where $v_{0p14} \overset{\text{D}}{=} 530.2$ is the birth velocity of 14-MeV protons,

$$\left\langle \frac{\Delta E}{E} \right\rangle_k = \frac{2A_k}{(1+A_k)^2} \langle 1 - \cos\theta \rangle_k \tag{7.79}$$

is the average relative energy loss of a 14-MeV proton in a single act of elastic scattering off a nucleus with atomic mass A_k, σ_{nk} is the cross-section of such scattering, θ is the scattering angle in the center-of-mass system. To within the experimental errors, one can assume isotopic invariance of all the differential cross-sections — i.e. that 14-MeV protons are scattered exactly as 14-MeV neutrons, and there is no difference between the T and ^{3}He target nuclei. Also, for deuterium, we add up the non-elastic and elastic cross-sections to

TABLE 7.4: Constants for nuclear scattering of 14-MeV protons and neutrons.

scatterer	p	D	T (^{3}He)
$\sigma_{nk,el}$ [barn]	0.69	0.61	0.98
$\sigma_{nk,tot}$ [barn]	0.69	0.80	0.98
$\langle 1-\cos\theta\rangle$	1.0	0.70	0.70
$\sigma_{nk,tot}\left\langle\frac{\Delta E}{E}\right\rangle_k$ [barn]	0.35	0.25	0.26

the total one. By using the experimental results for the total and differential cross-sections from Refs. [20–23], we arrive at the values given in Table 7.4.

From Table 7.4 one sees that, to a good accuracy, one can assume a universal value of the product $\sigma_{nk,tot}\left\langle\frac{\Delta E}{E}\right\rangle_k = 0.25$ barn for any D-T-^{3}He fuel mixture, which yields

$$\chi_{p14,n} \overset{\text{D}}{=} 0.015\,\frac{v_{0p14}}{\bar{A}} = \frac{7.95}{\bar{A}}. \tag{7.80}$$

The relaxation coefficient due to the Coulomb stopping can be calculated as [8]

$$\rho\chi_{(\alpha),c} = a_{(\alpha)} v_{0(\alpha)} \left(k_{e(\alpha)} + k_{i(\alpha)}\right), \tag{7.81}$$

where

$$a_{(\alpha)} = \frac{5}{2} - \frac{3}{2}\left[1 + \frac{2.4\times10^{-3}}{5\times10^{-4} + x_{e(\alpha)}^3} + c_{(\alpha)} x_{e(\alpha)}^3\right]^{-1} \tag{7.82}$$

is a dimensionless coefficient determined by the dependence of the friction force, acting on the decelerated particle, on the energy of this particle, and

$$x_{e(\alpha)} = \left(\frac{m_e\, v_{0(\alpha)}^2}{2T_F}\right)^{1/2} \overset{\text{D}}{=} \frac{v_{0(\alpha)}}{187.5\sqrt{T_F}}; \tag{7.83}$$

the temperature T_F is defined in Eq. (7.33). The effective "absorption coefficient" $k_{(\alpha)}$ is defined as the ratio $F_{0(\alpha)}/E_{0(\alpha)}$, where $E_{0(\alpha)} = \frac{1}{2} m_u A_{(\alpha)} v_{0(\alpha)}^2$ is the initial energy of the corresponding fast particle, and $F_{0(\alpha)}$ is the initial value of the friction force decelerating this particle. In evaluating $F_{0(\alpha)}$, we can restrict ourselves to the stopping powers by the free plasma electrons and ions only (i.e. neglect the contribution of the bound electrons) because, by the time fusion reactions become noticeable, both the fuel and the neighboring

target shells are sufficiently highly ionized. As a result, we have [8]

$$v_{0(\alpha)}\rho^{-1}k_{e(\alpha)} = \frac{4\pi\, e^4\, Z_{(\alpha)}^2}{E_{0(\alpha)}\, v_{0(\alpha)}}\, \frac{n_e}{\rho\, m_e}\, \Phi(x_{e(\alpha)})\, L_{e(\alpha)} \stackrel{\text{D}}{=}$$
$$\stackrel{\text{D}}{=} \frac{yZ_{mol}}{ZA_{mol}} \left(\frac{1746}{v_{0(\alpha)}}\right)^3 \frac{Z_{(\alpha)}^2}{A_{(\alpha)}}\, \frac{x_{e(\alpha)}^3}{x_{e(\alpha)}^3 + 1.33}\, L_{e(\alpha)}, \tag{7.84}$$

$$v_{0(\alpha)}\rho^{-1}k_{i(\alpha)} = \frac{4\pi\, e^4\, Z_{(\alpha)}^2}{E_{0(\alpha)}\, v_{0(\alpha)}}\, \frac{n_i}{\rho\, m_i}\, y^2 \left(1 + \frac{m_i}{m_{(\alpha)}}\right)^{1/2} L_{i(\alpha)} \stackrel{\text{D}}{=}$$
$$\stackrel{\text{D}}{=} \left(\frac{yZ_{mol}}{ZA_{mol}}\right)^2 \left(\frac{143}{v_{0(\alpha)}}\right)^3 \frac{Z_{(\alpha)}^2}{A_{(\alpha)}} \left(1 + \frac{\bar{A}}{A_{(\alpha)}}\right)^{1/2} L_{i(\alpha)}. \tag{7.85}$$

Here, the function $\Phi(x) = 2\pi^{-1/2}\left(\int_0^x e^{-t^2}\, dt - xe^{-x^2}\right)$ is approximated as $x^3/(x^3 + 1.33)$. For the Coulomb logarithms $L_{e(\alpha)}$ and $L_{i(\alpha)}$ we use the expressions from Ref. [4], reduced to the case of quantum scattering off the free electrons (but not the ions) and high projectile velocities $v_{0(\alpha)}$ compared to the thermal velocity $\sqrt{T_i/m_i}$ of the ions:

$$L_{e(\alpha)} = \ln\left[1 + \frac{\Lambda_{e(\alpha)}}{1 + 0.5\left(\Lambda_{e(\alpha)}\right)^{-1/2}}\right], \tag{7.86}$$

$$\Lambda_{e(\alpha)} = \frac{4T_F\, \eta_{(\alpha)}}{\hbar\omega_{pe}} \stackrel{\text{D}}{=} 139\, T_F\, \eta_{(\alpha)} \left(\frac{ZA_{mol}}{\rho y Z_{mol}}\right)^{1/2}, \tag{7.87}$$

$$L_{i(\alpha)} = \ln\left\{\frac{2m_{(\alpha)}m_i}{m_{(\alpha)} + m_i}\, \frac{v_{0(\alpha)}\sqrt{2T_F\eta_{(\alpha)}/m_e}}{\hbar\omega_{pe}\left[1 + (1.781\, yZ_{(\alpha)}e^2/\hbar v_{0(\alpha)})^2\right]^{1/2}}\right\} \stackrel{\text{D}}{=}$$
$$\stackrel{\text{D}}{=} 7.207 + \frac{1}{2}\ln\left[\left(\frac{\bar{A}}{1 + \bar{A}/A_{(\alpha)}}\right)^2 \frac{\bar{A}_e}{\rho y}\, \frac{T_F\, \eta_{(\alpha)}\, v_{0(\alpha)}^2}{1 + \left(39\, yZ_{(\alpha)}/v_{0(\alpha)}\right)^2}\right]. \tag{7.88}$$

The effects of the Fermi degeneracy of the free electrons are accounted for by using T_F instead of T_e; the function

$$\eta_{(\alpha)} = 0.353 + x_{e(\alpha)}^2\, \frac{2.34 + x_{e(\alpha)}^3}{11 + x_{e(\alpha)}^3} \tag{7.89}$$

accounts for possible "subsonic" (with respect to the electron thermal velocity) motion of the projectile at $v_{0(\alpha)} \lesssim \sqrt{T_F/m_e}$.

For alphas and 3-MeV protons, for which nuclear scattering is ignored, we can split the total energy dissipation $\chi_{(\alpha)}\mathcal{E}_{(\alpha)}$ between the electron and the ion plasma components by using a simple approximation (which introduces an error $\lesssim 20\%$)

$$\chi_{e(\alpha)} = \chi_{(\alpha)}\, f_{e(\alpha)}, \qquad \chi_{i(\alpha)} = \chi_{(\alpha)}\, [1 - f_{e(\alpha)}], \tag{7.90}$$

$$f_{e(\alpha)} = \frac{T_{(\alpha)}}{T_{(\alpha)} + T_e}, \tag{7.91}$$

with the values of $T_{(\alpha)}$ from Table 7.3. For the 14-MeV protons, we adopt the following

two-term approximation

$$\chi_{ep14} = \chi_{p14,n} f_{ep14,n} + \chi_{p14,c} \frac{T_{p14}}{T_{p14} + T_e}, \tag{7.92}$$

$$\chi_{ip14} = \chi_{p14,n}(1 - f_{ep14,n}) + \chi_{p14,c} \left(1 - \frac{T_{p14}}{T_{p14} + T_e}\right), \tag{7.93}$$

where $T_{p14} = 300$ keV, and $f_{ep14,n}$ is equal to the corresponding coefficient for the 14-MeV neutrons given by Eq. (6.27), i.e.

$$f_{ep14,n} \stackrel{\text{D}}{=} \left[1 + (1 + \bar{A})^2 T_e/750\right]^{-1}. \tag{7.94}$$

The diffusion coefficient $d_{(\alpha)}$ is affected (reduced) by the magnetic field. For the Coulomb stopping, Liberman and Velikovich [7] have found that in the important particular case of $F_{(\alpha)} \propto E_{(\alpha)}^{1/2}$ one has

$$d_{(\alpha)} = \frac{v_{0(\alpha)}^2}{9\,\rho\,\chi_{(\alpha)} + 4\Omega_{(\alpha)}^2/(\rho\,\chi_{(\alpha)})}, \tag{7.95}$$

where

$$\Omega_{(\alpha)} = \frac{eZ_{(\alpha)}B}{m_{(\alpha)}c} \stackrel{\text{D}}{=} 964.9 \frac{Z_{(\alpha)}B}{A_{(\alpha)}}. \tag{7.96}$$

Since without magnetic field, when $\Omega_{(\alpha)} = 0$, a more accurate formula for the general case of $-1 < \partial \ln F_{(\alpha)}/\partial \ln E_{(\alpha)} < \frac{1}{2}$ will be [8]

$$d_{(\alpha)}|_{B=0} = \frac{v_{0(\alpha)}^2}{8\,\rho\,\chi_{(\alpha)}}, \tag{7.97}$$

we adopt the following expression for the diffusion coefficient $d_{(\alpha)}$ of alphas and 3-MeV protons:

$$d_{(\alpha)} = \frac{v_{0(\alpha)}^2}{8\,\rho\,\chi_{(\alpha)} + 4\Omega_{(\alpha)}^2/(\rho\,\chi_{(\alpha)})}. \tag{7.98}$$

For the 14-MeV protons, for which nuclear scattering is also important, a more accurate formula will be

$$d_{p14} = \frac{v_{0p14}^2}{10\,\rho\,\chi_{p14,n} + 8\,\rho\,\chi_{p14,c} + 4\Omega_{p14}^2/[\rho(\chi_{p14,n} + \chi_{p14,c})]}. \tag{7.99}$$

8. FINITE DIFFERENCE SCHEME

1. Finite difference equations

We distinguish between the integer and half-integer numerical grid nodes. Integer nodes correspond to fixed values of the variable $m = m_j$, $j = 1, \ldots, N+1$ and discrete times $t = t_k$, $k = 1, 2, \ldots$. Half-integer nodes correspond to $m = m_j + \frac{1}{2}\Delta m_j$, $t = t_k + \frac{1}{2}\Delta t_k$. The values of m, r, u, κ_e^*, κ_r^*, $\hat{\kappa}_e^*$, $\hat{\kappa}_r^*$, F_{em}^*, F_{rm}^* are assigned to integer nodes, the values of all the remaining variables — to half-integer nodes. Below, the indices j and k are omitted; the system of notation is illustrated in Fig. 8.1.

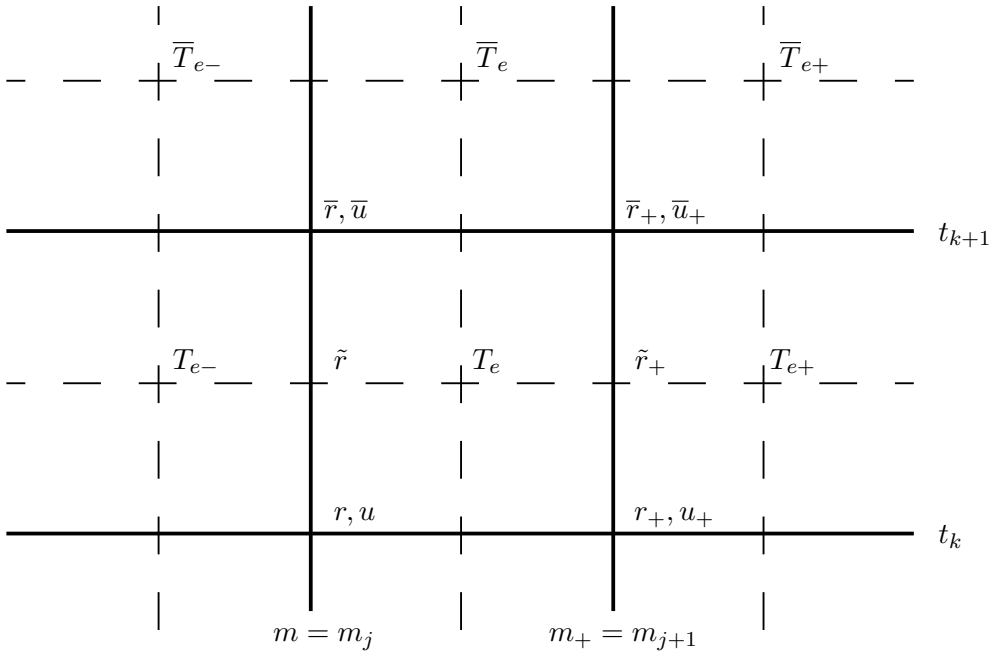

$$\Delta m = m_+ - m, \qquad \Delta t = t_{k+1} - t_k$$

FIG. 8.1: Numerical grid.

The finite difference scheme that we adopt for Eqs. (3.22)–(3.34) is as follows:

$$\frac{\overline{r} - r}{\Delta t} = \frac{1}{2}(u + \overline{u}), \tag{8.1}$$

$$\frac{\overline{u} - u}{\Delta t} + 2\,\tilde{r}^s\,\frac{P - P_-}{\Delta m + \Delta m_-} = \frac{2}{\tilde{r}}\,\frac{\eta_{ten}\Sigma - \eta_{ten-}\Sigma_-}{\Delta m + \Delta m_-}, \tag{8.2}$$

$$\epsilon_{eT}\,\frac{\overline{T}_e - T_e}{\Delta t} = \frac{1}{\Delta m}\left[\overline{r}^s\,\frac{2\hat{\kappa}^*_e}{\overline{r}_+ - \overline{r}_-}\,(\overline{T}_{e-} - \overline{T}_e) - \overline{r}^s_+\,\frac{2\,\hat{\kappa}^*_{e+}}{\overline{r}_{+2} - \overline{r}}\,(\overline{T}_e - \overline{T}_{e+})\right] - \\ -\chi_{ei}\,(\overline{T}_e - \overline{T}_i) - \chi_{er}\,(\overline{T}_e - \overline{T}_r) + Q_e, \tag{8.3}$$

$$\epsilon_{iT}\,\frac{\overline{T}_i - T_i}{\Delta t} = \frac{1}{\Delta m}\left[\overline{r}^s\,\frac{2\hat{\kappa}^*_i}{\overline{r}_+ - \overline{r}_-}\,(\overline{T}_{i-} - \overline{T}_i) - \overline{r}^s_+\,\frac{2\,\hat{\kappa}^*_{i+}}{\overline{r}_{+2} - \overline{r}}\,(\overline{T}_i - \overline{T}_{i+})\right] + \\ +\chi_{ei}\,(\overline{T}_e - \overline{T}_i) + Q_i, \tag{8.4}$$

$$4\,a_{SB}\,T_r^3\,\overline{V}\,\frac{\overline{T}_r - T_r}{\Delta t} + a_{SB}\,T_r^4\,\left(\frac{\overline{V} - V}{\Delta t} + \frac{1}{3}\dot{V}\right) = \chi_{er}\,(\overline{T}_e - \overline{T}_r) + \\ +\frac{1}{\Delta m}\left[\overline{r}^s\,\frac{2\hat{\kappa}^*_r}{\overline{r}_+ - \overline{r}_-}\,(\overline{T}_{r-} - \overline{T}_r) - \overline{r}^s_+\,\frac{2\,\hat{\kappa}^*_{r+}}{\overline{r}_{+2} - \overline{r}}\,(\overline{T}_r - \overline{T}_{r+})\right], \tag{8.5}$$

$$\frac{\overline{B}\,\overline{V} - BV}{\Delta t} = \frac{1}{\Delta m}\left[\overline{r}^s\,\frac{c^2}{4\pi}\,\frac{\eta_{\perp-} + \eta_\perp}{\overline{r}_+ - \overline{r}_-}\,(\overline{B}_- - \overline{B}) - \overline{r}^s_+\,\frac{c^2}{4\pi}\,\frac{\eta_\perp + \eta_{\perp+}}{\overline{r}_{+2} - \overline{r}}\,(\overline{B} - \overline{B}_+)\right], \tag{8.6}$$

$$\frac{\overline{V}\,\overline{\mathcal{E}}_{(\alpha)} - V\mathcal{E}_{(\alpha)}}{\Delta t} + \frac{2}{3}\,\mathcal{E}_{(\alpha)}\,\dot{V} + \chi_{(\alpha)}\overline{\mathcal{E}}_{(\alpha)} = Q_{(\alpha)} + \\ + \frac{1}{\Delta m}\left[\overline{r}^{s}\,\frac{d_{(\alpha)-} + d_{(\alpha)}}{\overline{r}_{+} - \overline{r}_{-}}\,\left(\overline{\mathcal{E}}_{(\alpha)-} - \overline{\mathcal{E}}_{(\alpha)}\right) - \overline{r}^{s}_{+}\,\frac{d_{(\alpha)} + d_{(\alpha)+}}{\overline{r}_{+2} - \overline{r}}\,\left(\overline{\mathcal{E}}_{(\alpha)} - \overline{\mathcal{E}}_{(\alpha)+}\right)\right], \quad (8.7)$$

$$\frac{\overline{X}_D - X_D}{\tau} = -\overline{X}_T\,q_{DT} - 2\,X_D\,q_{DD} - \overline{X}_{He}\,q_{DHe}, \quad (8.8)$$

$$\overline{X}_T = \frac{X_T + \frac{1}{2}\,\tau\,X_D\,q_{DD}}{1 + \tau\,q_{DT}}, \quad (8.9)$$

$$\overline{X}_{He} = \frac{X_{He} + \frac{1}{2}\,\tau\,X_D\,q_{DD}}{1 + \tau\,q_{DHe}}, \quad (8.10)$$

$$\begin{cases} \overline{X}_B = \dfrac{X_B}{1 + \tau_{BH} X_H}, \;\; \overline{X}_H = \overline{X}_B + X_H - X_B, \;\; \text{when} \;\; X_B < X_H, \\ \overline{X}_H = \dfrac{X_H}{1 + \tau_{BH} X_B}, \;\; \overline{X}_B = \overline{X}_H + X_B - X_H, \;\; \text{when} \;\; X_B > X_H. \end{cases} \quad (8.11)$$

In Eq. (8.7) index (α) runs through the values α, $p3$, and $p14$. In the above equations we introduced the following quantities:

$$\tilde{r} = r + \frac{1}{2}\,u\,\Delta t, \quad (8.12)$$

$$\Delta m = m_{+} - m, \quad (8.13)$$

$$P = -\eta_{sca}\,\dot{V} + P_e + P_i + \frac{B^2}{8\pi} + \frac{1}{3}\,a_{SB}\,T_r^4 + \frac{2}{3}\,(\mathcal{E}_{\alpha} + \mathcal{E}_{p3} + \mathcal{E}_{p14}), \quad (8.14)$$

$$\dot{V} = \frac{(u_{+} + \overline{u}_{+})\,\tilde{r}^{s}_{+} - (u + \overline{u})\,\tilde{r}^{s}}{2\,\Delta m}, \quad (8.15)$$

$$\Sigma = \frac{1}{2\,\Delta m}\left[\frac{u_{+} + \overline{u}_{+}}{\tilde{r}_{+}} - \frac{u + \overline{u}}{\tilde{r}}\right], \quad (8.16)$$

$$\epsilon_{eT} \equiv \frac{\partial \epsilon_e}{\partial T_e}, \quad \epsilon_{iT} \equiv \frac{\partial \epsilon_i}{\partial T_i}, \quad \epsilon_{eV} \equiv \frac{\partial \epsilon_e}{\partial V}, \quad \epsilon_{iV} \equiv \frac{\partial \epsilon_i}{\partial V}, \quad (8.17)$$

$$Q_e = Q_B + Q_{dr} + Q_{ecl} + Q_{en} + \chi_{e\alpha}\,\overline{\mathcal{E}}_{\alpha} + \chi_{ep3}\,\overline{\mathcal{E}}_{p3} + \chi_{ep14}\,\overline{\mathcal{E}}_{p14} - (P_e + \epsilon_{eV})\,\dot{V}, \quad (8.18)$$

$$Q_i = Q_{icl} + Q_{in} + \chi_{i\alpha}\,\overline{\mathcal{E}}_{\alpha} + \chi_{ip3}\,\overline{\mathcal{E}}_{p3} + \chi_{ip14}\,\overline{\mathcal{E}}_{p14} - (P_i + \epsilon_{iV})\,\dot{V} + \\ + \eta_{sca}\,(\dot{V})^2 + \eta_{ten}\,(\Sigma)^2, \quad (8.19)$$

$$Q_B = \overline{r}^{s}\frac{1}{2}\left(\frac{c}{4\pi}\right)^2 (\eta_{\perp -} + \eta_{\perp})\left(\frac{\overline{B}_{-} - \overline{B}}{\overline{r}_{+} - \overline{r}_{-}}\right)\left(\frac{\tilde{B}_{-} - \tilde{B}}{\Delta m}\right) + \\ + \overline{r}^{s}_{+}\frac{1}{2}\left(\frac{c}{4\pi}\right)^2 (\eta_{\perp} + \eta_{\perp +})\left(\frac{\overline{B} - \overline{B}_{+}}{\overline{r}_{+2} - \overline{r}}\right)\left(\frac{\tilde{B} - \tilde{B}_{+}}{\Delta m}\right), \quad (8.20)$$

$$\tau = \Delta t\,\frac{X_D}{V\,A_{mol}}, \quad \tau_{BH} = \frac{\Delta t}{V\,A_{mol}}\,q_{BH}, \quad \tilde{B} = \frac{1}{2}(B + \overline{B}). \quad (8.21)$$

Coefficients κ^{*}_{e}, $\hat{\kappa}^{*}_{e}$, κ^{*}_{i}, $\hat{\kappa}^{*}_{i}$, κ^{*}_{r}, $\hat{\kappa}^{*}_{r}$ are defined at the integer nodes of numerical grid, i.e. at the boundaries between the grid intervals. They are evaluated according to the following

formulae:

$$\hat{\kappa}_e^* = \min\left[\kappa_e^*; \quad F_{em}^* \frac{0.5(r_+ - r_-)}{|T_e - T_{e-}|}\right], \tag{8.22}$$

$$\hat{\kappa}_i^* = \min\left[\kappa_i^*; \quad F_{im}^* \frac{0.5(r_+ - r_-)}{|T_i - T_{i-}|}\right], \tag{8.23}$$

$$\hat{\kappa}_r^* = \min\left[\kappa_r^*; \quad F_{rm}^* \frac{0.5(r_+ - r_-)}{|T_r - T_{r-}|}\right], \tag{8.24}$$

$$\kappa_e^* = 0.5\,(\kappa_{e-} + \kappa_e), \quad F_{em}^* = \begin{cases} F_{em-}, & T_{e-} \geq T_e, \\ F_{em}, & T_{e-} < T_e, \end{cases} \tag{8.25}$$

$$\kappa_i^* = 0.5\,(\kappa_{i-} + \kappa_i), \quad F_{im}^* = \begin{cases} F_{im-}, & T_{i-} \geq T_i, \\ F_{im}, & T_{i-} < T_i, \end{cases} \tag{8.26}$$

$$\kappa_r^* = 0.5\,(\kappa_{r-} + \kappa_r), \quad F_{rm}^* = \begin{cases} F_{rm-}, & T_{r-} \geq T_r, \\ F_{rm}, & T_{r-} < T_r. \end{cases} \tag{8.27}$$

The quantities F_{em}, F_{im}, and F_{rm} are defined in Eqs. (7.1), (7.66), and(7.36). The new values of the specific volume are calculated from the formula

$$\overline{V} = \frac{\left(\overline{r}_+ + \frac{1}{2}\,\overline{u}_+\,\Delta t\right)^{s+1} - \left(\overline{r} + \frac{1}{2}\,\overline{u}\,\Delta t\right)^{s+1}}{(s+1)\,\Delta m}, \tag{8.28}$$

which implies rigorous conservation of mass in each mesh interval Δm.

For the coefficients of the total viscosity η_{sca} and η_{ten}, the following expressions are used

$$\eta_{sca} = \frac{\eta_{i,sc}}{V} + \begin{cases} 0, & u_+ \geq u, \\ \dfrac{\Delta m}{V\,\langle\tilde{r}^s\rangle}\,\left[\mu_{1av,sc} u_s + \mu_{2av,sc}(u - u_+)\right], & u_+ < u, \end{cases} \tag{8.29}$$

$$\eta_{ten} = \frac{\eta_{i,tn}}{V}\langle\tilde{r}^{2s+2}\rangle + \begin{cases} 0, & u_+ \geq u, \\ \dfrac{\Delta m\,\langle\tilde{r}^{s+2}\rangle}{V}\,\left[\mu_{1av,tn} u_s + \mu_{2av,tn}(u - u_+)\right], & u_+ < u, \end{cases} \tag{8.30}$$

where

$$\langle\tilde{r}^s\rangle = (1 - \sigma_{av,sc})\,\tilde{r}^s + \sigma_{av,sc}\,\tilde{r}_+^s, \tag{8.31}$$

$$\langle\tilde{r}^{s+2}\rangle = (1 - \sigma_{av,tn})\,\tilde{r}^{s+2} + \sigma_{av,tn}\,\tilde{r}_+^{s+2}, \tag{8.32}$$

$$\langle\tilde{r}^{2s+2}\rangle = (1 - \sigma_{av,tn})\,\tilde{r}^{2s+2} + \sigma_{av,tn}\,\tilde{r}_+^{2s+2}, \tag{8.33}$$

u_s is the adiabatic sound velocity defined in Eq. (5.10). In each of the Eqs. (8.29) and (8.30), the first and the second terms on the right-hand side represent, respectively, the physical and the artificial components of the viscosity. From Eqs. (8.29)–(8.32) it is seen that the adopted version of the artificial viscosity contains six dimensionless parameters: $\mu_{1av,sc}$ is the coefficient of the linear scalar viscosity, $\mu_{2av,sc}$ the coefficient of the quadratic scalar viscosity (the Neumann-Richtmyer viscosity), $\mu_{1av,tn}$ the coefficient of the linear "tensor" viscosity, $\mu_{2av,tn}$ the coefficient of the quadratic "tensor" viscosity, and $0 < \sigma_{av,sc} \leq 1$ and

$0 \le \sigma_{av,tn} \le 1$ are two free parameters of the approximation. The choice of specific values for these 6 parameters is discussed in Ref. [3]. A recommended set of values for the "center" and "closed cavity" left boundary conditions is given in Table 8.1. In the case of the "open halfspace" left boundary, when the artificial t-viscosity is turned off, one has to assign a non-zero value of $\mu_{2av,sc}$ (say, $\mu_{2av,sc} = 2$).

TABLE 8.1: Recommended values of the 6 parameters of the artificial viscosity for `IFLBND = 0,1`.

$\mu_{1av,sc}$	$\mu_{2av,sc}$	$\sigma_{av,sc}$	$\mu_{1av,tn}$	$\mu_{2av,tn}$	$\sigma_{av,tn}$
0.1	0	1	0	2	0.1

2. Conservation laws

The finite difference equations (8.1)–(8.10) ought to be augmented by the finite difference expressions for the momentum and various energy components. Omitting for simplicity the trivial factor $K(s)$ given by Eq. (3.18), we adopt the following expressions for the electron, ion, radiative, magnetic, and fast-product components of the internal energy content in a Lagrangian mesh interval Δm (assigned to the half-integer nodes of the grid):

$$\Delta E_e = \epsilon_e \, \Delta m, \qquad \Delta E_i = \epsilon_i \, \Delta m, \qquad \Delta E_r = a_{SB} T_r^4 V \, \Delta m,$$
$$\Delta E_B = \frac{1}{8\pi} B^2 V \, \Delta m, \qquad \Delta E_{(\alpha)} = \mathcal{E}_{(\alpha)} V \, \Delta m. \tag{8.34}$$

The momentum and the kinetic energy are naturally assigned to the integer rather than half-integer grid nodes — together with the velocities u. In doing so, we assume, in compliance with Eq. (8.2), that each integer node has a mass equal to the arithmetic mean of the masses of the two adjacent mesh intervals. The momentum and the kinetic energy of a mass interval Δm (assigned to half-integer nodes) is defined as the arithmetic mean of the momenta and kinetic energies of the corresponding left and right integer nodes:

$$\Delta p \;=\; \begin{cases} \dfrac{1}{2}\Delta m_1 \, u_1 + \dfrac{1}{4}(\Delta m_1 + \Delta m_2) u_2, & j = 1, \\ \dfrac{1}{4}\left[(\Delta m_- + \Delta m) u + (\Delta m + \Delta m_+) u_+\right], & j = 2, \ldots, N-1, \\ \dfrac{1}{4}(\Delta m_{N-1} + \Delta m_N) u_N + \dfrac{1}{2}\Delta m_N u_{N+1}, & j = N; \end{cases} \tag{8.35}$$

$$\Delta E_{kin} \;=\; \begin{cases} \dfrac{1}{4}\Delta m_1 \, u_1^2 + \dfrac{1}{8}(\Delta m_1 + \Delta m_2) u_2^2, & j = 1, \\ \dfrac{1}{8}\left[(\Delta m_- + \Delta m) u^2 + (\Delta m + \Delta m_+) u_+^2\right], & j = 2, \ldots, N-1, \\ \dfrac{1}{8}(\Delta m_{N-1} + \Delta m_N) u_N^2 + \dfrac{1}{4}\Delta m_N u_{N+1}^2, & j = N. \end{cases} \tag{8.36}$$

Next, define the momentum flux density

$$\Pi = \begin{cases} \dfrac{1}{2}(P_{bl} - P_1), & j = 1, \\ \dfrac{1}{2}\left[\tilde{r}^s(P_- - P) - \dfrac{1}{\tilde{r}}\left(\eta_{ten-}\Sigma_- - \eta_{ten}\Sigma\right)\right], & j = 2, \ldots, N, \\ \dfrac{1}{2}\left[\tilde{r}^s_{N+1}(P_N - P_{br}) - \dfrac{1}{\tilde{r}_{N+1}}\,\eta_{ten,N}\Sigma_N\right], & j = N+1, \end{cases} \tag{8.37}$$

the flux density of the internal energy (work by pressure forces)

$$\mathcal{F}_{kin} = \begin{cases} \dfrac{1}{2}(u_1 + \overline{u}_1)P_{bl}, & j = 1, \\ \dfrac{1}{4}(u + \overline{u})\left[\tilde{r}^s(P_- + P) - \dfrac{1}{\tilde{r}}(\eta_{ten-}\Sigma_- + \eta_{ten}\Sigma)\right], & j = 2, \ldots, N, \\ \dfrac{1}{2}(u_{N+1} + \overline{u}_{N+1})\tilde{r}^s_{N+1}P_{br}, & j = N+1, \end{cases} \tag{8.38}$$

the electron, ion, and radiation heat flux densities

$$\mathcal{F}_e = \begin{cases} 0, & j = 1, \\ \overline{r}^s\,\dfrac{2\hat{\kappa}^*_e}{\overline{r}_+ - \overline{r}_-}\,(\overline{T}_{e-} - \overline{T}_e), & j = 2, \ldots, N, \\ 0, & j = N+1, \end{cases} \tag{8.39}$$

$$\mathcal{F}_i = \begin{cases} 0, & j = 1, \\ \overline{r}^s\,\dfrac{2\hat{\kappa}^*_i}{\overline{r}_+ - \overline{r}_-}\,(\overline{T}_{i-} - \overline{T}_i), & j = 2, \ldots, N, \\ 0, & j = N+1, \end{cases} \tag{8.40}$$

$$\mathcal{F}_r = \begin{cases} 0, & j = 1 \wedge \texttt{IFLBND} = \texttt{0}, \texttt{1}, \\ \dfrac{1}{4}ca_{SB}(T^4_{rlex} - T^3_{r,1}\overline{T}_{r,1}), & j = 1 \wedge \texttt{IFLBND} = -\texttt{1}, \\ \overline{r}^s\,\dfrac{2\hat{\kappa}^*_r}{\overline{r}_+ - \overline{r}_-}\,(\overline{T}_{r-} - \overline{T}_r), & j = 2, \ldots, N, \\ \dfrac{1}{4}ca_{SB}\overline{r}^s_{N+1}(T^3_{r,N}\overline{T}_{r,N} - T^4_{rex}), & j = N+1, \end{cases} \tag{8.41}$$

and the flux densities of the energy of fast fusion products

$$\mathcal{F}_{(\alpha)} = \begin{cases} 0, & j = 1 \wedge \texttt{IFLBND} = \texttt{0}, \texttt{1}, \\ -\dfrac{2d_{(\alpha),1}}{\overline{r}_2 - \overline{r}_1}\,\overline{\mathcal{E}}_{(\alpha),1}, & j = 1 \wedge \texttt{IFLBND} = -\texttt{1}, \\ \overline{r}^s\,\dfrac{d_{(\alpha)-} + d_{(\alpha)}}{\overline{r}_+ - \overline{r}_-}\,(\overline{\mathcal{E}}_{(\alpha)-} - \overline{\mathcal{E}}_{(\alpha)}), & j = 2, \ldots, N, \\ \overline{r}^s_{N+1}\,\dfrac{2d_{(\alpha),N}}{\overline{r}_{N+1} - \overline{r}_N}\,\overline{\mathcal{E}}_{(\alpha),N}, & j = N+1. \end{cases} \tag{8.42}$$

across the left boundary of the j-th mesh interval (j-th integer node of the grid). Expressions (8.38)–(8.42) for the flux densities account for the boundary conditions (4.1)–(4.15).

Having adopted the above discretized definitions of the momentum, energy, and fluxes, one readily ascertains that the numerical scheme (8.1)–(8.11) has the following conservative properties. First of all, when just the equations of hydrodynamics are considered, the numerical scheme (8.1)–(8.4), (8.28) is fully conservative provided that $\epsilon_{eT} = constant$, $\epsilon_{iT} = constant$, and $\epsilon_{eV} = \epsilon_{iV} = 0$ because the increments of the momentum Δp and of the total energy $\Delta E = \Delta E_{kin} + \Delta E_e + \Delta E_i$ in any mesh interval for any time step can be cast in the divergent form

$$\frac{\overline{\Delta p} - \Delta p}{\Delta t} = \Pi + \Pi_+, \tag{8.43}$$

$$\frac{\overline{\Delta E} - \Delta E}{\Delta t} = \mathcal{F}_{kin} - \mathcal{F}_{kin+} + \mathcal{F}_e - \mathcal{F}_{e+} + \mathcal{F}_i - \mathcal{F}_{i+} + Q_{cl} + Q_n + Q_{dr}. \tag{8.44}$$

Moreover, the total energy $\Delta E = \Delta E_{kin} + \Delta E_e + \Delta E_i + \Delta E_\alpha + \Delta E_{p3} + \Delta E_{p14}$ is still conserved when the diffusion equations (8.7) for the energy density of fast fusion products are added to the hydrodynamic equations (8.1)–(8.4) (because expressions (8.18) and (8.19) for Q_e and Q_i contain "new" values $\overline{\mathcal{E}}_\alpha$, $\overline{\mathcal{E}}_{p3}$, and $\overline{\mathcal{E}}_{p14}$). The conservation of energy is however violated by the radiation diffusion equation (8.5) because the volumetric heat capacity of radiation $4a_{SB}T_r^3$ is a strong function of temperature, and is taken from the previous time step.

A special attention should be paid to the magnetic energy ΔE_B. From Eq. (3.27) one derives the following equation for the specific (per unit mass) density $B^2V/8\pi$ of the magnetic energy:

$$\frac{\partial}{\partial t}\left(\frac{B^2V}{8\pi}\right) + \frac{B^2}{8\pi}\frac{\partial V}{\partial t} = \frac{\partial}{\partial m}\left[\left(\frac{c}{4\pi}\right)^2 r^s \eta_\perp B \frac{\partial B}{\partial r}\right] - \left(\frac{c}{4\pi}\right)^2 \eta_\perp V \left(\frac{\partial B}{\partial r}\right)^2. \tag{8.45}$$

The second term on the right-hand side of Eq. (8.45) is the Joule heating. For our numerical scheme to be conservative with respect to the magnetic energy ΔE_B, the discretized form of Eq. (8.45) should look like

$$\frac{1}{8\pi}\frac{\overline{B}^2\overline{V} - B^2V}{\Delta t} + \frac{B^2}{8\pi}\dot{V} = \frac{1}{\Delta m}\left(\mathcal{F}_B - \mathcal{F}_{B+}\right) - Q_B, \tag{8.46}$$

where $\mathcal{F}_B$ and Q_B are the finite-difference approximations of the diffusion flux and the Joule heating,

$$\mathcal{F}_B \approx \left(\frac{c}{4\pi}\right)^2 r^s \eta_\perp B \frac{\partial B}{\partial r}, \qquad Q_B \approx \left(\frac{c}{4\pi}\right)^2 \eta_\perp V \left(\frac{\partial B}{\partial r}\right)^2. \tag{8.47}$$

When we multiply Eq. (8.6) by

$$\frac{1}{4\pi}\tilde{B} \equiv \frac{1}{8\pi}(B + \overline{B}) \tag{8.48}$$

we obtain

$$\frac{1}{8\pi}\frac{\overline{B}^2\overline{V} - B^2V}{\Delta t} + \left(\frac{B\overline{B}}{8\pi}\right)\frac{\overline{V} - V}{\Delta t} = \frac{1}{\Delta m}\left(\frac{c}{4\pi}\right)^2 \left[\overline{r}^s \frac{\eta_{\perp-} + \eta_\perp}{\overline{r}_+ - \overline{r}_-}\left(\overline{B}_- - \overline{B}\right)\tilde{B} - \right.$$
$$\left. - \overline{r}_+^s \frac{\eta_\perp + \eta_{\perp+}}{\overline{r}_{+2} - \overline{r}}\left(\overline{B} - \overline{B}_+\right)\tilde{B}\right]. \tag{8.49}$$

Although the term $\left(\frac{B\overline{B}}{8\pi}\right)\frac{\overline{V}-V}{\Delta t}$ is not exactly $\frac{B^2}{8\pi}\dot{V}$, it approaches $\frac{B^2}{8\pi}\dot{V}$ in the limit of $\Delta t \to 0$ (or at $u \to 0, \overline{u} \to 0$). Finally, we can rewrite Eq. (8.49) in the form

$$\frac{1}{8\pi}\frac{\overline{B}^2\overline{V}-B^2V}{\Delta t}+\left(\frac{B\overline{B}}{8\pi}\right)\frac{\overline{V}-V}{\Delta t}=\frac{1}{\Delta m}\left(\frac{c}{4\pi}\right)^2\left[\overline{r}^s\frac{\eta_{\perp-}+\eta_\perp}{\overline{r}_+-\overline{r}_-}\frac{\tilde{B}_-+\tilde{B}}{2}(\overline{B}_--\overline{B})-\right.$$
$$\left.-\overline{r}_+^s\frac{\eta_\perp+\eta_{\perp+}}{\overline{r}_{+2}-\overline{r}}\frac{\tilde{B}+\tilde{B}_+}{2}(\overline{B}-\overline{B}_+)\right]-\left(\frac{c}{4\pi}\right)^2\frac{1}{2\Delta m}\times$$
$$\times\left[\overline{r}^s\frac{\eta_{\perp-}+\eta_\perp}{\overline{r}_+-\overline{r}_-}(\overline{B}-\overline{B}_-)(\tilde{B}-\tilde{B}_-)+\overline{r}_+^s\frac{\eta_\perp+\eta_{\perp+}}{\overline{r}_{+2}-\overline{r}}(\overline{B}_+-\overline{B})(\tilde{B}_+-\tilde{B})\right], \quad (8.50)$$

which leads us to the expression (8.20) for the Joule heating Q_B and the following expression for the flux density $\mathcal{F}_B$ of the magnetic energy,

$$\mathcal{F}_B=\frac{1}{2}\left(\frac{c}{4\pi}\right)^2\overline{r}^s(\eta_{\perp-}+\eta_\perp)(\tilde{B}_-+\tilde{B})\frac{\overline{B}_--\overline{B}}{\overline{r}_+-\overline{r}_-}. \quad (8.51)$$

The finite difference approximation to the artificial viscosity is constructed in such a way that the viscous dissipation of the kinetic energy is strictly non-negative and heats up only the ion plasma component [see Eq. (8.19)]. However, the increment of the specific entropy may, strictly speaking, sometimes be negative because Eqs. (8.3) and (8.4) are written for the internal energy rather than the specific entropy and contain the "old" value of pressure P. The entropy disbalance decreases in direct proportion with the value of the time step Δt. Note also that, since the equation of motion (8.2) contains the "old" pressure P, our numerical scheme is an explicit one and is subject to the Courant restriction on the values of the time step Δt.

All the relaxation and diffusion terms in Eqs. (8.3)–(8.7) use the "new" values of of the corresponding principal variables $\overline{T}_e, \ldots, \overline{\mathcal{E}}_\alpha, \ldots$. This removes the problem of numerical stability with respect to these processes but does not imply that these processes do not impose any additional restrictions on the values of Δt: such restrictions may be dictated by strong dependence of the corresponding diffusion and relaxation coefficients on dynamic variables when the values of the coefficients are taken from the previous time step.

The numerical scheme for the equations of nuclear kinetics (8.8)–(8.10) is chosen in such a form that it admits large relative changes in the concentrations of tritium, X_T, and helium-3, X_{He}, (but not in the concentration of deuterium X_D) in one time step. The initial values of X_T and X_{He} can be arbitrarily small, while the initial value of X_D should always be on the order of unity.

9. NUMERICAL ALGORITHM

Once the "old" values r, u, T_e, ... of all the principal variables are known, the thermodynamic functions and the kinetic coefficients have been calculated, and the value of the next time step Δt is specified, one can solve the finite difference equations (8.1)–(8.10) to calculate the "new" values of the principal dependent variables $\overline{r}$, $\overline{u}$, $\overline{T}_e$, ... This step is realized in the `subroutine UPSLOI`, and the scheme of solution of Eqs. (8.1)–(8.10) described below is in fact a block-scheme of this subroutine. The `subroutine UPSLOI` consists of 5 major

blocks `NEWXDT`, `NEWRU`, `NEWEAL`, `NEWHZ`, and `NEWTTT`, each of which solves a certain subgroup of equations (8.1)–(8.11).

I. Block `NEWXDT`. In this block, new concentrations $\overline{X}_T$, $\overline{X}_{He}$, $\overline{X}_D$, $\overline{X}_B$, and $\overline{X}_H$ are calculated from Eqs. (8.8)–(8.11).

II. Block `NEWRU`. In this block, equations (8.1) and (8.2) are solved and the values of $\overline{r}$, $\overline{u}$, and $\overline{V}$ are calculated. The solution is obtained through the following steps.

1. The radii at half-step $\tilde{r}$ are calculated from Eq. (8.12) .
2. The values of $\overline{u}$ are calculated by solving the system of linear equations (8.2). The scheme of solution is as follows. First of all, we introduce a representation

$$\overline{u} = A\,\overline{u}_+ + B, \tag{9.1}$$

where A and B (not to be mixed up with the magnetic field strength B) are arrays of unknown coefficients. Since the general form of Eq. (8.2) is

$$\alpha\overline{u}_- + \beta\overline{u} + \gamma\overline{u}_+ + \delta = 0, \tag{9.2}$$

where α, β, γ, and δ are known, we substitute into it the expression $\overline{u}_- = A_-\,\overline{u} + B_-$ and obtain the following recurrent formulae for calculating the arrays A and B:

$$A = \mathcal{T}\left[\eta_s\tilde{r}_+^s + \eta_t\left(\frac{\tilde{r}_+}{\tilde{r}}\right)^{s+1}\right]/\Omega, \tag{9.3}$$

$$B = \Big\{u + \mathcal{T}\Big[2(P_{nv-} - P_{nv}) + \eta_s(u_+\tilde{r}_+^s - u\tilde{r}^s) - \eta_{s-}(u\tilde{r}^s - u_-\tilde{r}_-^s - B_-\tilde{r}_-^s) + \\ + \eta_t\left(\frac{\tilde{r}_+}{\tilde{r}}\right)^{s+2}\left(u_+\frac{\tilde{r}}{\tilde{r}_+} - u\right) - \eta_{t-}\left(u - (u_- + B_-)\frac{\tilde{r}}{\tilde{r}_-}\right)\Big]\Big\}/\Omega, \tag{9.4}$$

$$\Omega = 1 + \mathcal{T}\left[\eta_s\tilde{r}^s + \eta_{s-}(\tilde{r}^s - A_-\tilde{r}_-^s) + \eta_t\left(\frac{\tilde{r}_+}{\tilde{r}}\right)^{s+2} + \eta_{t-}\left(1 - A_-\frac{\tilde{r}}{\tilde{r}_-}\right)\right], \tag{9.5}$$

where

$$\eta_s = \frac{\eta_{sca}}{\Delta m}, \qquad \eta_t = \frac{\eta_{ten}}{\Delta m\,\tilde{r}_+^{s+2}}, \tag{9.6}$$

$$\mathcal{T} = \frac{\Delta t}{\Delta m + \Delta m_-}\,\tilde{r}^s, \tag{9.7}$$

$$P_{nv} = P_e + P_i + \frac{B^2}{8\pi} + \frac{1}{3}a_{SB}T_r^4 + \frac{2}{3}(\mathcal{E}_\alpha + \mathcal{E}_{p3} + \mathcal{E}_{p14}). \tag{9.8}$$

The boundary conditions are fulfilled as follows.

Left boundary, $j = 1$:

a) "center", `IFLBND=0`:

$$A_1 = B_1 = 0; \tag{9.9}$$

for $j = 2$ in this case we set $A_-/\tilde{r}_- = 0$ and $(u_- + B_-)/\tilde{r}_- = 0$;

b) "closed cavity", `IFLBND=1`:

$$\begin{aligned} &\Delta m_- = 0, \quad \eta_{sca-} = \eta_{ten-} = 0, \\ &P_{nv-} = P_{bl}(t+\frac{1}{2}\Delta t) + \frac{B_1^2}{8\pi} + \frac{1}{3}a_{SB}T_{r,1}^4 + \frac{2}{3}(\mathcal{E}_{\alpha,1} + \mathcal{E}_{p3,1} + \mathcal{E}_{p14,1}); \end{aligned} \tag{9.10}$$

here B_1, $T_{r,1}$, $\mathcal{E}_{\alpha,1}$, $\mathcal{E}_{p3,1}$, $\mathcal{E}_{p14,1}$ are the values of corresponding quantities in the first (from the left) mesh cell, i.e. at $j = 1$;

c) "open halfspace", `IFLBND=-1`:

$$\begin{aligned} &\Delta m_- = 0, \quad \eta_{sca-} = \eta_{ten-} = 0, \\ &P_{nv-} = P_{bl}(t+\frac{1}{2}\Delta t) + \frac{1}{8\pi}B_{bl}^2\left(t+\frac{1}{2}\Delta t\right) + \frac{1}{3}a_{SB}T_{rlex}^4(t+\frac{1}{2}\Delta t). \end{aligned} \tag{9.11}$$

Right boundary, $j = N + 1$:

$$\begin{aligned} &\Delta m = 0, \quad \eta_{sca} = \eta_{ten} = 0, \\ &P_{nv} = P_{br}(t+\frac{1}{2}\Delta t) + \frac{1}{8\pi}B_{br}^2\left(t+\frac{1}{2}\Delta t\right) + \frac{1}{3}a_{SB}T_{rex}^4(t+\frac{1}{2}\Delta t); \end{aligned} \tag{9.12}$$

in particular, this implies $A_{N+1} = 0$, $\overline{u}_{N+1} = B_{N+1}$. Once the coefficients $A \equiv A_j$, $B \equiv B_j$ are calculated for $j = 1, 2, \ldots, N+1$, the values of $\overline{u} \equiv \overline{u}_j$ are obtained through a recursive run in the opposite direction from Eq. (9.1).

In the process of solving for $\overline{u}$, the values of $\dot{V}$ and of the viscous heating $\eta_{sca}(\dot{V})^2 + \eta_{ten}(\Sigma)^2$ are calculated as well; the latter is added to the ion heating Q_i, while the values of $\dot{V}$ are memorized to be used when solving Eqs. (8.3)–(8.7).

3. The new radii are found from

$$\overline{r} = \tilde{r} + \frac{1}{2}\,\overline{u}\,\Delta t, \tag{9.13}$$

while the new values of the specific volume $\overline{V}$ are calculated from Eq. (8.28); the old values V are being kept until the exit from `subroutine UPSLOI`.

If initially the "closed cavity" boundary condition is chosen, the central void cavity may close in the process of implosion, i.e. the inner (left) radius r_1 of the target — which initially must of course be positive — may reach the value $r_1 = 0$. We use the following criterion of void closure: the void cavity closes at a given time step if

$$\tilde{r}_1 = r_1 + \frac{1}{2}u_1\Delta t \le \frac{1}{2}r_1, \quad \text{or} \quad \overline{r}_1 = \tilde{r}_1 + \frac{1}{2}\overline{u}_1\Delta t \le 0.01\,\tilde{r}_1. \tag{9.14}$$

Once this criterion is fulfilled, the value of `IFLBND` is changed from `IFLBND=1` to `IFLBND=0`, the values of $\overline{r}_1$ and $\overline{u}_1$ are set equal to $\overline{r}_1 = \overline{u}_1 = 0$, and the amount of kinetic energy $\frac{1}{4}\Delta m_1 u_1^2$ is added to the ion component of the internal energy by assigning

$$Q_{i,1} = Q_{i,1} + \frac{1}{4}u_1^2/\Delta t. \tag{9.15}$$

III. Block `NEWEAL`. In this block the linear equations (8.7) for the energy density $\overline{\mathcal{E}}_{(\alpha)}$ of fast fusion products are solved. Each of the three diffusion equations is solved independently from the other two according to the following scheme. First of all, we note that the necessary boundary conditions (see section 4) will be fulfilled after we rewrite Eq. (8.7) as

$$\begin{aligned}
&\overline{V}\,\overline{\mathcal{E}}_{(\alpha)} - V\mathcal{E}_{(\alpha)} + \frac{2}{3}\,\Delta t\,\dot{V}\,\mathcal{E}_{(\alpha)} + \Delta t\,\chi_{(\alpha)}\overline{\mathcal{E}}_{(\alpha)} = \\
&\quad = \Delta t\,Q_{(\alpha)} + \frac{\Delta t}{\Delta m}\left\{\begin{array}{ll} 0, & j=1\wedge \texttt{IFLBND}=0,1,\\ -\dfrac{2d_{(\alpha)}}{\overline{r}_+-\overline{r}}\,\overline{\mathcal{E}}_{(\alpha)}, & j=1\wedge \texttt{IFLBND}=-1,\\ \overline{r}^s\,\dfrac{d_{(\alpha)-}+d_{(\alpha)}}{\overline{r}_+-\overline{r}_-}\,\left(\overline{\mathcal{E}}_{(\alpha)-}-\overline{\mathcal{E}}_{(\alpha)}\right), & j>1,\end{array}\right\} - \\
&\qquad - \frac{\Delta t}{\Delta m}\left\{\begin{array}{ll} \overline{r}^s_+\dfrac{d_{(\alpha)}+d_{(\alpha)+}}{\overline{r}_{+2}-\overline{r}}\,\left(\overline{\mathcal{E}}_{(\alpha)}-\overline{\mathcal{E}}_{(\alpha)+}\right), & j<N,\\ \overline{r}^s_+\dfrac{2d_{(\alpha)}}{\overline{r}_+-\overline{r}}\,\overline{\mathcal{E}}_{(\alpha)}, & j=N.\end{array}\right\}
\end{aligned} \tag{9.16}$$

Once we introduce a representation

$$\overline{\mathcal{E}}_{(\alpha)} = A_{(\alpha)}\overline{\mathcal{E}}_{(\alpha)+} + B_{(\alpha)}, \tag{9.17}$$

the coefficients $A_{(\alpha)}$ and $B_{(\alpha)}$ can be calculated from the following recurrent formulae

$$A_{(\alpha)} = \frac{F_{(\alpha)+}}{\Delta m\,\Omega_{(\alpha)}}, \tag{9.18}$$

$$B_{(\alpha)} = \frac{1}{\Omega_{(\alpha)}}\left[V\mathcal{E}_{(\alpha)} + \Delta t\left(Q_{(\alpha)} - \frac{2}{3}\mathcal{E}_{(\alpha)}\dot{V}\right) + \left\{\begin{array}{ll} 0, & j=1,\\ \dfrac{F_{(\alpha)}B_{(\alpha)-}}{\Delta m}, & j>1,\end{array}\right\}\right], \tag{9.19}$$

$$\begin{aligned}
\Omega_{(\alpha)} = \overline{V} + \Delta t\,\chi_{(\alpha)} &+ \left\{\begin{array}{ll} 0, & j=1\wedge \texttt{IFLBND}=0,1,\\ \dfrac{\Delta t}{\Delta m}\,\dfrac{2d_{(\alpha)}}{\overline{r}_+-\overline{r}}, & j=1\wedge \texttt{IFLBND}=-1,\\ \dfrac{F_{(\alpha)}(1-A_{(\alpha)-})}{\Delta m}, & j>1,\end{array}\right\} + \\
&+ \left\{\begin{array}{ll} \dfrac{F_{(\alpha)+}}{\Delta m}, & j<N,\\ \dfrac{\Delta t}{\Delta m}\,\overline{r}^s_+\,\dfrac{2d_{(\alpha)}}{\overline{r}_+-\overline{r}}, & j=N,\end{array}\right\}
\end{aligned} \tag{9.20}$$

$$F_{(\alpha)} = \overline{r}^s\,\frac{\Delta t}{\overline{r}_+-\overline{r}_-}\,(d_{(\alpha)-}+d_{(\alpha)}). \tag{9.21}$$

Having calculated the values of $A_{(\alpha)}$ and $B_{(\alpha)}$, one obtains $\overline{\mathcal{E}}_{(\alpha)}$ from Eq. (9.17). The boundary conditions are satisfied by setting either $\overline{\mathcal{E}}_{(\alpha),N+1}=0$ or $F_{(\alpha),N+1}=0$.

After the values of $\overline{\mathcal{E}}_{(\alpha)}$ have been found, the energy dissipation rates $\chi_{e(\alpha)}\overline{\mathcal{E}}_{(\alpha)}$ and $\chi_{i(\alpha)}\overline{\mathcal{E}}_{(\alpha)}$ are added to the electron and ion heating rates Q_e and Q_i, respectively.

IV. Block `NEWHZ`. In this block the diffusion equation (8.6) for the magnetic field $\overline{B}$ is solved. To satisfy explicitly the boundary conditions, we rewrite it as

$$\overline{BV} - BV = \frac{\Delta t}{\Delta m}\left\{\begin{array}{ll} 0, & j=1 \wedge \texttt{IFLBND}=0,1, \\ \dfrac{c^2}{4\pi}\dfrac{2\eta_\perp}{\overline{r}_+ - \overline{r}}(\overline{B}_{bl}-\overline{B}), & j=1 \wedge \texttt{IFLBND}=-1, \\ \dfrac{c^2}{4\pi}\overline{r}^s\dfrac{\eta_{\perp -}+\eta_\perp}{\overline{r}_+ - \overline{r}_-}(\overline{B}_- - \overline{B}), & j>1, \end{array}\right\} -$$

$$-\frac{\Delta t}{\Delta m}\left\{\begin{array}{ll} \dfrac{c^2}{4\pi}\overline{r}^s_+\dfrac{\eta_\perp+\eta_{\perp +}}{\overline{r}_{+2}-\overline{r}}(\overline{B}-\overline{B}_+), & j<N, \\ \dfrac{c^2}{4\pi}\overline{r}^s_+\dfrac{2\eta_\perp}{\overline{r}_+-\overline{r}}(\overline{B}-\overline{B}_{br}), & j=N, \end{array}\right\}. \tag{9.22}$$

Once we introduce a representation

$$\overline{B} = \mathcal{A}\overline{B}_+ + \mathcal{B}, \tag{9.23}$$

the coefficients $\mathcal{A}$ and $\mathcal{B}$ can be calculated from the following recurrent formulae

$$\mathcal{A} = \left\{\begin{array}{ll} \dfrac{F_+}{\Delta m\,\Omega}, & j<N, \\ \dfrac{c^2}{4\pi}\dfrac{\Delta t}{\Delta m\,\Omega}\overline{r}^s_+\dfrac{2\eta_\perp}{\overline{r}_+-\overline{r}}, & j=N, \end{array}\right. \tag{9.24}$$

$$\mathcal{B} = \frac{1}{\Omega}\left[BV + \left\{\begin{array}{ll} 0, & j=1 \wedge \texttt{IFLBND}=0,1, \\ \dfrac{c^2}{4\pi}\dfrac{\Delta t}{\Delta m}\dfrac{2\eta_\perp}{\overline{r}_+-\overline{r}}B_{bl}, & j=1 \wedge \texttt{IFLBND}=-1, \\ \dfrac{F\mathcal{B}_-}{\Delta m}, & j>1, \end{array}\right\}\right], \tag{9.25}$$

$$\Omega = \overline{V} + \left\{\begin{array}{ll} 0, & j=1 \wedge \texttt{IFLBND}=0,1, \\ \dfrac{c^2}{4\pi}\dfrac{\Delta t}{\Delta m}\dfrac{2\eta_\perp}{\overline{r}_+-\overline{r}}, & j=1 \wedge \texttt{IFLBND}=-1, \\ \dfrac{F(1-\mathcal{A}_-)}{\Delta m}, & j>1, \end{array}\right\} +$$

$$+\left\{\begin{array}{ll} \dfrac{F_+}{\Delta m}, & j<N, \\ \dfrac{c^2}{4\pi}\dfrac{\Delta t}{\Delta m}\overline{r}^s_+\dfrac{2\eta_\perp}{\overline{r}_+-\overline{r}}, & j=N, \end{array}\right\}, \tag{9.26}$$

$$F = \frac{c^2}{4\pi}\overline{r}^s\frac{\Delta t}{\overline{r}_+-\overline{r}_-}(\eta_{\perp -}+\eta_\perp). \tag{9.27}$$

Having calculated the values of $\mathcal{A}$ and $\mathcal{B}$, one obtains $\overline{B}$ from the recurrent formula(9.23). The boundary condition at the right boundary is satisfied by setting $B_{N+1} = B_{br}$.

V. Block `NEWTTT`. In this block, three coupled systems of linear equations (8.3)–(8.5) for $\overline{T}_e$, $\overline{T}_i$, and $\overline{T}_r$ are solved. First of all, to fulfill the boundary conditions for the radiation diffusion, we rewrite Eq. (8.5) in the form

$$4\,a_{SB}\,T_r^3\,\overline{V}\,(\overline{T}_r - T_r) + a_{SB}\,T_r^4\,\left(\overline{V} - V + \frac{1}{3}\dot{V}\Delta t\right) = \chi_{er}\,(\overline{T}_e - \overline{T}_r)\Delta t + \\ + \left\{\begin{array}{ll} 0, & j = 1 \wedge \texttt{IFLBND} = 0, 1; \\ \dfrac{ca_{SB}}{4}\,\dfrac{\Delta t}{\Delta m}\,(T_{rlex}^4 - T_r^3\overline{T}_r), & j = 1 \wedge \texttt{IFLBND} = -1; \\ \overline{r}^s\,\dfrac{\Delta t}{\Delta m}\,\dfrac{2\hat{\kappa}_r^*}{(\overline{r}_+ - \overline{r}_-)}\,(\overline{T}_{r-} - \overline{T}_r), & j > 1, \end{array}\right\} - \\ - \left\{\begin{array}{ll} \overline{r}_+^s\,\dfrac{\Delta t}{\Delta m}\,\dfrac{2\hat{\kappa}_{r+}^*}{(\overline{r}_{+2} - \overline{r})}\,(\overline{T}_r - \overline{T}_{r+}), & j < N, \\ \dfrac{ca_{SB}}{4}\,\overline{r}_+^s\dfrac{\Delta t}{\Delta m}\,(T_r^3\overline{T}_r - T_{rex}^4), & j = N, \end{array}\right\}. \tag{9.28}$$

Then, we cast Eqs. (8.3), (8.4) and (9.28) in the matrix form

$$\|G\| \cdot \|\overline{T}\| = \|F_+\| \cdot \|\overline{T}_+\| + \|Q\|, \tag{9.29}$$

where

$$\|\overline{T}\| = \left\|\begin{array}{c} \overline{T}_e \\ \overline{T}_r \\ \overline{T}_i \end{array}\right\|, \qquad \|G\| = \left\|\begin{array}{ccc} G_{11} & G_{12} & G_{13} \\ G_{21} & G_{22} & G_{23} \\ G_{31} & G_{32} & G_{33} \end{array}\right\}, \\ \|Q\| = \left\|\begin{array}{c} Q_1 \\ Q_2 \\ Q_3 \end{array}\right\}, \qquad \|F_+\| = \left\|\begin{array}{ccc} F_{e+} & 0 & 0 \\ 0 & F_{r+} & 0 \\ 0 & 0 & F_{i+} \end{array}\right\}. \tag{9.30}$$

Solution to Eq. (9.29) is obtained by assuming a representation

$$\|\overline{T}\| = \|A\| \cdot \|\overline{T}_+\| + \|B\|, \tag{9.31}$$

and using the following recurrence relations

$$\|A\| = \|G\|^{-1} \cdot \|F_+\|, \qquad \|B\| = \|G\|^{-1} \cdot \|Q\|, \tag{9.32}$$

to calculate the matrices $\|A\|$ and $\|B\|$. Here

$$G_{11} = \epsilon_{eT} + \chi_{er}\,\Delta t + \chi_{ei}\,\Delta t + F_e\,(1 - A_{11-}) + F_{e+}, \tag{9.33}$$

$$G_{12} = -\chi_{er}\,\Delta t - F_e\,A_{12-}, \tag{9.34}$$

$$G_{13} = -\chi_{ei}\,\Delta t - F_e\,A_{13-}, \tag{9.35}$$

$$G_{21} = -\chi_{er}\,\Delta t - \left\{ \begin{array}{ll} 0, & j = 1, \\ F_r\,A_{21-}, & j > 1, \end{array} \right\}, \tag{9.36}$$

$$G_{22} = 4a_{SB}\,T_r^3\,\overline{V} + \chi_{er}\,\Delta t + \left\{ \begin{array}{ll} 0, & j = 1 \wedge \texttt{IFLBND} = \texttt{0}, \texttt{1}, \\ \dfrac{ca_{SB}}{4}\dfrac{\Delta t}{\Delta m}\,T_r^3, & j = 1 \wedge \texttt{IFLBND} = -\texttt{1}, \\ F_r\,(1 - A_{22-}), & j > 1, \end{array} \right\} + \\ + \left\{ \begin{array}{ll} F_{r+}, & j < N, \\ \dfrac{c\,a_{SB}}{4}\,\overline{r}_+^s\,\dfrac{\Delta t}{\Delta m}\,T_r^3, & j = N, \end{array} \right\}, \tag{9.37}$$

$$G_{23} = \left\{ \begin{array}{ll} 0, & j = 1, \\ -F_r\,A_{23-}, & j > 1, \end{array} \right\}, \tag{9.38}$$

$$G_{31} = -\chi_{ei}\,\Delta t - F_i\,A_{31-}, \tag{9.39}$$

$$G_{32} = -F_i\,A_{32-}, \tag{9.40}$$

$$G_{33} = \epsilon_{iT} + \chi_{ei}\,\Delta t + F_i(1 - A_{33-}) + F_{i+}, \tag{9.41}$$

$$Q_1 = \epsilon_{eT}\,T_e + Q_e\,\Delta t + F_e\,B_{1-}, \tag{9.42}$$

$$Q_2 = a_{SB}\,T_r^4\,(3\overline{V} + V - \frac{1}{3}\dot{V}\,\Delta t) + \left\{ \begin{array}{ll} 0, & j = 1 \wedge \texttt{IFLBND} = \texttt{0}, \texttt{1}, \\ \dfrac{ca_{SB}}{4}\dfrac{\Delta t}{\Delta m}\,T_{rlex}^4, & j = 1 \wedge \texttt{IFLBND} = -\texttt{1}, \\ F_r\,B_{2-}, & j > 1, \end{array} \right\} + \\ + \left\{ \begin{array}{ll} 0, & j < N, \\ \dfrac{c\,a_{SB}}{4}\dfrac{\Delta t}{\Delta m}\,\overline{r}_+^s\,T_{rex}^4, & j = N, \end{array} \right\}, \tag{9.43}$$

$$Q_3 = \epsilon_{iT}\,T_i + Q_i\,\Delta t + F_i\,B_{3-}, \tag{9.44}$$

$$F_e = \overline{r}^s\,\frac{\Delta t}{\overline{r}_+ - \overline{r}_-}\,\frac{2\hat{\kappa}_e^*}{\Delta m}, \qquad F_r = \overline{r}^s\,\frac{\Delta t}{\overline{r}_+ - \overline{r}_-}\,\frac{2\hat{\kappa}_r^*}{\Delta m}, \qquad F_i = \overline{r}^s\,\frac{\Delta t}{\overline{r}_+ - \overline{r}_-}\,\frac{2\hat{\kappa}_i^*}{\Delta m}. \tag{9.45}$$

In addition, we set

$$F_{e,1} = F_{i,1} = F_{e,N+1} = F_{i,N+1} = F_{r,N+1} = 0 \tag{9.46}$$

to satisfy the boundary conditions. Once the matrix arrays $\|A\|$ and $\|B\|$ are calculated

(note that at each recursive step we have to invert the matrix $\|G\|$), the arrays $\overline{T}_e$, $\overline{T}_i$, and $\overline{T}_r$ are found in a reverse recursive run from Eq. (9.31).

10. EVALUATION OF THE TIME STEP

The numerical algorithm, implemented in the DEIRA code, does not allow to return to the "old" values of the principal variables (3.20) after the "new" ones have been found if too large a time step Δt has been chosen. Hence, a special attention should be paid to the procedure of evaluation of the next value of Δt. This procedure is realized in the `subroutine TSTEP`. It implements the following constraints on the value of Δt.

1) For the explicit method (8.2) of solving the hydrodynamic equation of motion to be numerically stable, the time step Δt must be restricted by the conditions [24]

$$\Delta t \le K_h \frac{r_2 - r_1}{2\left[(P_{bl} - P_{e,1} - P_{i,1})V_1\right]^{1/2}}, \quad \text{CFL condition \#1,} \tag{10.1}$$

$$\Delta t \le K_h \frac{r_{N+1} - r_N}{2\left[(P_{br} - P_{e,N} - P_{i,N})V_N\right]^{1/2}}, \quad \text{CFL condition \#2,} \tag{10.2}$$

$$\Delta t \le K_h \min_j \left\{ \frac{r_+ - r}{u_s\left(1 + \mu_{1av,sc} + \mu_{1av,tn}\right)} \right\}, \quad \text{CFL condition \#3,} \tag{10.3}$$

$$\Delta t \le K_h \min_j \left\{ \frac{r_+ - r}{4|u_+ - u|(\mu_{2av,sc} + \mu_{2av,tn})} \right\}, \quad \text{CFL condition \#4,} \tag{10.4}$$

$$\Delta t \le K_{VT} \min_j \left\{ \frac{r_+ - r}{2|u_+ - u|} \right\}, \quad \text{CFL condition \#5,} \tag{10.5}$$

where u_s is the adiabatic sound velocity [see Eq. (5.10)], $K_h = \texttt{czdt} < 1$ is a safety factor in the Courant-Friedrichs-Lewy (CFL) condition, $K_{VT} = \texttt{czdtvt} \ll 1$ is the user-defined limit on the maximum allowed relative change of the volume and temperature (any of T_e, T_i, and T_r) in each mesh cell; typically $K_h \lesssim 0.5$, $K_{VT} \lesssim 0.05$. If `iartvis` $= 1$, the condition (10.4) is applied by compression only, i.e. only when $u > u_+$.

2) Since the energy equations (8.3), (8.4) contain the "old" values of all the heating rates and heat capacities, an additional restriction on the value of Δt is needed to avoid large errors in simulating fast thermal processes. As such, we have adopted the condition

$$\Delta t \le K_Q \min_j \left\{ \frac{\epsilon_{min} + \epsilon_{eT}\, T_e + \epsilon_{iT}\, T_i}{|Q_{ecl} + Q_{en} + Q_{dr}| + |Q_{icl} + Q_{in}| + \chi_\alpha \mathcal{E}_\alpha + \chi_{p3}\mathcal{E}_{p3} + \chi_{p14}\mathcal{E}_{p14}} \right\}, \tag{10.6}$$

where $\epsilon_{min} = \texttt{eemin}$ is a user-defined "energy sensitivity threshold", $K_Q = \texttt{czdtq} \ll 1$ is a safety coefficient, whose typical values should be $K_Q \lesssim 0.05$.

3) For fixed values of the heat capacities, diffusion and relaxation coefficients, the conditions of numerical stability of the diffusion and relaxation terms in Eqs. (8.3)–(8.7) impose no restrictions on the value of Δt. On the other hand, within the framework of our numerical scheme, strongly non-linear heat and radiation waves with steep temperature gradients can propagate no faster than one mesh interval in one time step.

Clearly, adequate simulation of such waves requires an additional restriction on possible values of Δt. We introduce the corresponding upper limit on Δt by correcting the previous value of the time step Δt_- with the condition

$$\frac{\Delta t}{\Delta t_-} \le \begin{cases} 1 + K_\Delta, & \delta < K_{VT}/(1+K_\Delta), \\ 1, & K_{VT}/(1+K_\Delta) < \delta < K_{VT}\,(1+K_\Delta) \\ \dfrac{K_{VT}}{\delta}, & K_{VT}\,(1+K_\Delta) < \delta. \end{cases} \tag{10.7}$$

Here $K_\Delta = \texttt{czddt} \ll 1$ sets an upper limit for a possible increment of Δt in a single time step (typically $\texttt{czddt} \lesssim 0.05$), $K_{VT} = \texttt{czdtvt}$ is the upper limit on possible relative changes of V, T_e, T_i, and T_r in a single time step. The quantity δ is defined as

$$\delta = \max\{\delta_V;\quad \delta_{T_e};\quad \delta_{T_i};\quad \delta_{T_r}\}, \tag{10.8}$$

$$\delta_V = \max_j \left\{ \max\left\{ \frac{\overline{V}}{V};\quad \frac{V}{\overline{V}} \right\} - 1 \right\}, \tag{10.9}$$

$$\delta_{T_e} = \max_j \left\{ \max\left\{ \frac{\max\{\overline{T}_e;\ T_{min}\} + T_{min}}{T_e + T_{min}}; \frac{T_e + T_{min}}{\max\{\overline{T}_e;\ T_{min}\} + T_{min}} \right\} - 1 \right\} \tag{10.10}$$

Maximum relative changes of the ion, δ_{T_i}, and radiation, δ_{T_r}, temperatures are defined analogously to δ_{T_e}; $T_{min} = \texttt{Tfloor} > 0$ is the user-defined "floor" value for all three temperatures. Note that condition (10.7) allows a sharp drop but only a gradual rise of the Δt value in a single time step.

It should be noted here that in some cases, where temperature jumps are present in the initial conditions, or some processes are "turned on" abruptly, the step correction procedure (10.7) cannot prevent from a few "bad" steps to be made. Hence, as an additional precaution against eventual sudden pressure jumps (like, for example, by fast local phase transitions), one more constraint

$$\Delta t \le K_h \min_j \left\{ \frac{(\Delta r/V + \Delta r_+/V_+)\min(\Delta r; \Delta r_+)}{2|p_{e+} + p_{i+} - p_e - p_i|} \right\}, \quad \text{CFL condition \#6} \tag{10.11}$$

has been added to the standard CFL conditions (10.1)–(10.5), where

$$\Delta r = r_+ - r \equiv r_{j+1} - r_j, \quad \Delta r_+ = r_{j+2} - r_{j+1}. \tag{10.12}$$

It should be mentioned also that, when certain transport coefficients become too strong functions of their arguments, our procedure of Δt evaluation may become weakly unstable. Otherwise, in most practical cases it proved to be quite adequate in keeping the discretization errors under control.

11. FLOW CHART OF SUBROUTINES IN THE DELIRA CODE

The principal flow chart of the DELIRA code is shown in Fig. 11.1. The job starts with reading out the control parameters from the `namelist/input/` by calling the `subroutine RDINPT`. In `subroutine CHECKINPT` the read out values of the input parameters are checked for consistency. The `subroutine WHEADER` writes out the header for the current job. In `subroutine MATDB` some variables with various material properties are assigned, and the required EOS and opacity tables are loaded. The `subroutine JOBINIT` constructs the mesh and loads the initial values of all the principal variables; then, the `subroutine PRINTOUT` prints out the initial target state.

The main loop over the successive hydrocycles encompasses the code block between the two black dots in Fig. 11.1. It starts by calculating all the necessary thermodynamic functions in the `subroutine UPDEOS`, which, if the phase-flip kinetics is activated, is followed by calling the `subroutine PFKIN` plus one more time the `subroutine UPDEOS`. Then, the external energy deposition Q_{dr} is calculated in the `subroutine DRIVE`. After that, the `subroutine KINBUR` calculates all the transport and relaxation coefficients, thermonuclear burn rates, and the electron $(Q_{ecl} + Q_{en})$ and the ion $(Q_{icl} + Q_{in})$ components of the local heating by the charged fusion products and by the fast neutrons.

At the next step, the conditions for job termination, printout, and the write-out into the dump file for continuation are checked; if fulfilled, the output is written out by calling the subroutines `PRINHIS`, `PRINOUT`, `PRIPR_C` (profiles of cell-centered variables), `PRIPR_V` (profiles of vertex-centered variables), and the dump is written out by calling the `subroutine RWDUMP('w')`. Then, the new value of the time step Δt is calculated in the `subroutine TSTEP`. In the `subroutine EBALNC`, the relevant increments are added to various components of the liberated thermonuclear energy, the externally deposited energy from Q_{dr}, and some other energy-balance related quantities. And, finally, the "new" values of the principal dependent variables are calculated in the `subroutine UPSLOI`. After that, the control is returned back to the entrance point of the main loop, and the whole cycle is repeated for a new time step. Note that the sequential order of the subroutine calls shown in Fig. 11.1 is essential and must not be changed.

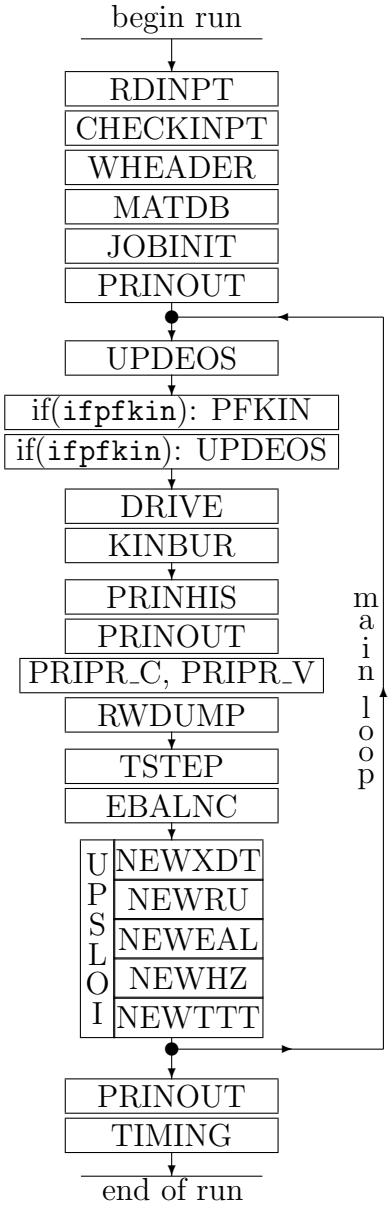

Figure 11.1

12. TEST PROBLEMS

In test simulations, the numerical results from the DEIRA code have been compared with analytic and self-similar solutions for one or several equations from the full system (3.1)–(3.14). The test problems can be grouped according to the specific physical processes under trial.

1. Hydrodynamics

A series of test problems used to verify the DELIRA (DEIRA) hydrodynamics is described in Ref. [3]. Test runs have been performed for the Guderley solution (in cylindrical and spherical geometries), for a planar piston with reflection of the shock wave from the rigid wall, for the problem of a homologous compression and expansion of a sphere. On the basis of these tests, the values of the six free parameters of the artificial viscosity have been chosen. In addition, a test run has been performed for the self-similar solution of a planar shock with heat conduction. The agreement with the exact solution was no worse than that observed earlier for the GITTAM code [25].

In all of the above tests, an infinitely fast relaxation between the electron and ion temperatures was assumed. To test the process of temperature relaxation, the following version of the planar piston problem was simulated. The equation of state is taken in the form

$$P_e = \frac{1}{2}\,\rho\, T_e, \qquad P_i = \frac{1}{2}\,\rho\, T_i, \qquad \epsilon_e = \frac{T_e}{2(\gamma-1)}, \qquad \epsilon_i = \frac{T_i}{2(\gamma-1)}, \tag{12.1}$$

a constant value of the electron-ion relaxation coefficient χ_{ei} is used, while the coefficients χ_{er}, κ_e, and κ_r are all set to be zero. The initial state of the gas with $\gamma = 5/3$ in the region $0 \le r \le R_0 = 1$ is taken as

$$\rho(0,r) = \rho_0 = 1, \qquad T_e(0,r) = T_i(0,r) = 0. \tag{12.2}$$

Starting from $t = 0$, a constant pressure P_1 is applied to the right boundary such that a strong shock propagates to the left with the speed $D = -1$. The post-shock gas parameters are given by

$$\rho_1 = \frac{\gamma+1}{\gamma-1}\,\rho_0 = 4, \qquad P_1 = \frac{2}{\gamma+1}\,\rho_0\, D^2 = \frac{3}{4}, \tag{12.3}$$

$$T_1 \equiv \frac{1}{2}\,(T_e + T_i)_1 = \frac{2(\gamma-1)}{(\gamma+1)^2}\,D^2 = \frac{3}{16}, \tag{12.4}$$

$$T_e = T_1 \left\{ 1 - \exp\left[-\frac{4(\gamma+1)}{D}\,\chi_{ei}\,(r - r_0) \right] \right\}, \tag{12.5}$$

$$T_i = T_1 \left\{ 1 + \exp\left[-\frac{4(\gamma+1)}{D}\,\chi_{ei}\,(r - r_0) \right] \right\}, \tag{12.6}$$

where $r_0 = R_0 - Dt$ is the shock position at time t. Comparison of the exact solution (12.5), (12.6) for $\chi_{ei} = 1$ with the DELIRA simulation on 40 mesh intervals at $t = 0.75$ is shown in Fig. 12.1.

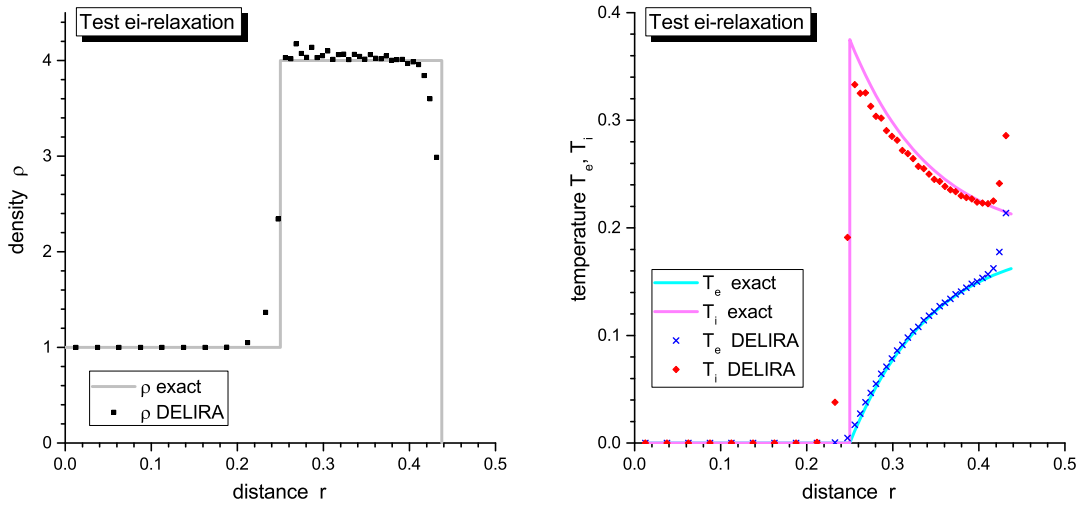

FIG. 12.1: Electron-ion temperature relaxation behind a strong-shock front.

2. Electron heat conduction and diffusion of radiation

Propagation of heat and radiation waves has been tested against motionless background by using the self-similar solution for a planar heat wave entering the half-space with a fixed temperature at the outer boundary and a power-law temperature dependence of the heat conduction coefficient. In such a case, the equation of heat conduction is

$$\rho c_V \frac{\partial T}{\partial t} = \frac{\partial}{\partial r}\left(\kappa_0 T^n \frac{\partial T}{\partial r}\right), \tag{12.7}$$

where c_V is the heat capacity per unit mass at constant volume. After introduction of the self-similar variables

$$\xi = \left(\frac{n+1}{2}\,\frac{\rho c_V}{\kappa_0 T_0^n}\right)^{1/2} \frac{r}{\sqrt{t}}, \qquad \tau = \frac{T}{T_0}, \tag{12.8}$$

Eq. (12.7) is reduced to

$$\frac{d^2\tau^{n+1}}{d\xi^2} + \xi\frac{d\tau}{d\xi} = 0. \tag{12.9}$$

This equation should be solved with the boundary conditions

$$\tau(0) = 1, \qquad \tau(\xi_0) = 0, \tag{12.10}$$

augmented by the condition for calculation of ξ_0. The latter can be obtained by integrating Eq. (12.9) and noticing that the product $\tau^n(d\tau/d\xi)$ must vanish at $\xi = \xi_0$ because the heat flux, proportional to $\tau^n(d\tau/d\xi)$, must be a continuous function of r:

$$\alpha \equiv \int_0^{\xi_0} \tau\, d\xi = -(n+1)\left.\frac{d\tau}{d\xi}\right|_{\xi=0}. \tag{12.11}$$

The constants ξ_0 and α define the penetration depth

$$r_f = \xi_0 \left[\frac{2\kappa_0 T_0^n}{(n+1)\rho c_V} t \right]^{1/2}, \tag{12.12}$$

and the energy

$$E \equiv \rho c_V \int_0^{r_f} T \, dr = \alpha T_0 \left(\frac{2\kappa_0 T_0^n \rho c_V}{n+1} t \right)^{1/2} \tag{12.13}$$

of the heat wave in the half-space. The values of these constants, calculated for certain n, are given in Table 12.1. To the accuracy of $\simeq 0.6\%$, one can make use of the approximations

$$\alpha \approx \left(\frac{n+1}{n+\pi/2} \right)^{1/2}, \quad 0 < n < \infty; \qquad \xi_0 \approx \left(1 + \frac{\pi}{2n} \right)^{1/2}, \quad 1 < n < \infty. \tag{12.14}$$

TABLE 12.1: Eigenvalues for a self-similar heat wave into a planar wall.

n	1	2	3	4	5	6	7
ξ_0	1.616121	1.335363	1.231172	1.176523	1.142817	1.119935	1.103380
α	0.887496	0.922297	0.940688	0.952049	0.959760	0.965336	0.969556

Three different types of heat waves have been tested, which are defined by the following combinations of the transport coefficients:

1) an electron conductivity wave with

$$\kappa_e = \kappa_{e0} T_e^3, \qquad \kappa_r = \chi_{er} = 0; \tag{12.15}$$

2) a radiation heat wave with

$$\kappa_e = \chi_{er} = 0, \qquad \kappa_r = \kappa_{r0} T_r^7; \tag{12.16}$$

3) an electron-radiation heat wave with

$$\kappa_e = \kappa_{e0} T_e^3, \qquad \kappa_r = 10^3 \kappa_{e0} T_r^3, \qquad \chi_{er} = \infty. \tag{12.17}$$

In practice, these tests have been run as different variants of the following planar target with the equation of state from Eq. (12.1) and $a_{SB} = 10^{-4}$:

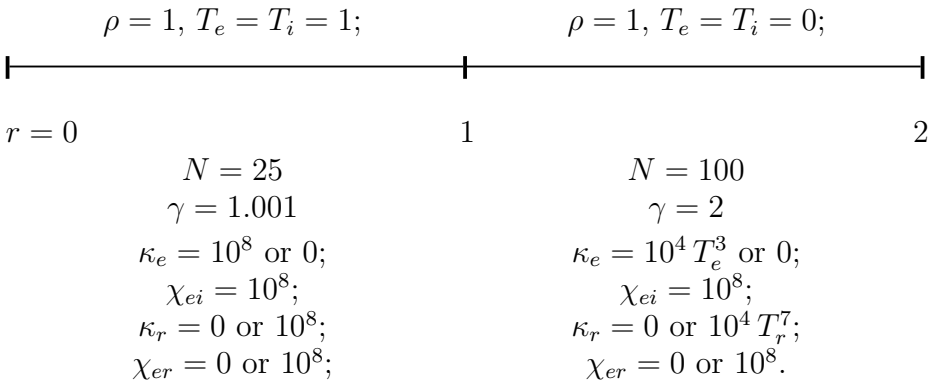

In all cases, a good agreement between the DELIRA results and the analytic solutions was observed, with the errors in the wave-front propagation $r_f(t)$ not exceeding 1–2%.

3. Diffusion of the energy of fast fusion products

The diffusion equations for the energy density of three charged species of the fast fusion products have been tested against the following three problems.

1. Non-stationary diffusion. Consider a motionless gas slab in the rerion $0 < r < 1$ with constant values of ρ, χ_α, and d_α. In the absence of the source term ($Q_\alpha = 0$), the diffusion equation (3.9) takes the form

$$\frac{\partial \mathcal{E}_\alpha}{\partial t} + \rho\chi_\alpha \mathcal{E}_\alpha = d_\alpha \frac{\partial^2 \mathcal{E}_\alpha}{\partial r^2}. \tag{12.18}$$

This equation has a partial solution

$$\mathcal{E}_\alpha = C_\alpha \exp\left[-\left(\rho\chi_\alpha + \frac{\pi^2 v_{0\alpha}^2}{32\rho\chi_\alpha}\right) t\right] \cos\left(\frac{\pi}{2} r\right), \tag{12.19}$$

which satisfies the boundary conditions (4.3) and (4.15). In Eq. (12.19), the relationship (7.98) between χ_α and d_α has been taken into account. Numerical simulations have been performed on a grid of 40 mesh zones for the ideal-gas equation of state (12.1) and the following initial state:

$$\rho(0, r) = 1, \quad T_e(0, r) = T_i(0, r) = 3 \times 10^{-7}, \quad \chi_\alpha = 1, \quad C_\alpha = 10^{-6}. \tag{12.20}$$

Under such conditions, the hydrodynamic motion can be neglected for times $t \le 1$. At $t = 1$, the values of $\mathcal{E}_\alpha(t, r)$, calculated with the DELIRA code for $v_{0\alpha} = 4\sqrt{2}/\pi$, deviate from the exact solution (12.19) by no more than 0.4%.

2. Stationary diffusion. Consider a stationary gaseous sphere of radius R with constant values of ρ, $\chi_{(\alpha)}$, and $d_{(\alpha)}$, inside which the source $Q_{(\alpha)}$ has a constant intensity. Beyond this sphere, the gas is assumed to be in the same state, but the source term vanishes, i.e. $Q_{(\alpha)} = 0$. Then, the equation of stationary diffusion

$$\frac{1}{r^2}\frac{\partial}{\partial r}\left(r^2 d_{(\alpha)} \frac{\partial \mathcal{E}_{(\alpha)}}{\partial r}\right) - \rho\chi_{(\alpha)}\mathcal{E}_{(\alpha)} + \rho Q_{(\alpha)} = 0 \tag{12.21}$$

has a solution

$$\mathcal{E}_{(\alpha)}(r) = \frac{Q_{(\alpha)}}{\chi_{(\alpha)}} \begin{cases} (1 - C\sinh\xi/\xi), & \xi < \xi_0, \\ D\exp(-\xi)/\xi, & \xi > \xi_0, \end{cases} \tag{12.22}$$

where

$$\begin{aligned} &\xi = \frac{\sqrt{8}}{v_{0(\alpha)}}\rho\chi_{(\alpha)}\, r, && \xi_0 = \frac{\sqrt{8}}{v_{0(\alpha)}}\rho\chi_{(\alpha)}\, R, \\ &C = (1 + \xi_0)\exp(-\xi_0), && D = \xi_0\cosh\xi_0 - \sinh\xi_0. \end{aligned} \tag{12.23}$$

Simulations have been performed in the region $0 \le r \le 3$ with $R = 1$ (40 mesh zones at $r \le 1$, and 60 between $1 < r \le 3$). The initial data and the values of constants have been set as follows:

$$\chi_\alpha = \frac{v_{0\alpha}}{\sqrt{8}}, \quad \chi_{p3} = \frac{v_{0p3}}{\sqrt{8}}, \quad \chi_{p14} = \frac{v_{0p14}}{\sqrt{8}}, \quad \rho(0,r) = 1,$$
$$T_e(0,r) = T_i(0,r) = 10 \text{ keV}, \quad X_D = X_T = X_{He} = \begin{cases} 1, & 0 \le r < 1, \\ 0, & 1 \le r \le 3. \end{cases} \tag{12.24}$$

The hydrodynamics and the heating and cooling of the plasma have been artificially turned off. The source terms Q_α, Q_{p3}, and Q_{p14} were calculated according to the formulae from section 6 2 (the depletion of fuel has been turned off as well); for $v_{0\alpha}$, v_{0p3}, and v_{0p14}, the values from Table 7.3 have been used. Under such conditions, a steady state is reached within $\Delta t \lesssim 0.01$. Table 12.2 compares the values of $\mathcal{E}_\alpha$, $\mathcal{E}_{p3}$, and $\mathcal{E}_{p14}$ from the DELIRA simulation with those from the analytic solution (12.22) for $t = 0.485$ at three characteristic radii.

TABLE 12.2: Stationary-diffusion test for the energy densities of fast fusion products.

	DELIRA simulation			analytic		
j	$\mathcal{E}_\alpha$	$\mathcal{E}_{p3}$	$\mathcal{E}_{p14}$	$\mathcal{E}_\alpha$	$\mathcal{E}_{p3}$	$\mathcal{E}_{p14}$
1	2.2154	2.185×10^{-3}	3.221×10^{-3}	2.2102	2.180×10^{-3}	3.213×10^{-3}
40 ($r = 1$)	1.1348	1.119×10^{-3}	1.650×10^{-3}	1.1529	1.137×10^{-3}	1.676×10^{-3}
83 ($r = 2$)	0.1819	1.793×10^{-4}	2.644×10^{-4}	0.20995	2.070×10^{-4}	3.052×10^{-4}

3. Adiabatic compression. In the limit of $\chi_\alpha = d_\alpha = 0$ and in the absence of sources ($Q_\alpha = 0$), Eq. (3.9) describes the adiabatic compression of fast fusion products with the adiabatic index $\gamma_\alpha = 5/3$. In particular, when a strong shock passes through a gas with the equation of state (12.1), the energy density of fast products should jump by a factor

$$\left(\frac{\gamma+1}{\gamma-1}\right)^{\gamma_\alpha} = 10.08 \quad \text{for } \gamma = \frac{5}{3}$$

across the shock front. A corresponding test run has been done for a planar piston problem with $\chi_\alpha = v_{0\alpha} = 10^{-7}$; the results are shown in Fig. 12.2.

FIG. 12.2: Adiabatic compression of $\mathcal{E}_\alpha$ across the shock front.

APPENDIX A: OPACITY MODEL DEIRA-3

1. General formulae

In the approximation that the radiation field locally has the Planckian spectrum $\mathcal{B}(\nu, T_r)$ with a temperature T_r in the comoving reference frame, the radiative energy transport can be described by the diffusion equation

$$\frac{\partial \mathcal{E}_r}{\partial t} + \mathbf{u}\cdot\nabla\mathcal{E}_r + \frac{4}{3}\mathcal{E}_r \mathrm{div}(\mathbf{u}) = \mathrm{div}\left(\frac{cl_R}{3}\nabla\mathcal{E}_r\right) + \\ + \int_0^\infty \tilde{k}_a(h\nu)\left[\mathcal{B}(\nu, T_e) - \mathcal{B}(\nu, T_r)\right] d\nu + \frac{4\sigma_T}{m_e c} n_e \mathcal{E}_r \cdot (T_e - T_r). \tag{A.1}$$

Here

$$\mathcal{E}_r \equiv \frac{1}{c}\int_0^\infty \mathcal{B}(\nu, T_r)\, d\nu = a_{SB} T_r^4 \tag{A.2}$$

is the energy density of radiation in the comoving frame,

$$a_{SB} = \frac{4\sigma_{SB}}{c} = \frac{\pi^2}{15\hbar^3 c^3} = 1.372 \times 10^{14} \text{ ergs cm}^{-3} \text{ keV}^{-4}, \tag{A.3}$$

σ_{SB} is the Stefan-Boltzmann constant, $\tilde{k}_a(h\nu)$ [cm^{-1}] is the absorption coefficient corrected for the stimulated emission,

$$\mathcal{B}(\nu, T_r) = \frac{8\pi h\nu^3}{c^2}\frac{1}{\exp(h\nu/T_r) - 1} \tag{A.4}$$

is 4π times the Planckian intensity. The last term on the right-hand side of Eq. (A.1) represents the Compton energy exchange between the free electrons and the radiation; $\sigma_T = 6.652 \times 10^{-25}$ cm^2 is the Thomson scattering cross-section.

The Rosseland mean free path l_R is defined as

$$l_R = l_R(\rho, T_e, T_r) = \frac{\displaystyle\int_0^\infty \frac{1}{\sigma_T n_e + \tilde{k}_a(h\nu)}\frac{\partial \mathcal{B}(\nu, T_r)}{\partial T_r}\, d\nu}{\displaystyle\int_0^\infty \frac{\partial \mathcal{B}(\nu, T_r)}{\partial T_r}\, d\nu}. \tag{A.5}$$

It can be written as

$$l_R = \int_0^\infty \frac{R(x)\, dx}{\sigma_T n_e + \tilde{k}_a(xT_r)}, \tag{A.6}$$

where

$$x = \frac{h\nu}{T_r}, \qquad R(x) = \frac{15}{4\pi^4}\frac{x^4 e^{-x}}{(1 - e^{-x})^2}. \tag{A.7}$$

When calculating l_R, it is physically reasonable to include the Compton scattering as an additive term in the opacity. In our case, l_R is treated as a function of two temperatures, T_e and T_r, whereas usually it is evaluated as a function of one temperature $T_e = T_r$ only. When just the values of $l_R(\rho, T_e)$ are available, one can take, as a first approximation, $l_R(\rho, T_e, T_r) = l_R(\rho, T_e)$ for all $T_r \neq T_e$. In the system of basic DELIRA equations, the radiative heat flux is written in the form

$$\frac{1}{3}\, c\, l_R\, \nabla \mathcal{E}_r = \frac{4}{3}\, c\, a_{SB}\, l_R\, T_r^3\, \nabla T_r; \tag{A.8}$$

accordingly, we define the coefficient of radiative heat conduction as

$$\kappa_r = \frac{4}{3}\, c\, a_{SB}\, l_R\, T_r^3. \tag{A.9}$$

Next, we define the radiation-matter temperature relaxation coefficient χ_{er} by the relationship

$$(T_e - T_r)\, \rho\, \chi_{er} = \int\limits_0^\infty \tilde{k}_a(h\nu)\, [\mathcal{B}(\nu, T_e) - \mathcal{B}(\nu, T_r)]\, d\nu + \frac{4\sigma_T}{m_e c}\, n_e \mathcal{E}_r \cdot (T_e - T_r). \tag{A.10}$$

From this we obtain

$$\chi_{er} = \chi_{er}(\rho, T_e, T_r) = \frac{4\sigma_T}{m_e c}\, \frac{n_e}{\rho}\, a_{SB}\, T_r^4 + \frac{\int\limits_0^\infty \tilde{k}_a(h\nu) \mathcal{B}(\nu, T_e)\, d\nu - \int\limits_0^\infty \tilde{k}_a(h\nu) \mathcal{B}(\nu, T_r)\, d\nu}{\rho(T_e - T_r)} =$$

$$= \frac{4\sigma_T}{m_e c}\, \frac{n_e}{\rho}\, a_{SB}\, T_r^4 + \frac{c\, a_{SB}}{\rho}\, \frac{T_e^4 \int\limits_0^\infty \tilde{k}_a(xT_e) P(x)\, dx - T_r^4 \int\limits_0^\infty \tilde{k}_a(xT_r) P(x)\, dx}{T_e - T_r}, \tag{A.11}$$

where

$$P(x) = \frac{15}{\pi^4}\, \frac{x^3 e^{-x}}{1 - e^{-x}}. \tag{A.12}$$

The Planckian mean free path l_P is defined as

$$l_P = l_P(\rho, T_e) = \frac{\int\limits_0^\infty \mathcal{B}(\nu, T_e)\, d\nu}{\int\limits_0^\infty \tilde{k}_a(h\nu) \mathcal{B}(\nu, T_e)\, d\nu} = \left[\int\limits_0^\infty \tilde{k}_a(xT_e) P(x)\, dx \right]^{-1}. \tag{A.13}$$

When one wants to evaluate $\chi_{er}(\rho, T_e, T_r)$ by simply using the known values of $l_P(\rho, T_e)$, one can, as a first approximation, take

$$\chi_{er} = \frac{4\sigma_T}{m_e c}\, \frac{n_e}{\rho}\, a_{SB}\, T_r^4 + \frac{c\, a_{SB}}{\rho}\, \frac{T_e^3}{l_P}. \tag{A.14}$$

When evaluating the absorption coefficient $\tilde{k}_a(h\nu)$, we take into account the free-free, free-bound, and bound-bound transitions:

$$\tilde{k}_a(h\nu) = \tilde{\sigma}_a(h\nu)\, \frac{\rho}{\bar{A}\, m_u} = \left[\tilde{\sigma}_{ph}(h\nu) + \frac{(Z^2)_{mol}}{Z^2 X_{mol}}\, \tilde{\sigma}_{ff}(h\nu) \right] \frac{\rho}{\bar{A} m_u}. \tag{A.15}$$

Here $\tilde{\sigma}_{ph}(h\nu)$ is the sum of the free-bound and the bound-bound absorption cross-sections, $\tilde{\sigma}_{ff}(h\nu)$ is the cross-section of the free-free absorption by one average atom (ion) — both corrected for the stimulated emission. When calculating $\tilde{\sigma}_{ff}(h\nu)$, we take into account the Fermi degeneracy of the ideal electron gas.

2. Basic formulae in the DEIRA units

In the DEIRA units ($[t] = 10^{-8}$ s, $[l] = 0.1$ cm, $[m] = 10^{-3}$ g, $[T] = 1$ keV) the basic formulae become

$$\kappa_r \;=\; 5484\, l_R\, T_r^3, \tag{A.16}$$

$$l_R \;=\; 16.6\, \frac{\bar{A}}{\rho} \int\limits_0^\infty \frac{R(x)\, dx}{\tilde{\sigma}_a(xT_r) + 0.6652\, yZ_{mol}/(ZX_{mol})}, \tag{A.17}$$

$$l_P \;=\; 16.6\, \frac{\bar{A}}{\rho} \left[\int\limits_0^\infty \tilde{\sigma}_a(xT_e) P(x)\, dx \right]^{-1}, \tag{A.18}$$

$$\chi_{er} \;=\; 1.290\, T_r^4\, \frac{yZ_{mol}}{ZA_{mol}} + \frac{4113}{16.6\, \bar{A}} \frac{T_e^4 \int\limits_0^\infty \tilde{\sigma}_a(xT_e) P(x)\, dx - T_r^4 \int\limits_0^\infty \tilde{\sigma}_a(xT_r) P(x)\, dx}{T_e - T_r}. \tag{A.19}$$

Here the total absorption cross-section $\tilde{\sigma}_a(h\nu)$ is in barns (10^{-24} cm^2); y is the degree of ionization in the average ion model.

3. General formulae for the absorption cross-section

We evaluate the absorption cross-section as

$$\tilde{\sigma}_a(h\nu) = \tilde{\sigma}_{ph}(h\nu) + \frac{(Z^2)_{mol}}{Z^2 X_{mol}}\, \tilde{\sigma}_{ff}(h\nu), \tag{A.20}$$

where $\tilde{\sigma}_{ff}(h\nu)$ is the free-free absorption cross-section by an average ion with atomic number Z, atomic mass $\bar{A}$, and ionization degree y (positive charge $+ye$).

a. Bound-bound and bound-free transitions

First of all we note that in the average ion approximation the ionization degree $0 < y < Z$ is not an integer. We define an integer i such that

$$i - 1 \le y < i; \qquad i = 1, 2, \ldots, Z. \tag{A.21}$$

We assume further that only two ion species, i and $i+1$, are present in plasma with fractional abundances $(i - y)$ and $[1 - (i - y)]$, respectively; $i = 1$ corresponds to a neutral atom, $i = Z$ — to a hydrogen-like ion. Then

$$\tilde{\sigma}_{ph}(h\nu) = (i - y)\, \tilde{\sigma}_{ph,i}(h\nu) + [1 - (i - y)]\, \tilde{\sigma}_{ph,i+1}(h\nu). \tag{A.22}$$

For the photoabsorption cross-section by ion i we adopt a simple approximation

$$\tilde{\sigma}_{ph,i}(h\nu) = a_i\, \alpha\, a_0^2 \left(\frac{e^2/a_0}{I_i} \right)^3 \times \begin{cases} \dfrac{1}{b_i} \left(\dfrac{h\nu}{I_i} \right)^2, & h\nu \le I_i, \\ \left[\left(\dfrac{h\nu}{I_i} \right)^3 + (b_i - 1) \left(\dfrac{h\nu}{I_i} \right) \right]^{-1}, & h\nu \ge I_i. \end{cases} \tag{A.23}$$

Here $\alpha = e^2/\hbar c$ is the fine-structure constant, $a_0 = \hbar^2/m_e e^2$ is the Bohr radius, I_i is the ionization potential of ion i, and a_i and b_i are dimensionless fitting constants. Note that the dependence $\tilde{\sigma}_{ph,i} \propto \nu^2$ at $h\nu < I_i$ is close to the Thomas-Fermi asymptotical behavior $\sigma_{ph} \propto \nu^{7/3}$ in the limit of low frequencies [26]. We set the value of a_i equal to

$$a_i = \begin{cases} \dfrac{8\pi Z^4}{3\sqrt{3}}, & i = Z, \quad \text{H-like ion,} \\ \dfrac{16\pi Z^4}{3\sqrt{3}}, & i \le Z-1, \quad \text{He-like and higher ions,} \end{cases} \tag{A.24}$$

to satisfy the Kramers asymptotical behavior for the photoabsorption by K-electrons in the limit of $h\nu \gg e^2 Z^2/a_0$. To determine the value of b_i, we invoke the Thomas-Reiche-Kuhn sum rule

$$\int_0^\infty \tilde{\sigma}_{ph,i}(h\nu)\, d\nu = \frac{\pi e^2}{m_e c}\,(Z+1-i). \tag{A.25}$$

This condition leads to the following equation for b_i

$$F(b_i) = \Lambda_i, \tag{A.26}$$

where

$$\Lambda_i = \frac{a_i}{6\pi^2(Z+1-i)} \left(\frac{e^2/a_0}{I_i}\right)^2, \tag{A.27}$$

and the function $F(x)$ is given by

$$F(x) = \left(\frac{1}{x} + \frac{3}{2}\,\frac{\ln x}{x-1}\right)^{-1}. \tag{A.28}$$

This function is monotonously increasing from $F(0) = 0$ to $F(\infty) = \infty$. For the H-like ions, which have $I_Z = \frac{1}{2}e^2 Z^2/a_0$, we obtain

$$\Lambda_Z = \frac{16}{9\pi\sqrt{3}} = 0.32671, \qquad b_Z = 0.7495. \tag{A.29}$$

b. Free-free transitions

The cross-section of free-free absorption in a partially degenerate plasma, as derived in Ref. [5], is given by

$$\tilde{\sigma}_{ff}(h\nu) = \frac{16\pi}{3\sqrt{3}}\,\alpha\, a_0^2\, \frac{\left(e^2/a_0\right)^2 T_e}{(h\nu)^3}\, \ln\left[\frac{1+\exp(\mu_e/T_e)}{1+\exp(\mu_e/T_e - h\nu/T_e)}\right]\, \langle y^2\rangle\, g_{ff}, \tag{A.30}$$

where μ_e is the chemical potential of the free electrons, g_{ff} is the Gaunt factor, and

$$\langle y^2\rangle = (i-y)\,(i-1)^2 + [1-(i-y)]\,i^2. \tag{A.31}$$

The chemical potential μ_e can be evaluated from the approximate formula

$$\exp\left(\frac{\mu_e}{T_e}\right) \approx \frac{1+\exp(E_F/T_e)}{1+\frac{3}{2}\sqrt{\pi}\,\left(T_e/E_F\right)^{3/2}}, \tag{A.32}$$

where

$$E_F = \frac{\hbar^2}{2m_e}\,\left(3\pi^2\,n_e\right)^{2/3} \tag{A.33}$$

is the Fermi energy of free electrons. Formula (A.32) has the correct asymptotical behavior in both the Fermi and Boltzmann limits; in the intermediate region its error does not exceed 6%. Even in the Born approximation, the Gaunt factor g_{ff} cannot be reduced to elementary functions; here we use an approximate expression from Ref. [5]

$$g_{ff} \approx \frac{\sqrt{3}}{\pi} \times \begin{cases} \ln\left[\dfrac{2\mu_e}{h\nu}\left(1+\sqrt{1-(h\nu/2\mu_e)^2}\right)\right], & h\nu < 2(\mu_e - 0.71T_e), \\ \ln\left[1+2\dfrac{0.71T_e}{h\nu}\left(1+\sqrt{1+h\nu/0.71T_e}\right)\right], & h\nu \geq 2(\mu_e - 0.71T_e). \end{cases} \tag{A.34}$$

For $\mu_e \simeq T_e \simeq h\nu$, the error of Eq. (A.34) may be as high as 20%, but in the Boltzmann limit $\exp(\mu_e/T_e) \ll 1$ this error is below 5% over the entire frequency range.

4. Absorption cross-section in the DEIRA units

Having adopted the units $[\sigma] = 10^{-24}$ cm^2 for the cross-sections, and $[\varepsilon] \equiv [h\nu] = [I_i] = 1$ keV for the photon energies and ionization potentials, we obtain

$$\tilde{\sigma}_a(\varepsilon) = \tilde{\sigma}_{ph}(\varepsilon) + \frac{(Z^2)_{mol}}{Z^2 X_{mol}}\,\tilde{\sigma}_{ff}(\varepsilon), \tag{A.35}$$

$$\tilde{\sigma}_{ph}(\varepsilon) = (i-y)\tilde{\sigma}_{ph,i}(\varepsilon) + [1-(i-y)]\tilde{\sigma}_{ph,i+1}(\varepsilon), \tag{A.36}$$

$$\tilde{\sigma}_{ph,i}(\varepsilon) = 4.1174\,\frac{a_i}{I_i^3} \times \begin{cases} \dfrac{1}{b_i}\left(\dfrac{\varepsilon}{I_i}\right)^2, & \varepsilon \leq I_i, \\ \left[\left(\dfrac{\varepsilon}{I_i}\right)^3 + (b_i-1)\dfrac{\varepsilon}{I_i}\right]^{-1}, & \varepsilon \geq I_i, \end{cases} \tag{A.37}$$

$$a_i = 4.8368\,(2-\delta_{iZ})\,Z^4, \tag{A.38}$$

$$F(b_i) = \Lambda_i = 1.2504 \times 10^{-5}\,\frac{a_i}{I_i^2(Z+1-i)}, \tag{A.39}$$

$$F(x) = \frac{x}{1+\dfrac{3}{2}\dfrac{x\ln x}{x-1}}; \tag{A.40}$$

$$\tilde{\sigma}_{ff}(\varepsilon) = 1463.7\,\frac{T_e}{\varepsilon^3}\ln\left[\frac{1+\exp(\mu_e/T_e)}{1+\exp(\mu_e/T_e)\exp(-\varepsilon/T_e)}\right]\,\langle y^2\rangle\,g_{ff}, \tag{A.41}$$

$$\langle y^2\rangle = (i-y)\,(i-1)^2 + [1-(i-y)]\,i^2, \tag{A.42}$$

$$g_{ff} = 0.55133 \times \begin{cases} \ln\left[\dfrac{2\mu_e}{\varepsilon}\left(1+\sqrt{1-(\varepsilon/2\mu_e)^2}\right)\right], & \varepsilon < 2(\mu_e - 0.71T_e), \\ \ln\left[1+2\dfrac{0.71T_e}{\varepsilon}\left(1+\sqrt{1+\varepsilon/0.71T_e}\right)\right], & \varepsilon \geq 2(\mu_e - 0.71T_e), \end{cases} \tag{A.43}$$

$$\exp\left(\frac{\mu_e}{T_e}\right) = \frac{1+\exp(E_F/T_e)}{1+634.03\dfrac{T_e^{3/2}ZA_{mol}}{\rho y Z_{mol}}}, \qquad E_F = 0.0260\,\left(\frac{\rho y Z_{mol}}{ZA_{mol}}\right)^{2/3}. \tag{A.44}$$

APPENDIX B: ARRAY `PROPMAT(I,IMAT)` FOR CONTROL OVER MATERIAL PROPERTIES

Control over various properties of each individual material `imat`, engaged in a given job, is exercised through the user-defined array `propmat(i,imat)`, `i` $= 1, 2, \ldots, 100$. The full list `imatlist(1:nmatrls)` of the `imat` values in a given job, together with the total number `nmatrls` of participating materials, is composed and calculated in `subroutine MATDB` anew at each job restart.

All required values of `propmat(i,imat)` must be assigned through the `namelist/input/` in the input file `"input/deinput.ii"`. Because no default values are envisaged for `propmat(i,imat)`, and because this array is not saved for continuation, all its required values must be reassigned in the `namelist/input/` by every job restart.

1. EOS parameters

For any participating material `imat`, the user must assign the value of `propmat(1,imat)`= EOS#; if it is not assigned, the code stops. A special role belongs to the variables

$$\texttt{propmat(27,imat)} = \bar{A}, \quad \text{and} \quad \texttt{propmat(28,imat)} = \bar{Z}, \tag{B.1}$$

which also must, strictly speaking, be assigned by the user for each material in a given job — with the only exception of the tabular EOS #3. The variables `propmat(27,imat)`, `propmat(28,imat)` have been introduced with the aim to be used for calculation of the transport and relaxation coefficients from appropriate analytical models, assuming that they may differ from $\bar{A}_{eos}$ and $\bar{Z}_{eos}$ in the EOS model for the same material `imat`.

When setting the values of `propmat(27,imat)` and `propmat(28,imat)`, the following rules should be kept in mind:

- if the value `propmat(1,imat)` $= 3$ is chosen for a given material `imat`, the values

  $$\texttt{propmat(27,imat)} = \bar{A}_{eos}, \quad \texttt{propmat(28,imat)} = \bar{Z}_{eos} \tag{B.2}$$

  are loaded automatically and unconditionally in the `subroutine MATDB` — independent of whether the user has set any values of `propmat(27,imat)`, `propmat(28,imat)` in the `namelist/input/`; in doing so, $\bar{A}_{eos}$ and $\bar{Z}_{eos}$ are taken from the "DEITA3" EOS table in the non-fuel layers, and calculated from the initial chemical composition in the fuel layers;

- for any value of `propmat(1,imat)` other than 3, the code stops whenever one of `propmat(27,imat)`, `propmat(28,imat)` has not been assigned a value via the `namelist/input/`.

Note that the values of `propmat(27,imat)`, `propmat(28,imat)` are not used when calculating EOS by calling the `subroutine EOSDRV`; if $\bar{A}$ or $\bar{Z}$ is needed for the EOS calculation (like in the EOS models #2 and #3), the values

$$\texttt{propmat(25,imat)} = \bar{A}_{eos}, \quad \text{and} \quad \texttt{propmat(26,imat)} = \bar{Z}_{eos}, \tag{B.3}$$

are used. Generally, the values of `propmat(25,imat)`, `propmat(26,imat)` are loaded automatically — when needed — and must not be assigned by the user in the `namelist/input/`; the only exception is the value of `propmat(25,imat)` for the EOS model #2, see section 5 2.

TABLE B.1: Array `propmat(i,imat)` of material properties

EOS#	1	2	3	4	5	7
type	polytropic	Fermi	DEITA3	lin.Mie-Grü	GWEOS	GLT
i=1	1.0	2.0	3.0	4.0	5.0	7.0
2	K_e	$\bar{y} = z_{ion}$	TAB3# m	ρ_0	n	GLT# m
3	K_i			c_0^2	c_V	
4	γ_e			ν	ρ_{cr}	
5	γ_i			Γ_e	T_{cr}	
6				Γ_i	P_{cr}	
7				c_{Ve}	$z_{ion} = \bar{y}$	
8				c_{Vi}		
9						
10	pf-Mxwl	pf-Mxwl	pf-Mxwl	pf-Mxwl	pf-Mxwl	pf-Mxwl
...				...		
25		$\bar{A}_{eos}$	$\bar{A}_{eos}$		A_{eos}	
26			$\bar{Z}_{eos}$		Z_{eos}	
27	$\bar{A}$	$\bar{A}$	$\bar{A}$	$\bar{A}$	$\bar{A}$	$\bar{A}$
28	$\bar{Z}$	$\bar{Z}$	$\bar{Z}$	$\bar{Z}$	$\bar{Z}$	$\bar{Z}$
29						
parameters for calculating the electron conduction coefficient κ_e and its flux limiter f_{le}						
model type	$\kappa_0 T^n$ $f_{le}\rho T^{3/2}$	ad hoc analytic	Spitzer $f_{le}\frac{\rho z_i T^{3/2}}{A_{mol}}$		Basko-met $f_{le}\frac{\rho z_i T\sqrt{T_F}}{A_{mol}}$	GLT $f_{le}\frac{\rho z_i T^{3/2}}{A_{mol}}$
30	1.0	2.0	3.0	4.0	5.0	7.0
31	κ_0					GLT# m
32	n		$(\ln\Lambda)_{min}$			
...				...		
37	f_{le}	f_{le}	f_{le}	f_{le}	f_{le}	f_{le}
38						
39	g_{ei}	g_{ei}	g_{ei}	g_{ei}	g_{ei}	
parameters for calculating the ion conduction coefficient κ_i and its flux limiter f_{li}						
model type	$\kappa_0 T^n$ $f_{le}\rho T^{3/2}$	ad hoc analytic	Spitzer $f_{le}\frac{\rho z_i T^{3/2}}{A_{mol}}$		Basko-met $f_{le}\frac{\rho z_i T\sqrt{T_F}}{A_{mol}}$	GLT $f_{le}\frac{\rho z_i T^{3/2}}{A_{mol}}$
40	1.0	2.0	3.0	4.0	5.0	7.0
41	κ_0					GLT# m
42	n		$(\ln\Lambda)_{min}$			
...				...		
47	f_{li}	f_{li}	f_{li}	f_{li}	f_{li}	f_{li}
parameters for calculating radiation opacities						
model type	$k_{R,0}\rho^\alpha T^\beta$ $k_{P,0}\rho^\alpha T^\beta$	ad hoc analytic	Kramers free-free			GLT
50	1.0	2.0	3.0			7.0
51	$k_{R,0}$	$k_{R,0}$				GLT# m
52	$k_{P,0}$	$k_{P,0}$				
53	α	T_0				
parameters for laser absorption coefficient (dielectric constant)						
model type	$k_{las} =$ $k_0\rho^\alpha T^\beta$	ad hoc analytic	Kramers free-free		Basko metal	GLT
60	1.0	2.0	3.0		5.0	7.0
61	k_0	k_0	$z_{ii,min}$	$z_{ii,min}$		GLT# m
62	α	T_0	$z_{ie,min}$	$z_{ie,min}$		
63	β					

Presently, calculation of all the transport and relaxation coefficients, initiated by calling the `subroutine KINBUR`, is organized through the arrays `XMOL(I), AMOL(I), ZMOL(I), Z2MOL(I), SMOL(I)`, representing the quantities X_{mol}, A_{mol}, Z_{mol}, $(Z^2)_{mol}$, and S_{mol}, defined

in Eqs. (2.7)–(2.9), in each target layer `I`. For any non-fuel layer `I`, these are set to be

$$\begin{aligned}
&\texttt{XMOL(I)} = 1,\\
&\texttt{AMOL(I)} = \texttt{propmat(27,imatz0(I))},\\
&\texttt{ZMOL(I)} = \texttt{propmat(28,imatz0(I))},\\
&\texttt{Z2MOL(I)} = \texttt{propmat(28,imatz0(I))}^2,\\
&\texttt{SMOL(I)} = \texttt{propmat(27,imatz0(I))}^{-1/2} \cdot \texttt{propmat(28,imatz0(I))}^{-2},
\end{aligned} \tag{B.4}$$

in the `subroutine JOBINIT`.

In addition to `propmat(1,imat)`, `propmat(27,imat)`, `propmat(28,imat)`, also the PF-Maxwell flag `propmat(10,imat)` must have a meaningful value (either 0, or 1, or 2) for every material `imat`. For the EOS models #1, #2, #3, and #4, the value `propmat(10,imat)` = 0 is assigned automatically in the `subroutine MATDB` — irrespective of whether this has been done in the `namelist/input/`. For the EOS models #5 and #7, the code stops if an appropriate value of `propmat(10,imat)` has not been assigned by the user in the `namelist/input/`.

---

[1] BASKO, M.M., Teplofiz. Vys. Temper. **23** (1985) 483 (English translation: Sov. High Temper. **23** (1985) 388).

[2] S. I. Braginskii, in *Reviews of Plasma Physics*, ed. M. A. Leontovich (Consultants Bureau, New York, 1965), Vol. 1, p. 205.

[3] BASKO, M.M., Zh. Vychisl. Matem. i Matem. Fiz. **30** (1990) 176 (in Russian).

[4] BASKO, M.M., Fiz. Plazmy **10** (1984) 1195 (English translation: Sov. J. Plasma Phys. **10** (1984) 689).

[5] BASKO, M.M., Equations of One-Dimensional Radiative Hydrodynamics with Heat Conduction and Kinetics of Thermonuclear Burn, Preprint ITEP-145, Inst. of Theor. Exp. Physics, Moscow (1985) (in Russian).

[6] FOWLER, W.A., CAUGHLAM, G.R., ZIMMERMAN, B.A., Ann. Rev. Astron. Ap. **13** (1975) 69.

[7] LIBERMAN, M.A., VELIKOVICH, A.L., J. Plasma Physics **31** (1984) 369.

[8] BASKO, M.M., Fiz. Plazmy **13** (1987) 967 (in Russian); Sov. J. Plasma Phys. **13** (1987) 558 (English translation).

[9] IMSHENNIK, V.S., MIKHAILOV, I.N., BASKO, M.M., MOLODTSOV, S.V., Zh. Eksp. Teor. Fiz. **90** (1986) 1669 (in Russian); Sov. Phys. — JETP **63** (1986) 980 (English translation).

[10] BOBROVA, N.A., SASOROV, P.V., Fiz. Plazmy **19** (1993) 789-795 (in Russian); Plasma Phys. Rep. **19**(6) (1993) 409-412 (English translation).

[11] MAX, C.E., McKEE, C.F., MEAD, W.C., Phys. Fluids **23** (8) (1980) 1620.

[12] LEE, ...

[13] LAMPE, M., Phys. Rev. **174** ...

[14] LAMPE, M., Phys. Rev. **170** (1968) 306.

[15] FERMI, E., TELLER, E., Phys. Rev. **72** (1947) 399.

[16] BRYSK, H., Plasma Physics **16** (10) (1974) 927.

[17] YAKOVLEV, D.G., URPIN, V.A., Astron. Zh. (Sov. Astronomy) **57** (3) (1980) 526 (in Russian).
[18] BRYSK, H., CAMPBELL, P.M., HAMMERLING, P., Plasma Physics **17** (6) (1975) 473.
[19] HUBBARD, W.B., LAMPE, M., Astrophys. J. Suppl. **18** No. 163 (1969) 297.
[20] Seagrave J.D., Phys. Rev. **97** (1955) 757.
[21] Kikuchi S., Sanada J., Suwa Sh., Hayashi I., Nisimura K., and Fukunaga K., , J. Phys. Soc. Jpn **15** (1960) 9.
[22] Kootsey J.M., Nucl. Phys. A **113** (1968) 65.
[23] Glöckle W., Witala H., Hüber D., Kamafda H., and Golak J., Phys. Rep. **274** (1996) 107.
[24] RICHTMYER, R.D., MORTON, K.W., Difference Methods for Initial-Value Problems, Interscience Publ., New York (1967).
[25] BASKO, M.M., SOKOLOVSKII, M.V., Preprint ITEP 89–89, Moscow (1989).
[26] VINOGRADOV, A.V., TOLSTIKHIN, O.I., Preprint FIAN No. 139 (1989) (in Russian).
[27] NEVINS, W.M., and SWAIN, R., Nucl. Fusion **40** (2000) 865.
[28] BASKO, M.M., Keldysh Institute Preprints, No. 112 (2018) 28 p.; doi: 10.20948/prepr-2018-112e; URL: http://library.keldysh.ru/preprint.asp?id=2018-112.